AN ABSTRACT OF THE DISSERTATION OF

Bassem Khalfi for the degree of Doctor of Philosophy in Electrical and Computer Engineering presented on June 11, 2018.

Title: Efficient Spectrum Sensing and Sharing Techniques for Dynamic Wideband Spectrum Access

Abstract approved: _____

Bechir Hamdaoui

Besides enabling an enhanced mobile broadband access, fifth-generation (5G) wireless mobile networks are envisioned to support the connectivity of massive, heterogeneous Internet of Things (IoT) devices. Connecting these devices through 5G systems and providing them with their needed data rates require huge amounts of spectrum and power resources, thus calling for the development and design of innovative, dynamic resource identification, access and sharing methods that make effective use of these limited resources. This thesis focuses specifically on wideband spectrum sensing, and presents innovative techniques that enable efficient identification and recovery of unused spectrum opportunities in wideband dynamic spectrum access. Recent research efforts have focused on leveraging compressive sampling (CS) theory to enable wideband spectrum sensing recovery at sub-Nyquist rates. However, these approaches suffer from the following shortcomings. First, they consider homogenous wideband spectrum, where all bands are assumed to have similar primary users (PU)s traffic characteristics whereas in practice, the wideband spectrum occupancy is heterogeneous. Second, the number of measurements that receiver hardware designs are able to perform is practically way smaller than the number of measurements required by the CS-based sensing approaches. Third, the number of measurements required by the CS-based sensing approaches depends on the number of occupied bands (i.e., sparsity level), which is often unknown in advance and changes over time. Forth, current wideband spectrum databases suffer

from scalability issues in that they incur lots of sensing overhead. This thesis proposes a set of new, complementary techniques that overcome these aforementioned challenges. More specifically, in this thesis,

1. We design efficient spectrum occupancy information recovery techniques for heterogeneous wideband spectrum access. Our proposed techniques exploit the block-like structure of spectrum occupancy behavior observed in wideband spectrum access networks to enable the development of compressed spectrum sensing algorithms. Our proposed spectrum sensing algorithms achieve more stable spectrum information recovery than that achieved by existing approaches.

2. We develop distributed CS-based spectrum sensing techniques for cooperative wideband spectrum access that require lesser measurements while overcoming time-variability of spectrum occupancy and addressing hidden terminal challenges. Also, we propose non-uniform sensing matrices design that exploits the heterogeneity in the wideband spectrum access to further improve the spectrum sensing recovery accuracy.

3. We develop scalable spectrum occupancy information recovery techniques for database-driven wideband spectrum access networks. The novelty of our developed techniques lies in combining the merit of compressive sampling theory with that of low-rank matrix theory to enable scalable and accurate wideband spectrum occupancy recovery at low sensing overhead.

4. We propose joint data and energy transfer optimization frameworks for powering mobile cellular devices through RF energy harvesting. Our proposed framework accounts for both the consumed power at the base station and the battery power available at the end users to ensure that end users achieve their required data rates with as little battery power consumption as possible. We also analytically derive closed-form expressions of the optimal power allocations required for meeting the data rate requirements of the downlink and uplink communications between the base station and its mobile users.

Efficient Spectrum Sensing and Sharing Techniques for Dynamic Wideband Spectrum Access

by

Bassem Khalfi

A DISSERTATION

submitted to

Oregon State University

in partial fulfillment of
the requirements for the
degree of

Doctor of Philosophy

Presented June 11, 2018
Commencement June 2018

Doctor of Philosophy dissertation of <u>Bassem Khalfi</u> presented on <u>June 11, 2018</u>.

APPROVED:

_____

Major Professor, representing Electrical and Computer Engineering

_____

Director of the School of Electrical Engineering and Computer Science

_____

Dean of the Graduate School

I understand that my dissertation will become part of the permanent collection of Oregon State University libraries. My signature below authorizes release of my dissertation to any reader upon request.

_____

Bassem Khalfi, Author

ACKNOWLEDGEMENTS

First and for most, thank God for giving me the strength to fulfill my dreams and for surrounding me with beautiful minds and hearts.

I would like to express my special appreciation and sincere gratitude to my advisor, Prof. Bechir Hamdaoui for his continuous support, his patience, his motivation and encouragement, and his continuous follow-up. His valuable feedback and fruitful discussions were behind all the works in this dissertation. Also, I would like to thank the rest of my committee members: Prof. Attila Yavuz, Prof, Huaping Liu, Prof. Maggie Niess, and Prof. Lizhong Chen for their insightful comments and encouragement. Also, I would like to thank my professors here at OSU and extend my thanks to former professors and teachers. Thank you all for your endeavors.

For my friends here in Corvallis and elsewhere, thank you for the fun we had and the continuous support.

A special thanks and love to my parents, my brothers, my sister, and my nephews for their unconditional love. Finally, many thanks and gratitude goes to my future wife Houweida for the support, love, and patience during these years as well as her family.

CONTRIBUTION OF AUTHORS

Adem Zaid helped with the idea and simulations in manuscript 3. Abdurrahman Elmaghbub helped with the simulations and discussion in manuscript 4. Mahdi Ben Ghorbel and Xi Zhang provided a valuable feedback and discussion for Manuscript 6. Nizar Zorba provided a valuable feedback and discussion for Manuscripts 2 and 6.

Manuscripts in this dissertation were written with valuable feedback from Dr. Mohsen Guizani.

TABLE OF CONTENTS

TABLE OF CONTENTS (Continued)

TABLE OF CONTENTS (Continued)

TABLE OF CONTENTS (Continued)

LIST OF FIGURES

LIST OF FIGURES (Continued)

LIST OF FIGURES (Continued)

LIST OF TABLES

LIST OF ALGORITHMS

Chapter 1: Introduction

The increasingly growing number of wireless devices (e.g., Internet of things (IoT)s devices), along with the continually rising demand for wireless bandwidth, has created a serious shortage problem in the wireless spectrum supply [65]. This foreseen spectrum shortage is shown to be due to the lack of efficient spectrum allocation and regulation methods rather than the scarcity of spectrum resources [137, 108]. As a result, dynamic spectrum access (DSA) has been promoted as a potential candidate for addressing this shortage problem. This is done by authorizing access to any unused spectrum opportunities by the non-legacy users [165, 63, 61, 78, 142, 79]. Spectrum awareness is one of the main features crucial to enabling DSA, which allows DSA users (aka secondary users (SU)s) to locate unused portions of the spectrum in time, frequency and/or space. For instance, one of the major challenging tasks encountered in DSA that spectrum awareness techniques address is protecting primary users (PU)s from interference. Broadly speaking, spectrum awareness techniques can be categorized into two classes: sensing-based approaches [58, 57, 68, 55, 54, 83, 127] and spectrum database-driven approaches [53, 102, 56, 59, 97, 50, 132, 120]. While the former class allows users to identify unused spectrum portions on their own via local measurements, the latter provides users with radio occupancy databases, which users can query to acquire spectrum occupancy information in their vicinity.

Due to its great potential, DSA has already found its way to standardization—e.g., IEEE 802.22 [2] for enabling opportunistic access in the TV bands and 3GPP's Licensed-Assisted Access (LAA) and LTE-U [26] for enabling spectrum access in the unlicensed 5 GHz band. Spectrum sensing is vital to enabling successful DSA, and as a result, has been studied thoroughly in the literature. Most of the sensing technique development effort, however, has been focused on narrow band access, and not until recently, has it attracted some attention for the wideband spectrum access case [158, 127, 64, 117].

Performing wideband spectrum sensing (WSS) through traditional methods has been shown ineffective, by incurring excessive delays, costly hardware, and/or high energy consumption; for instance, sequential sensing approaches require cheap hardware, but incur

high sensing delays, whereas, parallel sensing approaches overcome delay issues, but require more hardware [158]. Frequency-domain analysis methods, on the other hand, require sampling rates that are excessively high for the case of wideband, which can be feasible only through complex hardware circuitry and processing algorithms. Motivated by the fact that only a small number of bands are occupied at a given time (the number of occupied bands is termed sparsity level throughout [28]), and in an effort to address the high sampling rate limitation, researchers have exploited compressive sampling (CS) theory to make wideband spectrum sensing possible at sub-Nyquist sampling rates (e.g. [127, 115, 101, 103, 117, 125]). Despite the many attempts aimed to develop CS-based approaches that require fewer sensed measurements, there remains major challenges that need to be overcome when it comes to recovering spectrum occupancy information in dynamic wideband spectrum access.

1.1   Wideband Spectrum Sensing Challenges

Connecting massive numbers of emerging wireless devices requires enormous amounts of spectrum and power resources. This requires the development of new, innovative resources sensing and sharing algorithms and frameworks that can cope with these raising demands. When it comes to wideband spectrum sensing, there have recently been research efforts that leverage CS to enable wideband spectrum occupancy information recovery at sub-Nyquist rates. However, these approaches fail to address the following challenges:

- **Challenge 1: Wideband spectrum occupancy is heterogenous.** Existing research efforts have focused mainly on *homogenous* wideband access, meaning that the entire wideband spectrum is considered as a one single block with multiple bands, and the sparsity or occupancy level is estimated across all bands and considered to be the same for the entire wideband spectrum. However, in spectrum assignment, applications of similar types (TV, satellite, cellular, etc.) are often assigned bands within the same band block, and different application types exhibit different traffic occupancy patterns and behaviors. This suggests that wideband spectrum is block-like *heterogeneous*, in that band occupancy patterns are not the same across the different band blocks, and hence, sparsity levels may vary significantly from one block to another. This trend has also been confirmed by many

measurement studies [31, 28, 159].

- **Challenge 2: Receiver hardware is limited.** The number of hardware branches needed to enable the CS-based recovery can be high and unpractical. For example, even when the number of occupied bands is as small as 6, the number of needed branches for a total number of bands 50 can be as high as 16 [158]. In practice, however, the number of branches that reasonable receiver designs have is typically in the order of 4 to 8 [157], a number that is much smaller than the number of measurements required by the CS-based approaches. Therefore, hardware presents a major limitation on the applicability of such CS-based approaches.

- **Challenge 3: Sparsity levels are time varying.** The third challenge that these CS-based approaches also face is that the number of occupied bands (i.e., the sparsity level) changes over time. Most CS-based approaches, however, assume that the sparsity level is fixed, often done by setting it to the overall average occupancy of the spectrum [127, 68]. Therefore, the time variability of the sparsity of the wideband occupancy makes existing approaches either inaccurate or incur high overhead.

In general, from a practical viewpoint, cooperative spectrum sensing approaches are more effective than non-cooperative approaches, since they are designed with the aim of providing spectrum availability information not only to just one SU, but to multiple SUs, often located in different geographic locations. Clearly, having each SU perform the CS-based spectrum sensing task on its own can be costly and redundant, as it might suffice for one SU to perform sensing and share it with other SUs, thereby saving SUs' energy and computation resources. Despite all the known benefits of cooperation, there is another major challenge that needs to be addressed to enable cooperative CS-based sensing.

- **Challenge 4: Observed spectrum occupancies are not consistent across different users.** In practice, different SUs may observe different spectrum occupancy due to wireless channel impairments (e.g., fading, multipath, etc.), leading to inconsistent measurements across the different users. This presents a challenge when it comes to using CS-based sensed measurements to collaboratively recover spectrum occupancy information.

As an alternative to performing spectrum sensing at the SU, spectrum database-driven techniques have been proposed to provides SUs with the available bands. Building Spectrum database for a wideband spectrum faces a major challenge.

- **Challenge 5: Existing spectrum database-driven techniques are unsuited for wideband spectrum access.** Current spectrum database-driven approaches are primarily designed for TV white spaces [102], which represent only a small portion of the wideband spectrum that can potentially be shared. In addition, TV carrier frequencies are mostly below 1 GHz, and hence, these signals can propagate long distances, requiring only a small number of SUs to get the spectrum occupancy in a relatively wide region. Therefore, to extend spectrum databases to cover wider spectrum ranges, say 10 GHz bandwidth or more, a higher number of SUs must be deployed to be able to obtain a complete radio occupancy map covering the entire wideband spectrum, as well as to overcome the hidden terminal problem, where due to, for example, fading, different SUs may observe different primary signals, thereby leading to different occupancy decisions. Although collaborative filtering [118] reduces the network overhead (spectrum occupancy matrix has a low rank property), it fails to scale well with the number of bands. This limitation comes from the propagation nature of signals at different spectrum frequencies, and especially at high frequencies (e.g. millimeter waves) that is being adopted in 5G systems [121]. Note that SUs at different locations tend to observe a completely different spectrum occupancy, which can result in losing the low-rank property of the spectrum occupancy matrix.

In addition to these aforementioned challenges, the need for supporting massive numbers of IoT devices, inherently having limited resources, gives rise to another major challenge that ought to be overcome.

- **Challenge 6: IoTs have limited energy resources.** Maintaining the operation of wireless devices (e.g., massive IoTs) through next-generation wireless networks requires large amounts of spectrum and power resources. RF energy harvesting has been proposed as an alternative power supply to these devices, by having a base station powering wirelessly these distant devices while communicating with them [45, 80]. However, existing approaches do not account for the power cost at

the base station nor for the power levels at the devices' batteries. Furthermore, existing multiuser frameworks relying on dedicated RF energy harvesting do not account for ambient RF energy.

1.2   Thesis Contributions

This thesis proposes frameworks and algorithms that overcome these challenges. Specifically, it makes the following contributions:

1. It considers heterogeneous wideband spectrum access and exploits its inherent, block-like structure of its occupancy to design efficient compressed spectrum sensing techniques that are well suited for heterogeneous wideband spectrum. The thesis proposes a weighted ℓ_1-minimization occupancy information recovery algorithm that achieves more stable recovery than that achieved by existing approaches while accounting for the variations of spectrum occupancy across both the time and frequency dimensions. In addition, the proposed algorithm is shown to require a smaller number of sensing measurements when compared to the state-of-the-art approaches.

2. It designs techniques that leverage supervised learning to provide accurate realtime estimates of the spectrum occupancy levels, which are then exploited to provide accurate recovery of spectrum occupancy. In doing so, the proposed techniques are able to overcome the issue of time-variability of the number of occupied bands.

3. It develops a distributed compressive sampling based technique for cooperative wideband spectrum sensing that requires lesser numbers of measurements while overcoming time-variability of spectrum occupancy and addressing the hidden terminal problem. First, the wideband spectrum occupancy information is shown to almost surely be recovered with lesser numbers of spectrum measurements. Second, a non-uniform sensing matrices design is proposed, which exploits the heterogeneity in the wideband spectrum access to further improve the spectrum sensing recovery accuracy.

4. It proposes a framework for enabling scalable database-driven dynamic spectrum access and sharing. It brings together the merits of compressive sensing and collab-

orative filtering to provide accurate radio occupancy map while reducing the network overhead and overcoming the scalability issue that conventional approaches suffer from. We start from an observation that close-by users have a highly correlated spectrum observation and we propose to recover the spectrum occupancy matrix in the borough of each sensing node by minimizing the rank of local submatrices. Then, we combine the recovered matrix entries using a similarity criterion to get the global spectrum occupancy map. Through simulations, we show that the proposed framework minimizes the error while reducing the network overhead.

5. It proposes joint data and energy transfer optimization frameworks for powering mobile wireless devices through RF energy harvesting. We introduce a power utility that captures the power consumption cost at the base station and the used power from the users' batteries, and determine optimal power resource allocations that meet data rate requirements of downlink and uplink communications. Two types of harvesting capabilities are considered at each user: harvesting only from dedicated RF signals and hybrid harvesting from both dedicated and ambient RF signals. The developed frameworks increase the end users' battery lifetime at the cost of a slight increase in the base station power consumption.

1.3   List of Publications

1. **Bassem Khalfi**, Bechir Hamdaoui, and Mohsen Guizani, "Extracting and Exploiting Inherent Sparsity for Efficient IoT Support in 5G: Challenges and Potential Solutions", IEEE Wireless Communications Magazine, Vol. 24, No. 5, pp. 68-73, Oct. 2017.

2. **Bassem Khalfi**, Bechir Hamdaoui, Mohsen Guizani, and Nizar Zorba, "Efficient Spectrum Availability Information Recovery for Wideband DSA Networks: A Weighted Compressive Sampling Approach", IEEE Transactions on Wireless Communications, Vol. 17, No. 3, pp. 1688 - 1699, Apr. 2018.

3. **Bassem Khalfi**, Adem Zaid, and Bechir Hamdaoui, "When Machine Learning Meets Compressive Sampling for Wideband Spectrum Sensing", in Proceedings of International Wireless Communications and Mobile Computing Conference (IWCMC), Valencia, Spain, pp. 1120-1125, 26-30 Jun. 2017.

4. **Bassem Khalfi**, Abdurrahman Elmaghbub, and Bechir Hamdaoui, "Distributed Wideband Sensing for Faded Dynamic Spectrum Access with Changing Occupancy", submitted to IEEE Global Communications Conference (Globecom) Abu Dhabi, UAE, 9-13 Dec. 2018.

5. **Bassem Khalfi**, Bechir Hamdaoui, and Mohsen Guizani, "AirMap: Scalable Spectrum Occupancy Recovery Using Local Low-Rank Matrix Approximation", submitted to IEEE Global Communications Conference (Globecom) Abu Dhabi, UAE, 9-13 Dec. 2018.

6. **Bassem Khalfi**, Bechir Hamdaoui, Mahdi Ben Ghorbel, Mohsen Guizani, Xi Zhang, Nizar Zorba, "Optimizing Joint Data and Power Transfer in Energy Harvesting Multiuser Wireless Networks", IEEE Transactions on Vehicular Technology, Vol. 66, No. 12, pp. 10989-11000, Dec. 2017.

7. Bechir Hamdaoui, **Bassem Khalfi**, and Mohsen Guizani, "Compressed Wideband Spectrum Sensing: Concept, Challenges and Enablers", IEEE Communications Magazine, Vol. 56, No. 4, pp. 136-141, Apr. 2018.

8. **Bassem Khalfi**, Bechir Hamdaoui, Mohsen Guizani and Nizar Zorba, "Exploiting Wideband Spectrum Occupancy Heterogeneity for Weighted Compressive Spectrum Sensing", in proceedings of IEEE Conference on Computer Communications Workshops (INFOCOM WKSHPS), Atlanta, GA, USA, 2017, pp. 613-618.

9. **Bassem Khalfi**, Bechir Hamdaoui, Mehdi Ben Ghorbel, Mohsin Guizani, and Xi Zhang, "Joint Data and Power Transfer Optimization for Energy Harvesting Wireless Networks", in proceedings of IEEE Conference on Computer Communications Workshops (INFOCOM WKSHPS), San Francisco, CA, 2016, pp. 742-747.

Extracting and Exploiting Inherent Sparsity for Efficient IoT Support in 5G: Challenges and Potential Solutions

Bassem Khalfi, Bechir Hamdaoui, and Mohsen Guizani

Chapter 2: Manuscript 1: Extracting and Exploiting Inherent Sparsity for Efficient IoT Support in 5G: Challenges and Potential Solutions

Bassem Khalfi, Student Member, IEEE, Bechir Hamdaoui, Senior Member, IEEE, and Mohsen Guizani, Fellow Member, IEEE

Abstract

Besides enabling an enhanced mobile broadband, next generation of mobile networks (5G) are envisioned for the support of massive connectivity of heterogeneous Internet of Things (IoT)s. These IoTs are envisioned for a large number of use-cases including smart cities, environment monitoring, smart vehicles, etc. Unfortunately, most IoTs have very limited computing and storage capabilities and need cloud services. Hence, connecting these devices through 5G systems requires huge spectrum resources in addition to handling the massive connectivity and improved security. This article discusses the challenges facing the support of IoTs through 5G systems. The focus is devoted to discussing physical layer limitations in terms of spectrum resources and radio access channel connectivity. We show how sparsity can be exploited for addressing these challenges especially in terms of enabling wideband spectrum management and handling the connectivity by exploiting device-to-device communications and edge-cloud. Moreover, we identify major open problems and research directions that need to be explored towards enabling the support of massive heterogeneous IoTs through 5G systems.

2.1 Introduction

The foreseen success of the Internet of Things (IoT) and its applications is the result of three major trends. First, fifth-generation (5G) systems have promises for meeting stringent QoS requirements that legacy systems fail to meet. Examples of such requirements are high data rates, low energy consumption, low latency, high capacity, and improved security. These expected improvements make 5G an ideal candidate for ensuring required connectivity and services for massive and heterogenous IoT devices [1]. The

second trend is the emergence of cloud computing services, which are believed to play a vital role in making IoT a success by enabling diverse IoT services and applications that were not possible before. Bringing computing and storage resources closer to the IoT devices by means of edge computing has great promises for lowering energy consumption by releasing the devices from the burden of having to deal with some or most of the computation and energy needed for task execution [4]. The third trend is the adoption of device-to-device (D2D) communications envisioned for public safety with the potential for enabling more decentralized network management and local traffic offloading [10]. D2D offers 5G real-time assurances and better spectrum and resource allocation efficiency [10]. These (technological) trends have jointly led to a common belief that the success of IoT applications is rather a possible reality.

Indeed, telecom industries believe that IoT is the main driver of 5G, as the major use-cases for 5G involve IoT devices (e.g., consumer or industrial IoTs). For instance, IoT will shift the focus of mobile system designs from enabling traditional broadband communications to support not only enhanced broadband communications but especially massive IoTs with heterogeneous services requirements. However, there are major challenges that need to be addressed in order for 5G to support these massive IoTs. The first challenge lies in the enormous amounts of spectrum and bandwidth resources that these massive numbers of IoT devices need. We envision that dynamic spectrum access (DSA) is to be needed now more than ever, as it is commonly viewed as a potential solution for overcoming such resource demand challenge. Second, large numbers of newly emerging IoT applications are desperately in need for cloud offloading services due to their limited computation and storage capabilities, as well as to their low latency requirements. Empowering such IoTs with cloud offloading capabilities is therefore crucial to the successful support of key time-critical IoT applications like virtual reality, video surveillance, and precision healthcare, just to name a few. Third, current cellular systems are designed for users' profiles that are different from the services requested by IoTs. In fact, current mobile systems are designed for limited numbers of connections and high-rate downlink data traffic, whereas IoTs require massive numbers of connections mostly for low-rate uplink traffic with various delay constraints [9].

In this paper, we discuss some potential solutions that can be used to overcome these aforementioned challenges. Specifically, we leverage three key technology enablers, D2D, compressive sensing, and edge cloud, to address bandwidth resource shortages and

network edge traffic bottlenecks that 5G systems face. The potential of some of these technologies has already been recognized by ongoing research efforts such as the METIS project led by different research groups from various telecom companies. The main contribution of this work lies in the exploitation of key sparsity properties that are inherent to dynamic spectrum access and IoT traffic to develop efficient techniques that offer better IoT connectivity, alleviate congestion bottlenecks at network edges, and enable efficient dynamic wideband spectrum access and sharing. The paper also identifies some open research challenges that still need to be overcome in order to enhance 5G's support of IoTs.

We want to mention that even though this work focuses on the support of IoTs via cellular/5G systems, depending on the IoT application, IoT devices can also be connected via various other means, such as WiFi, ZigBee, LoRa, etc [11]. In fact, recent studies [6] show that by 2021, only about 7% of IoT devices will be connected via cellular systems.

The remainder of this article is organized as follows. Section 2.2 discusses IoT connectivity challenges. Section 2.3 presents the different approaches that can be used to exploit 5G sparsity to overcome these challenges. Finally, Section 2.4 presents some open challenges and new research directions.

2.2 Challenges 5G Faces in Support of IoTs

Besides accommodating enhanced broadband mobile communications, 5G is anticipated to support a wide range of IoT applications with various heterogeneous requirements [1]. Fig. 2.1 illustrates 5G support to diverse IoT devices, where base station is augmented with edge cloud services. The traffic generated by such IoTs is different from that generated by cellular systems in many aspects. First, unlike the case of broadband access, most of the IoT traffic is in the uplink. Moreover, IoTs' messages are typically small in size and sparse in time. Furthermore, IoT devices are limited in energy and computation resources. These IoT devices' characteristics make their access to 5G systems different from classical cellular devices. Given these traffic characteristics and resource constraints, IoTs can be classified, as illustrated by Table 2.1, into three classes based on their required services.

- **Massive IoTs (mIoTs)**: This class of IoTs includes large numbers of low-power, low-cost devices that generate low-rate, small-sized, delay-tolerant uplink traffic. Examples of such mIoTs are those envisioned for smart cities, smart homes, smart parking, environmental monitoring, etc.

- **Ultra-reliable, low-latency IoTs (uIoTs)**: These IoTs need very low latency, high availability, and high reliability, but do not require high data rates. Examples of uIoTs are those envisioned for vehicle-to-everything (V2E) services, emergency management, remote healthcare, manufacturing control, smart grids, etc.

- **Hybrid IoTs**: These IoTs require both high data rates and low latency and are used in applications like virtual/augmented reality, video surveillance, law enforcement, etc.
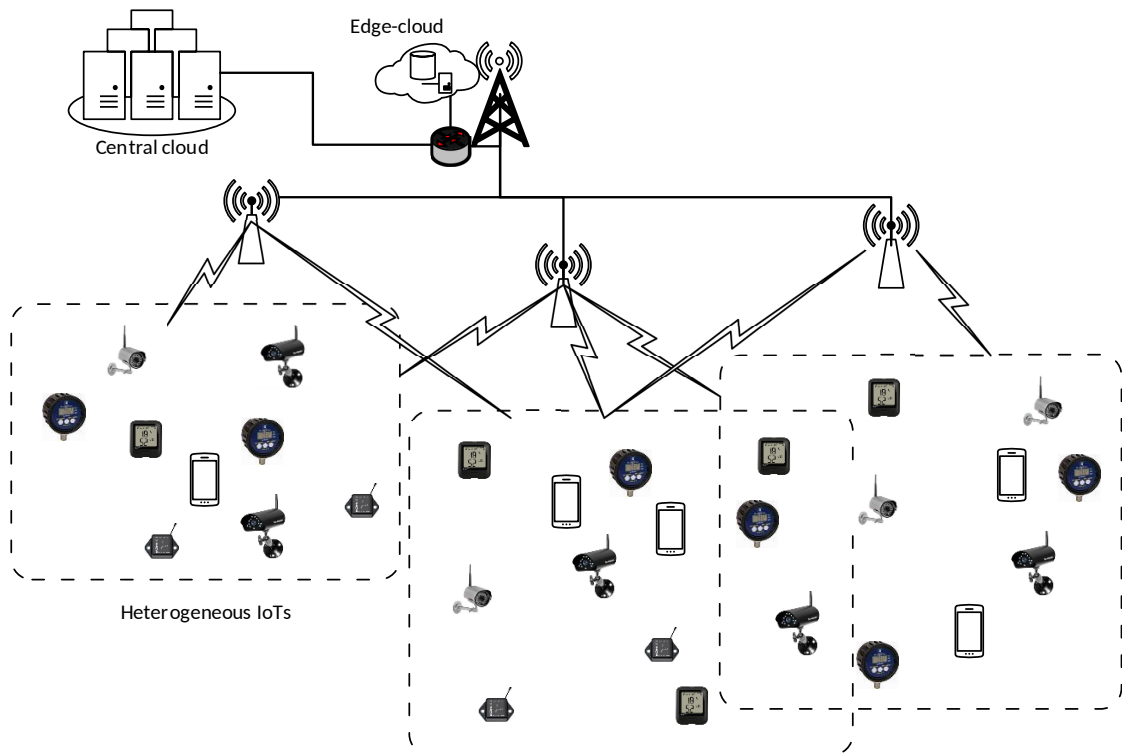
Figure 2.1: 5G support to massive and heterogenous IoTs with different service requirements enabled via edge-cloud or central cloud.

Table 2.1: Classification of heterogeneous IoTs

Type/class of IoTs	Service characteristics
Massive IoTs (mIoTs)	Requires scalable connectivity and generates small-sized, delay-tolerant uplink traffic
ultra-IoTs (uIoTs)	Requires reliable, low-latency, and highly available network connections
Hybrid	Includes low-latency, high-rate services

The connectivity of these heterogeneous IoTs will be ensured through heterogeneous networks with diverse ranges and data rates including cellular systems, WiFi, Bluetooth, Zigbee, Z-Wave, Sigfox, LoRA, Weightless, etc [11]. In particular, we focus in this work on cellular systems as there have been significant efforts towards developing standards relative to IoTs such as LTE-MTC, NB-LTE-M, and NB-IoT. With that being said, it is worth acknowledging that it is anticipated that only a small portion (about 7%) of IoTs will be connected through cellular systems by 2021 [6].

2.2.1 Wideband Dynamic Spectrum Access Challenges

Serving these diverse, massive and heterogeneous IoTs calls for the development of new intelligent resource management approaches. Of particular importance is the need for efficient spectrum resource usage and access at higher frequency ranges. Spectrum regulation agencies such as FCC and Ofcom have already issued notices for considering and using millimeter wave spectrum with the aim to meet the enormous bandwidth needs these massive IoTs are anticipated to require. Though spectrum policy makers are taking the necessary steps towards enabling and opening up wideband spectrum for 5G access, much remains to be done when it comes to developing resource allocation techniques. Although there is a general consensus among the researchers that dynamic spectrum access (DSA) will be a key for enabling efficient spectrum resource sharing at the millimeter wave range, there are key challenges that need to be addressed to be able to enable wideband DSA. Wideband spectrum sensing is one of such challenges that we focus on in this paper.

Spectrum sensing is the process by which unlicensed spectrum users identify unused portions of the licensed spectrum to use opportunistically. Despite the huge research

efforts dedicated to developing efficient sensing techniques, not much has been done when it comes to exploiting the sparsity properties that are intrinsic to the wideband spectrum access. As will be discussed later, intelligently extracting and exploiting the sparsity properties inherent to the heterogenous occupancy nature of the wideband spectrum can significantly improve the sensing efficiency of the available portions of the wideband spectrum, and thus increase the overall spectrum utilization.

With the opening up of the wideband spectrum access recently enabled by spectrum policy makers, and with the device characteristics and traffic heterogeneity nature of these massive IoTs, traditional single-band spectrum sensing approaches are no longer effective and hence, new sensing approaches need to be developed. The main reason for why traditional approaches are not efficient for wideband DSA is that they do require high numbers of sensing measurements; that is, in order to fully recover spectrum occupancy information, high (Nyquist) sampling rates are required, which can incur significant sensing overhead in terms of energy, computation, and communication. Motivated by the sparsity nature of spectrum occupancy and in an effort to address the overhead caused by these high sampling rates, researchers have recently been focusing on exploiting compressed sampling theory to develop wideband spectrum sensing approaches that can recover information at sub-Nyquist sampling rates [5]. In Section 2.3.1, we present a novel wideband spectrum sensing technique that extracts key sparsity properties inherent to the wideband spectrum occupancy heterogeneity nature [15] and exploits them through compressive sensing theory to improve the efficiency of spectrum sensing. An illustration of the wideband spectrum occupancy is shown in Fig. 2.2.

2.2.2   Network Edge Traffic Challenges

Cloud offloading has been adopted as a potential solution for overcoming the resource limitation of IoT devices, as it exempts them from having to deal with the computation, storage, and device-to-network communication burdens resulting from the running of the IoT applications. Researchers have recently started exploring new ways to take cloud offloading to a higher level: bring cloud computing infrastructures closer to end-users, leading to what is commonly known today as Edge Clouds or Cloudlets. Enabling IoT devices with edge cloud offloading capabilities is a key requirement for the 5G network architecture, crucial to successfully supporting IoT applications at scale, characterized

Occupancy 10%   Occupancy 10%   ...   Occupancy 5%

Service provider 1   Service provider 2
Occupancy 7%   Occupancy 13%

| F1 | F2 | F3 | ⋮ | ⋮ | ⋮ | ⋮ | ⋮ | ⋮ | ⋮ | ⋮ | ⋮ | ⋮ | ⋮ | ⋮ | ⋮ | ⋮ | ⋮ | ⋮ | ⋮ | ⋮ | Fn |

(a)

Wideband $B\ Hz$

(b)
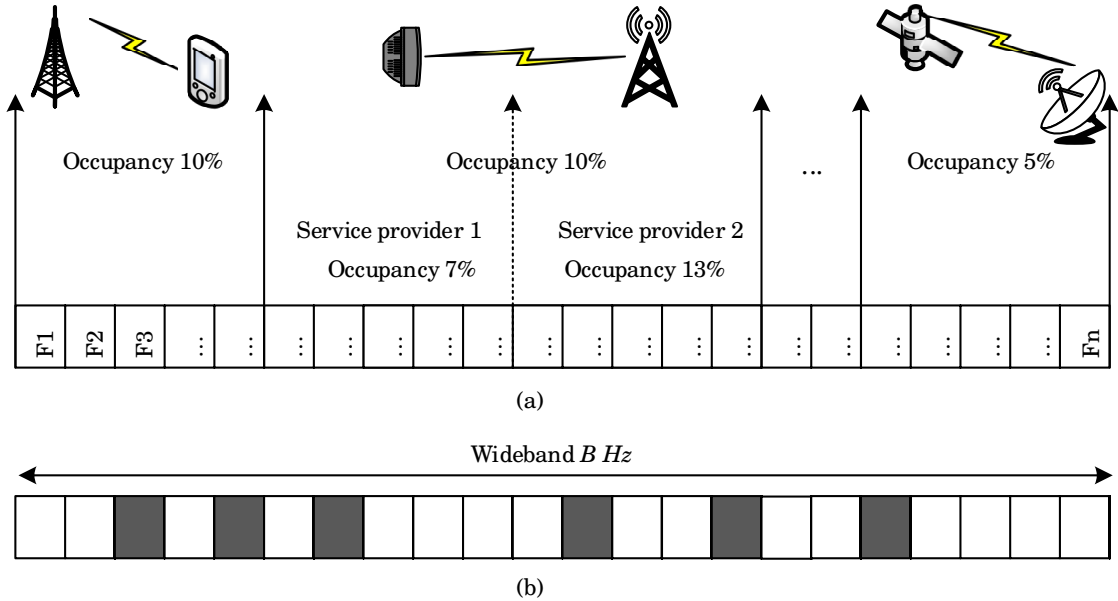
Figure 2.2: n frequency bands occupied by heterogeneous applications with different occupancy rates. The grey bands are occupied by primary users while the white bands are vacant. (a) is the statistical allocation while (b) is a realization of allocation in a given region at a given time slot. (a) reveals that the wideband spectrum is stochastically under-utilized and (b) is an instantaneous realization of this under-utilization.

with diverse and more stringent QoS requirements. In addition to relieving the device from having to run its application locally, edge cloud offloading eliminates the need for having to send massive amounts of IoT data through the Internet, thereby generating lesser Internet congestions and, more importantly, improving IoT device responsiveness, essential to the support of time-critical IoT applications, such as realtime video surveillance, augmented reality, and remote health care.

With edge cloud offloading, IoT devices can replicate their memory objects (often small-sized) and transfer them to their associated Cloudlets. Despite these apparent resource elasticity benefits of edge cloud offloading, the massive numbers of devices each 5G cell is expected to support will render the network edges of 5G major traffic bottlenecks, thereby significantly limiting cloud offloading performance gains [3]. In Section 2.3.2, we present techniques that leverage existing technologies such as D2D and

compressive sensing theory to exploit key sparsity properties unique to IoT to alleviate congestion bottlenecks and overcome access scalability issues at 5G network edges.

2.3 Extracting and Exploiting Sparsity for Efficient IoT Support in 5G

Having identified some key challenges facing the adoption of IoTs in 5G, we now present potential solutions that leverage compressive sensing theory to overcome these challenges.

2.3.1 Enabling Efficient Wideband Spectrum Sensing

In order to serve the massive numbers of IoTs, spectrum sensing techniques suitable for wideband spectrum access and sharing need to be carefully developed. We discussed in Section 2.2.1 the shortcomings of conventional sensing approaches when applied to wideband spectrum sensing. More specifically, the key limitations of such existing approaches lie in their high sampling rates and hardware capabilities needed to be able to recover sensing information for wideband spectrum access. However, since (wideband) spectrum is heavily under-utilized [15] in that the number of occupied bands is significantly less than the total number of bands (i.e., the vector representing spectrum occupancy information is sparse), compressive sensing theory is an ideal candidate for fully recovering spectrum occupancy information while using sampling rates lower than sub-Nyquist rates [12]. In other words, the recovery of the (sparse) spectrum occupancy vector can be done with a fewer number of sensing measurements.

With compressive sensing, the occupancy information of a spectrum consisting of n bands can be recovered with only $m = O\big(k\log(n/k)\big)$ measurements where $m < n$ and k is the number of occupied bands, referred to as the sparsity level. The spectrum occupancy information vector, $\boldsymbol{x}_{n\times 1}$, is then recovered by minimizing the ℓ_0-norm of $\boldsymbol{x}_{n\times 1}$ subject to a constraint on the error $\|\boldsymbol{y}_{m\times 1} - \Phi\Psi\boldsymbol{x}_{n\times 1}\|_{\ell_2}^2$, where $\boldsymbol{y}_{m\times 1}$ is the vector representing the m measurements, Φ is a full-rank sensing matrix, and Ψ is the discrete inverse Fourier transform Matrix. Due to its NP-hardness nature, recovery heuristics (e.g., ℓ_1-norm minimization and orthogonal matching pursuit [12]) have been proposed in the literature for solving such problems. From a practical viewpoint, the implementation of wideband spectrum sensing requires the use of m amplifiers and then mixing the

received amplified signals with pseudo-random waveforms at Nyquist rates. After that, an integrator is applied followed by an analog-to-digital converter that takes samples at sub-Nyquist rate. This architecture is known as analog-to-information converter (AIC) sampler [12].

An observation we make by investigating the existing compressive sensing-based approaches is that they consider that the occupancy of wideband spectrum is *homogenous*, meaning that the entire wideband spectrum is considered as one single block with multiple bands, and the sparsity level is estimated across all bands and considered to be the same for the entire wideband spectrum. However, in wideband spectrum assignment, applications of similar types (TV, satellite, cellular, etc.) are often assigned bands within the same block, suggesting that wideband spectrum is *heterogeneous*. That is, band occupancy patterns are not the same across the different blocks, since different application/user types within each block can exhibit different traffic behaviors, and hence, wideband spectrum occupancy may vary significantly from one block to another as illustrated in Fig. 2.2. This trend has indeed also been confirmed by recent measurement studies [15].

Incorporating this fine-grained sparsity structure into the formulation of wideband spectrum occupancy recovery allows us to improve the recovery performance and enhance the detection accuracy of wideband spectrum sensing. Specifically, such a block-like sparsity structure allowed us to formulate the problem as a weighted ℓ_1-minimization problem, thereby resulting in an algorithm that provides faster spectrum occupancy recovery with lesser sensing overhead [8]. The basic idea behind our algorithm is that the spectrum blocks that are more likely to be occupied are favored during the search. In addition, blocks corresponding to critical applications or for which some occupancy information is known are captured through careful design of block weights [8]. In essence, any additional knowledge about spectrum utilization behavior can be incorporated and exploited so that faster recovery of spectrum occupancy information can be achieved. Fig. 2.3 illustrates some of these design elements, where the blocks that are more likely to be unoccupied are encouraged to be sparser than the blocks which are more likely to be occupied. Since the number of occupied bands changes over time, the design of the weights $\boldsymbol{w}$ can be based on the average occupancy of every spectrum block i, $\bar{k}_i$, such that $w_i = 1/\bar{k}_i$ [8]. Furthermore, if each block occupancy, $\hat{k}_i$, can be estimated through learning (e.g., using regression techniques), better performance can be achieved when setting

$w_i = 1/\hat{k}_i$. In Fig. 2.4, we show the performance of the proposed weighted compressive spectrum sensing approach with band occupancy prediction (using different regression models), and compare it to a conventional wideband spectrum sensing approach [12]. Note that in the non-cooperative case where IoTs perform wideband spectrum sensing individually, there is no signaling overhead (information exchange with the other network entities to perform this task). However, in the cooperative case where multiple IoTs are involved in the sensing task, the signaling overhead becomes proportional to the number of cooperating IoTs. Table 2.2 shows the signaling overhead associated with each of the approaches discussed in this paper.
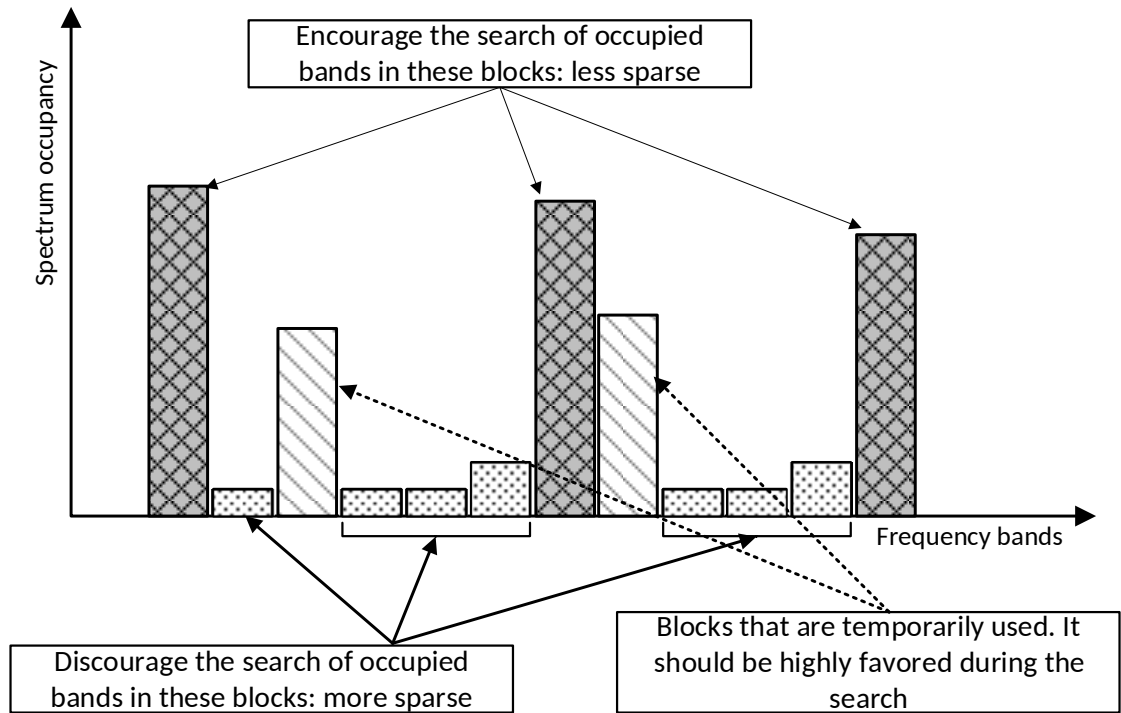
Figure 2.3: Sparsity-promoting wideband spectrum sensing.

2.3.2 Overcoming Network Edge Traffic Bottlenecks

As discussed in Section 2.2.2, the massive IoT traffic that 5G cells are required to support to enable edge cloud offloading will create severe congestion bottlenecks at the 5G
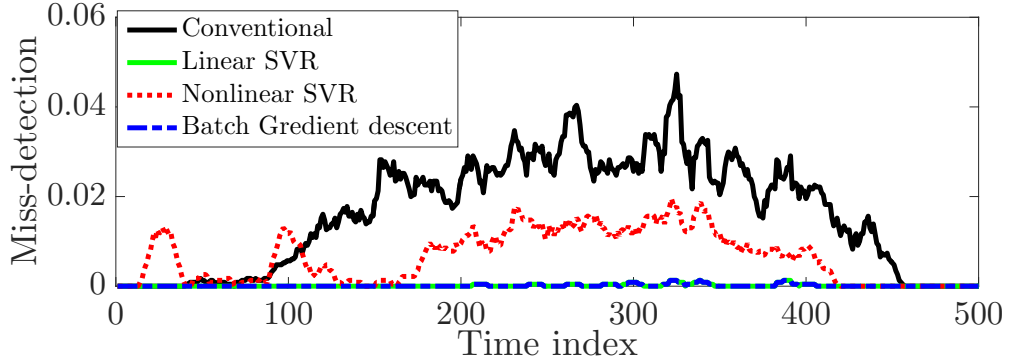
Figure 2.4: Miss-detection performance evaluation of weighted compressive sensing under different regression techniques.

network edges. One possible solution proposed in [2] to overcome this challenge lies in leveraging D2D and compressive sensing theory to reduce the number of connections established between the base stations and the IoTs, and to reduce the amount of of-floading traffic. D2D communication technology has been adopted in LTE-advanced systems but only for public safety communications. When appropriately exploited, D2D can offer great advantages. Higher throughput, low latency, better availability and new services among other advantages make D2D an ideal candidate to help in the adoption and support of IoTs by 5G.

With the use of compressive sensing, instead of having all IoTs push their data to the base stations, the base stations can pull the data from only a subset of devices and use compressive sensing to recover the data of all IoTs. Here the sparsity that allowed the exploitation of compressive sensing comes from the fact/assumption that at a given time, only a few IoT devices experience changes in their memory and hence only few will need to upload their memory updates to the edge clouds. Specifically, considering mIoTs with delay-tolerant requirements, every node multicasts to its neighbors a weighted value of the updated data replica with a defined coefficient that corresponds to the coefficient of the sensing matrix. When a node receives the weighted data replicas from other nodes, it adds its corresponding update, if any, and multicasts it during its time slot. After exchanging the data replicas, the nodes turn to the sleep mode for energy saving purposes. The base station pulls the measurements from few nodes, compared to the total number of mIoTs, where the number of these nodes should satisfy a condition that

depends on the total number of nodes and the number of nodes that have data updates. Since most of the mIoTs have no update, then the vector corresponding to the memory replicas is sparse. Compressive sensing theory can accurately recover the data replicas for each IoT and support the corresponding ones through cloud services. The proposed protocol shows that signaling overhead is considerably reduced (only m connections are established with BS), congestion is avoided and latency is improved by placing cloud services at the edge. The main shortcoming of this approach is that it only works with homogeneous IoTs and assumes a fixed sparsity level.

Potential improvements can be achieved through weighted compressive sensing as discussed previously in the wideband spectrum sensing context. In addition, learning and prediction approaches can also be used in conjunction with the recovery approach to improve the performance. This has been considered in [13] where a data gathering approach is proposed based on compressive sensing. The proposed scheme takes advantage of the correlation between data and introduces an autoregressive (AR) model in the recovery approach. IoTs can also be leveraged for performing wideband spectrum sensing but with a focus on reducing the reported measurements' cost [7], which can be combined with the work of [13]. Under the assumption that the sensed signal is sparse, a sparser basis can be found and can lead to a more compressed signal than the frequency domain basis. The IoTs report the measurements to network nodes that perform simple addition of the measurements coming from the IoTs and report them to the base station. This way, a constant communication cost is maintained (communication overhead is proportional to the number of network nodes). At the base station, the different measurements are exploited to recover the wideband spectrum occupancy.

Table 2.2 summarizes the main proposed works that exploit sparsity features to enable the support of massive and heterogeneous IoTs.

Table 2.2: Summary of the techniques exploiting sparsity.

Ref.	Application	Comments	Sparsity	Signaling overhead
[12]	Wideband spectrum sensing	without cooperation	fixed sparsity	no signaling overhead
		with cooperation		proportional to number of SUs
[8]	Wideband spectrum sensing	Exploited spectrum heterogeneity	varying sparsity	no signaling overhead
[2]	Upload memory replicas of mIoTs	Exploited D2D communications	fixed sparsity	m connections with the BS
[13]	Adaptive data gathering	Exploited correlation	varying sparsity	m transmissions to the sink
[7]	Compressed measurement reporting	Exploited signal's stationarity+ D2D	fixed sparsity	for p active IoTs and n network nodes: $n + p$ transmissions
[14]	Wideband spectrum sensing	Two-step approach to adjust the number of measurements	varying sparsity	no signaling overhead

2.4 Open Research Problems and Directions

Despite the efforts made in exploiting the hidden sparsity structure for supporting IoTs through cellular systems, there remains key challenges that need to be overcome. We summarize here some of the research directions that we believe are worth investigating in the future.

Wideband spectrum occupancy behaviors: Although some research efforts aiming to exploit spectrum occupancy sparsity to reduce traffic overhead have already been made, these approaches are either generic (not specific to wideband spectrum access) or achieve limited performance improvements due to the assumptions made. For instance, the spectrum occupancy heterogeneity structure inherent to dynamic wideband spectrum access is a feature that when exploited properly can allow for the design of more efficient compressive sampling approaches [8]. Also, a common limitation of these existing approaches lies in the fact that the spectrum occupancy sparsity level is considered constant and does not change over time. Therefore, designing efficient recovery algorithms that exploit such features and structures in spectrum occupancy, finding bounds on the minimum required number of sensed measurements, and deriving error bounds on the achieved performances are some important challenges that remain open and hence require further investigation.

Cooperative wideband spectrum sensing: As the demand for spectrum resources continues to rise with the emergence of 5G, devising efficient techniques for enabling dynamic spectrum sharing and access of wideband spectrum resources is needed more than ever. Of particular importance is cooperative spectrum sensing. Considering and studying cooperative wideband spectrum sensing approaches under the observed heterogeneous structure of the spectrum occupation has great potential for improving spectrum sensing accuracy and reducing sensing overhead and is still an open research problem that requires further investigation. Although this problem can be casted as a low-rank matrix minimization, deriving theoretical performance that consider tradeoffs between sensing overhead (delay, energy, etc.) and sensing accuracy while accounting for the time-variability of the spectrum occupation has not been investigated.

IoT heterogeneity: Although there have been some research efforts that aim to leverage compressive sampling to reduce traffic jams, more work remains to be done when it comes to incorporating QoS. The heterogeneity nature of IoT devices and their

applications mandate that different IoT types may come with different QoS requirements. For instance, what IoTs designated for smart vehicle applications need is different from what those designed for collecting agriculture data (e.g., air temperature, humidity, soil moisture, etc.) need. QoS with respect to IoT is an area that has not received much attention, and hence, there remains challenges that need to be overcome.

Energy harvesting: Energy availability and consumption continue to present a major challenge for IoTs due to their limited energy resources. Relying on energy harvesting and dedicated wireless energy transfer technologies emerge as key solutions to such challenges. Although there have recently been a research focus on developing energy harvesting techniques for wireless systems in general, not much has been done when it comes to developing energy harvesting techniques aimed for IoT devices and applications.

Security and privacy: Most of these compressive sampling-based data reporting techniques that have been proposed so far do not address security and privacy concerns. For instance, users' privacy may not be protected in the data reporting process. Existing traditional encryption protocols cannot be applied as they are to these proposed approaches, and hence, new privacy-preserving techniques need to be carefully designed so that compressive sampling can be exploited to reduce traffic, yet without compromising the privacy of users involved in the data reporting process.

2.5   Conclusion

IoTs have recently gained tremendous research attention as they are the main driver for a wide range of various applications. Of particular interest is the focus on leveraging compressive sampling theory and D2D communication technology to exploit some sparsity structures inherent to the spectrum resource access and sharing in 5G to overcome key challenges that 5G systems will face. Specifically, we focus on two key challenges that pertain to the support of IoTs in 5G: spectrum resource availability and traffic jams at network edges. We present some potential solutions for overcoming these two challenges, and identify some open research problems that remain to be addressed.

Acknowledgement

Bibliography

[1] 3GPP TR 23.799 V1.0.0. 3rd generation partnership project; technical specification group services and system aspects; study on architecture for next generation system (release 14). Technical report, 3GPP, Sept. 2016.

[2] Sherif Abdelwahab, Bechir Hamdaoui, Mohsen Guizani, and Taieb Znati. Replisom: Disciplined tiny memory replication for massive iot devices in LTE edge cloud. *IEEE Internet of Things Journal*, 3(3):327–338, 2016.

[3] Andrea Biral, Marco Centenaro, Andrea Zanella, Lorenzo Vangelista, and Michele Zorzi. The challenges of M2M massive access in wireless cellular networks. *Digital Communications and Networks*, 1(1):1–19, 2015.

[4] Flavio Bonomi, Rodolfo Milito, Jiang Zhu, and Sateesh Addepalli. Fog computing and its role in the internet of things. In *Proceedings of the first edition of the MCC workshop on Mobile cloud computing*, pages 13–16. ACM, 2012.

[5] Yunfei Chen and Hee-Seok Oh. A survey of measurement-based spectrum occupancy modeling for cognitive radios. *IEEE Communications Surveys & Tutorials*, 18(1):848–859, 2014.

[6] Visual Networking Index Cisco. Global mobile data traffic forecast update, 2016–2021. *White Paper*, 2017.

[7] Youngjune Gwon and HT Kung. Scaling network-based spectrum analyzer with constant communication cost. In *Proceedings of IEEE INFOCOM*, pages 737–745, 2013.

[8] Bassem Khalfi, Bechir Hamdaoui, Mohsen Guizani, and Nizar Zorba. Exploiting wideband spectrum occupancy heterogeneity for weighted compressive spectrum

sensing. In *Computer Communications Workshops (INFOCOM WKSHPS), IEEE Conference on*, pages 1–6, 2017.

[9] MA Mehaseb, Y Gadallah, A Elhamy, and H Elhennawy. Classification of LTE uplink scheduling techniques: An M2M perspective. *IEEE Communications Surveys & Tutorials*, 18(2):1310–1335, 2016.

[10] Afif Osseiran, Jose F Monserrat, and Patrick Marsch. *5G Mobile and Wireless Communications Technology*. Cambridge University Press, 2016.

[11] Maria Rita Palattella, Mischa Dohler, Alfredo Grieco, Gianluca Rizzo, Johan Torsner, Thomas Engel, and Latif Ladid. Internet of things in the 5g era: Enablers, architecture, and business models. *IEEE Journal on Selected Areas in Communications*, 34(3):510–527, 2016.

[12] Zhijin Qin, Yue Gao, Mark D Plumbley, and Clive G Parini. Wideband spectrum sensing on real-time signals at sub-Nyquist sampling rates in single and cooperative multiple nodes. *IEEE Trans. on Signal Processing*, 64(12):3106–3117, 2015.

[13] Jin Wang, Shaojie Tang, Baocai Yin, and Xiang-Yang Li. Data gathering in wireless sensor networks through intelligent compressive sensing. In *Proceedings of IEEE INFOCOM*, pages 603–611, 2012.

[14] Yue Wang, Zhi Tian, and Chunyan Feng. Sparsity order estimation and its application in compressive spectrum sensing for cognitive radios. *IEEE Trans. on wireless communications*, 11(6):2116–2125, 2012.

[15] Mümtaz Yılmaz, Damla Gürkan Kuntalp, and Akan Fidan. Determination of spectrum utilization profiles for 30 MHz–3 GHz frequency band. In *Proc. of IEEE International Conference on Communications (COMM)*, pages 499–502, 2016.

Efficient Spectrum Availability Information Recovery for Wideband DSA Networks: A Weighted Compressive Sampling Approach

Bassem Khalfi, Bechir Hamdaoui, Mohsen Guizani, and Nizar Zorba

Chapter 3: Manuscript 2: Efficient Spectrum Availability Information Recovery for Wideband DSA Networks: A Weighted Compressive Sampling Approach

Bassem Khalfi, Student Member, IEEE, Bechir Hamdaoui, Senior Member, IEEE, Mohsen Guizani, Fellow Member, IEEE, and Nizar Zorba, Member, IEEE

Abstract

There have recently been research efforts that leverage compressive sampling to enable wideband spectrum sensing recovery at sub-Nyquist rates. These efforts consider homogenous wideband spectrum, where all bands are assumed to have similar PU traffic characteristics. In practice, however, wideband spectrum is not homogeneous, in that different bands could present different occupancy patterns. In fact, applications of similar types are often assigned spectrum bands within the same block, dictating that wideband spectrum is indeed heterogeneous. In this paper, we consider heterogeneous wideband spectrum and exploit its inherent, block-like structure to design efficient compressive spectrum sensing techniques that are well suited for heterogeneous wideband spectrum. We propose a weighted ℓ_1-minimization sensing information recovery algorithm that achieves more stable recovery than that achieved by existing approaches while accounting for the variations of spectrum occupancy across both the time and frequency dimensions. In addition, we show that our proposed algorithm requires a smaller number of sensing measurements when compared to the state-of-the-art approaches.

Index terms— Wideband spectrum sensing; compressive sampling; heterogeneous wideband spectrum occupancy.

3.1 Introduction

Spectrum sensing is a key component of cognitive radio networks (CRNs), essential for enabling dynamic and opportunistic spectrum access [4, 16]. It essentially allows secondary users (SUs) to know whether and when a licensed band is available prior to using it so as to avoid harming primary users (PUs). Due to its vital role, over the last

decade or so, a tremendous amount of research has focused on developing techniques and approaches that enable efficient spectrum sensing [31]. Most of the focus has, however, been on single-band spectrum sensing, and the focus on wideband spectrum sensing has recently received increased attention [40, 37, 32, 27].

The key advantage of wideband spectrum sensing over its single-band counterpart is that it allows SUs to locate spectrum opportunities in wider frequency ranges by performing sensing across multiple bands simultaneously. Being able to perform wideband spectrum sensing is becoming a crucial requirement of next-generation CRNs, especially with the emergence of IoT [5] and 5G [14]. This requirement is becoming even more stringent with FCC's new rules for opening up mmWave bands for wireless broadband devices in frequencies above 24 GHz [1]. The challenge, however, with wideband sensing lies in its high sampling rate requirement, which can incur significant sensing overhead in terms of energy, computation, and communication. Motivated by the sparsity feature inherent in spectrum occupancy [9] and in an effort to address the high sampling rate limitation, researchers have exploited compressive sampling to make wideband spectrum sensing possible at sub-Nyquist sampling rates (e.g. [37, 32, 27, 28, 33, 35]).

These research efforts have focused mainly on *homogenous* wideband spectrum, meaning that the entire wideband spectrum is considered as one single block with multiple bands, and the sparsity level is estimated across all bands and considered to be the same for the entire wideband spectrum. However, in spectrum assignment, applications of similar types (TV, satellite, cellular, etc.) are often assigned bands within the same band block, and different application types exhibit different traffic occupancy patterns and behaviors. This suggests that wideband spectrum is block-like *heterogeneous*, in that band occupancy patterns are not the same across the different band blocks. Therefore, sparsity levels may vary significantly from one block to another. This trend that has also been confirmed by recent measurement studies [9, 49]. With this being said, in this paper, we leverage *compressive sampling theory* [6] to exploit this *spectrum occupancy heterogeneity* to design efficient *wideband spectrum sensing* techniques.

3.1.1   Related Work

There has recently been a growing interest in using compressive sampling theory [6] to enable wideband spectrum sensing [42, 43, 32, 27, 35, 28, 45, 33, 38, 20, 39]. A

common factor among these works is that the sparsity level is assumed to be fixed over time. In an effort to relax this assumption, [47] proposes a two-step algorithm, where at each sensing period, the sparsity level is first measured and then used to determine the total number of measurements. The issue, however, with this approach lies in its computational complexity. To overcome this issue, other efforts have been devoted to developing methods that leverage existing concepts like asymptotic random matrix [38] and stretching [25] theories to estimate these sparsity levels from measurements. There have also been some other efforts [20] that mitigate this realtime change in sparsity levels by proposing approaches that do not require knowledge of these sparsity levels on an instant by instant basis. Such approaches, however, still assume that the sparsity level is bounded and that PU's signal is wide-sense stationary which is not usually guaranteed in practice.

Other efforts also aimed to exploit additional knowledge about the signal to further improve the sensing information recovery [46, 13, 29, 48, 8, 21, 3]. For instance, the authors in [46] propose a ℓ_1-minimization-based recovery approach that exploits knowledge about the support[1] of the sparse signal. The authors in [13] also exploit signal support information, but for recovering signals with noisy measurements. Their technique is shown to be more stable and robust than standard ℓ_1-minimization approaches when 50% of the support is estimated correctly. This approach has been generalized for multiple weights in [29], addressing the case where the support is estimated with different confidence levels. These approaches, however, work well in applications where the support does not change much over time, like in real-time dynamic MRI [46] and video/audio decoding [13, 29] applications. In the wideband spectrum sensing case where the signal support changes over time, an estimate of the support is too difficult to acquire in advance, making these approaches unsuitable. There have also been attempts that exploit block sparsity information in signals to further improve signal recovery [21, 3]. These attempts, however, were not in the context of wideband spectrum sensing.

Unlike these previous works and as motivated by the block-like wideband spectrum sparsity structure, our proposed framework considers time-varying and heterogeneous wideband spectrum occupancy. We exploit this fine-grained sparsity structure to propose, which to the best of our knowledge, the first spectrum sensing information recovery scheme for *heterogeneous* wideband spectrum sensing with *noisy* measurements. We want

---

[1]The support corresponds to the signal components that are non-zero.

to emphasize that the use of spectrum recovery methods as the approach for locating spectrum vacancies has benefits over the use of detection methods (e.g., [10, 23]). They, for instance, allow us to determine not only whether there is a signal or not in the wideband, but also which band(s) this signal is occupying. Also, they help to identify the type of signals/devices operating in such bands, a capability of great importance to dynamic spectrum sharing [19]. This work focuses on spectrum recovery methods.

3.1.2 Our Key Contributions

- We develop an algorithm that exploits *spectrum occupancy heterogeneity* inherent in wideband spectrum access to provide an efficient spectrum sensing information recovery.

- We prove that our recovery algorithm is more stable and robust than existing approaches, and reduces sensing overhead by requiring small numbers of measurements.

- We derive lower bounds on the probability of spectrum occupancy and use them to determine the sparsity levels that lead to further reduction in the sensing overhead.

It is important to mention that our proposed weighted compressive sampling framework, including the derived theoretical results, is not restricted to wideband spectrum sensing applications. It can be applied to any other application where the signal to be recovered possesses block-like sparsity structure. This includes applications such as sparse target counting and localization [24] and medical imaging and DNA microarrays [21], to name a few. We are therefore hoping that this work can be found useful for solving problems in other disciplines and domains.

The remainder of the paper is structured as follows. In Section 3.2, we present our system model and the PU bands' occupancy model. Next, our proposed approach along with its performance analysis are presented in Section 3.3. The numerical evaluations are then presented in Section 3.4. Finally, our conclusions are given in Section 3.5.

3.2   Wideband Spectrum Sensing Model

In this section, we begin by presenting the studied heterogeneous wideband spectrum model. Then, we present the spectrum sensing preliminaries and setup.

3.2.1   Wideband Occupancy Model

We consider a heterogeneous wideband spectrum access system containing n frequency bands as illustrated by Fig. 3.1(a). We assume that wideband spectrum accommodates multiple different types of user applications, where applications of the same type are allocated frequency bands within the same block. Therefore, we consider that wideband spectrum has a block-like occupation structure, where each block (accommodating applications of similar type) has different occupancy behavioral characteristics. The wideband spectrum can then be grouped into g disjoint contiguous blocks, $\mathcal{G}_i, i = 1, ..., g$, with $\mathcal{G}_i \bigcap \mathcal{G}_j = \emptyset$ for $i \neq j$. Each block, $\mathcal{G}_i$, is a set of n_i contiguous bands. Like previous works [41], the state of each band i, $\mathcal{H}_i$, is modeled as $\mathcal{H}_i \sim$ Bernoulli(p_i) with parameter $p_i \in [0, 1]$ (p_i is the probability that band i is occupied by a PU). Assuming that the bands' occupancies within a block are independent of one another, then the average number of occupied bands is $\bar{k}_j \sum_{i \in \mathcal{G}_j} p_i$ for $j = 1, ..., g$.

Recall that one of the things that distinguish this work from others is the fact that we consider a *heterogeneous* wideband spectrum; formally, this means that the average number $\bar{k}_j$ of the occupied bands in block j can vary significantly from one block to another. The average occupancies, however, of the different bands within a given block are close to one another; i.e., $p_i \approx p_j$ for all $i, j \in \mathcal{G}_j$. Our proposed framework exploits such a block-like occupancy structure stemming from the wideband spectrum heterogeneity to design efficient compressive wideband spectrum sensing techniques. For this, we assume that the blocks have sufficient different average sparsity levels (otherwise, blocks with similar sparsity levels are merged into one block with a sparsity level corresponding to their average). This is supported by practical observations where typically each block of bands is assigned to a particular application, and the average occupancy could be quite different from one block to another [49, 26, 18]. These averages are often available via measurement studies, and can easily be estimated, or provided by spectrum operators [26].
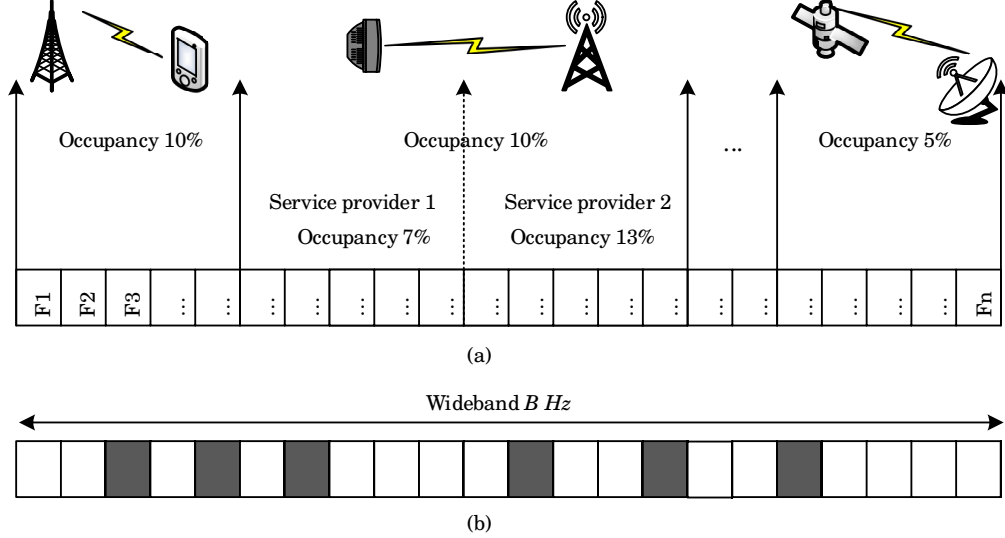
Figure 3.1: n bands occupied by heterogeneous applications with different occupancy rates. Grey bands are occupied by PUs and white bands are vacant. (a) is the statistical allocation; (b) is a realization of allocation in a given region at a given time slot.

3.2.2 Secondary System Model

We consider a SU performing the sensing of the entire wideband spectrum as illustrated by Fig. 3.2. The time-domain signal $\boldsymbol{r}(t)$ received by the SU can be expressed as

$$r(t) = h(t) \otimes s(t) + w(t) = \sum_{i=1}^{n_{sig}} h_i(t) \otimes s_i(t) + w(t), \qquad (3.1)$$

where $h_i(t)$ is the channel impulse between the primary transmitters and SU_i, $s(t)$ is the PUs' signal, $w(t)$ is an additive white Gaussian noise with mean 0 and variance σ^2, $\otimes$ is the convolution operator, and n_{sig} is the number of active PUs. Ideally, we should take samples with at least twice the maximum frequency, $f_{\max}$, of the signal to recover the signal successfully. Let the sensing window be $[0, mT_0]$ with $T_0 = 1/(2f_{\max})$. Assuming a normalized number of Nyquist samples per band, the vector of the taken samples is $\boldsymbol{r} = [r(0), ..., r((m_0 - 1)T_0)]^T$ where $r(i) = r(t)|_{t=iT_0}$, $i = 0, 1, \ldots, (m_0 - 1)T_0$, and $m_0 = n$. The sensing window length is (reasonably) assumed to be sufficiently small when compared to the time it takes a band state to change, so that each band's
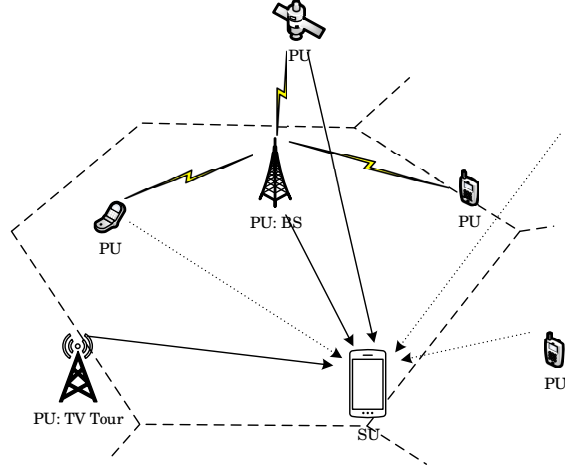
Figure 3.2: A *SU* performing wideband spectrum sensing. Received signals are coming from *PU*s with different energy levels.

occupancy remains constant during each sensing window.

We perform a discrete Fourier transform of the received signal $\boldsymbol{r}(t)$; i.e.,

$$\boldsymbol{r}_f = \boldsymbol{h}_f \boldsymbol{s}_f + \boldsymbol{w}_f = \boldsymbol{x} + \boldsymbol{w}_f, \tag{3.2}$$

where $\boldsymbol{h}_f$, $\boldsymbol{s}_f$, and $\boldsymbol{w}_f$ are the Fourier transforms of $\boldsymbol{h}(t)$, $\boldsymbol{s}(t)$, and $\boldsymbol{w}(t)$, respectively. The vector $\boldsymbol{x}$ contains a faded version of the PUs' signals operating in the different bands. Given the occupancy of the bands by their *PU*s (as illustrated in Fig. 3.1(b)) and in the absence of interference, the vector $\boldsymbol{x}$ can be considered *sparse*, where a vector $\boldsymbol{x} \in \mathbb{R}^n$ is *k-sparse* if it has (with or without a basis change) at most k non-zero elements [11]; i.e., $supp(\boldsymbol{x}) = \|\boldsymbol{x}\|_{\ell_0} = |\{i : x_i \neq 0\}| \leq k$. The set of $k-$sparse vectors in $\mathbb{R}^n$ are denoted by $\Sigma_k = \{\boldsymbol{x} \in \mathbb{R}^n : \|\boldsymbol{x}\|_{\ell_0} \leq k\}$.

In practice, however, there will likely be interference coming from other nearby cells and users, and hence, $\boldsymbol{x}$ could rather be *nearly sparse*, where a vector $\boldsymbol{x} \in \mathbb{R}^n$ is *nearly sparse* (or also compressible [11]) if most of its components obey a fast power law decay. The $k-$sparsity index of $\boldsymbol{x}$ is then defined as $\sigma_k(\boldsymbol{x}, \|.\|_{\ell_p}) = \min_{\boldsymbol{z} \in \Sigma_k} \|\boldsymbol{x} - \boldsymbol{z}\|_{\ell_p}$.

Since wideband spectrum is large, the number of required samples can be huge, making the sensing operation prohibitively costly and the needed hardware capabilities beyond possible. To overcome this issue, compressive sampling theory has been leveraged

to reduce the number of needed measurements, as the wideband spectrum occupancy vector is sparse or nearly sparse. After performing the compressive sampling, the resulted signal can be written as

$$\boldsymbol{y} \;\; = \;\; \Psi\mathcal{F}^{-1}(\boldsymbol{x} + \boldsymbol{w}_f) = \mathcal{A}\boldsymbol{x} + \boldsymbol{\eta}, \tag{3.3}$$

where $\boldsymbol{y} \in \mathbb{R}^m$ is the measurement vector, $\mathcal{F}^{-1}$ is the inverse discrete Fourier transform since $\boldsymbol{x}$ is sparse in the Fourier basis, and Ψ is the sensing matrix assumed to have a full rank, i.e. $rank(\Psi) = m$. Throughout the paper, we consider a uniform sampling where all the coefficients of Ψ are drawn from the same distribution. Note that while spectrum occupancy heterogeneity in this work is exploited in the recovery, it can also be exploited to design an efficient non-uniform sampling. The sensing noise $\boldsymbol{\eta}$ is equal to $\Psi\mathcal{F}^{-1}\boldsymbol{w}_f$.

It is worth mentioning that without resorting to compressive sampling theory, wideband spectrum sensing requires wideband antennas and Nyquist-rate analog-to-digital converters (ADC), which are very challenging to build [51, 17, 2, 2, 22]. Compressive sampling overcomes this by allowing sub-Nyquist-rate sampling as illustrated by Fig. 3.3, where the signal is first amplified by m amplifiers and mixed with a pseudo-random waveform at a Nyquist rate ($f_s = 2f_{\max}$). Then, an integrator is applied followed by an ADC sampling at a sub-Nyquist rate (f_s/n). The implementation aspects of the proposed compressive sensing approach are beyond the scope of this paper.

Different from classical wideband compressive sensing, this paper takes advantage of the wideband occupancy heterogeneity to design efficient spectrum occupancy recovery approaches. Specifically, we show that exploiting band occupancy variability across the different blocks indeed improves the recovery accuracy, and thus, the ability to locate spectrum availability.

3.3 The Proposed Wideband Spectrum Sensing Information Recovery

The sensing matrix and recovery algorithm are the main challenging components in compressive sampling design. While the former consists of minimizing the number of measurements, the latter consists of ensuring a stable and robust recovery. In this
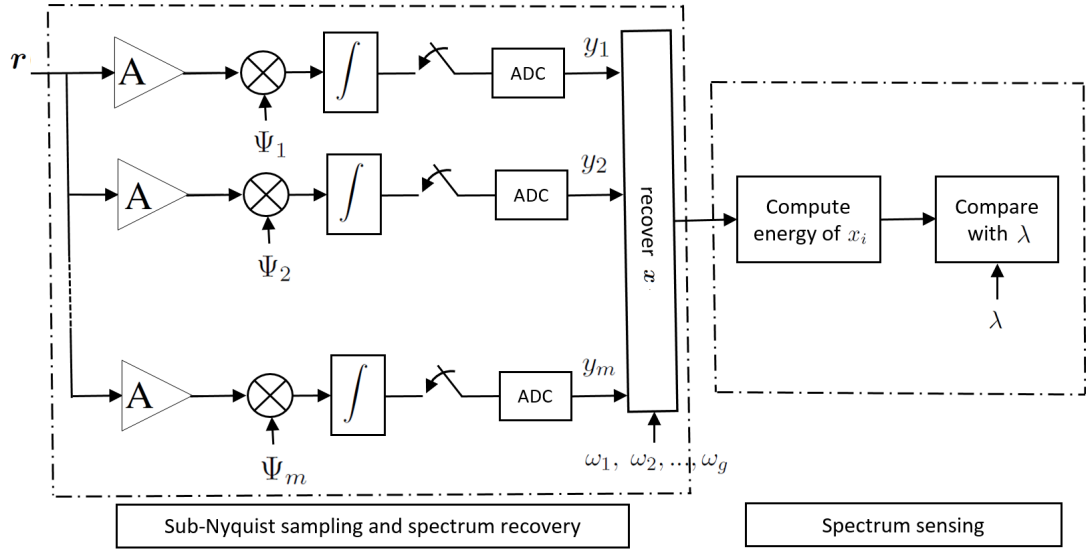
Figure 3.3: Illustration of an SU receiver architecture.

work, our proposed recovery algorithm outperforms existing approaches by 1) requiring smaller numbers of measurements (better sensing matrix) and by 2) reducing the recovery error (more stable and robust recovery). In this section, we start by providing some background on signal recovery using classical compressive sampling. Then, we present our proposed approach and analyze its performance by bounding its achievable mean square errors and its required number of measurements.

3.3.1 Background

The spectrum recovery task can be very computationally costly, a fact that motivated the use of direct signal processing approaches, such as detection [10, 23]. While these approaches succeed in identifying the presence of signals in the wideband spectrum, they fail to locate which portions/bands of the spectrum are occupied/unoccupied. In addition, being able to identify which signal types are occupying the bands is important and can be very useful for DSA applications (e.g., spectrum access policy enforcement) [19]. Such objectives can, however, be achieved via spectrum recovery approaches, which can indicate not only whether there is a signal in the wideband or not, but also which bands

are occupied and which signal types are occupying them.

In wideband spectrum recovery approaches, an SU's aim is to recover the frequency-domain version of the received signal. Exploiting the fact that the signal is sparse, an ideal recovery can be performed by minimizing the ℓ_0-norm of the signal. This is, however, NP-hard [7]. It turns out that minimizing the ℓ_1-norm recovers the sparsest solution with a bounded error that depends on the noise variance and the solution structure [6]. This can be formulated as

$$\mathscr{P}_1 : \underset{x}{\text{minimize}} \quad \|\boldsymbol{x}\|_{\ell_1}$$
$$\text{subject to} \quad \|\mathcal{A}\boldsymbol{x} - \boldsymbol{y}\|_{\ell_2} \leq \epsilon \tag{3.4}$$

Here, ϵ is a user-defined parameter chosen such that $\|\boldsymbol{\eta}\|_{\ell_2} \leq \epsilon$. This formulation is known also as Least Absolute Shrinkage and Selection Operator (LASSO) [6].

Although LASSO is shown to achieve good performance when applied for wideband spectrum sensing recovery, it does not capture, nor exploit the block-like occupancy structure information that is inherent to the wideband spectrum, where the occupancy is heterogeneous across the different blocks of the spectrum. As shown later, it is the exploitation of this block-like occupancy structure that is behind the performance again achieved by our proposed recovery algorithm.

3.3.2   The Proposed Recovery Algorithm

Intuitively, our key idea is to incorporate and exploit the variability of sparsity levels across the different spectrum blocks to perform intelligent solution search. We essentially encourage more search of the non-zero elements of the signal $\boldsymbol{x}$ in the blocks that have higher average sparsity levels. Such a variability in the block sparsity levels can be incorporated in the formulation through carefully designed weights. More specifically, we propose the following weighted ℓ_1-minimization recovery scheme:

$$\mathscr{P}_1^{\omega} : \quad \underset{\boldsymbol{x}}{\text{minimize}} \quad \sum_{l=1}^{g} \omega_l \|\boldsymbol{x}_l\|_{\ell_1}$$
$$\text{subject to} \quad \|\mathcal{A}\boldsymbol{x} - \boldsymbol{y}\|_{\ell_2} \leq \epsilon. \tag{3.5}$$

where $\boldsymbol{x} = [\boldsymbol{x}_1^T, ..., \boldsymbol{x}_g^T]^T$, $\boldsymbol{x}_l^T$ is a $n_l \times 1$ vector, and ω_l is the weight assigned to block l for $l \in \{1, ..., g\}$. The question that arises here now is how to design and select these weights. Intuitively, the higher the average sparsity level of a block, the greater the number of occupied bands within that block. This means that if we consider two blocks with two different average sparsity levels, say $\bar{k}_1$ and $\bar{k}_2$, such that $\bar{k}_1 < \bar{k}_2$, then to encourage the search for more occupied bands in the second block, the weight ω_2 assigned to the second block should be smaller than the weight ω_1 assigned to the first block. Following this intuition, we set the weights to be inversely proportional to the average sparsity levels. More specifically,

$$\omega_i = \frac{1/\bar{k}_i}{\sum_{j=1}^{g} 1/\bar{k}_j} \quad \forall\, i \in \{1, ..., g\} \tag{3.6}$$

Remark 1. *Some insights into the proposed scheme*

Consider a two-block spectrum with $\bar{k}_1 > \bar{k}_2$, and hence, with $\omega_2 > \omega_1$. For this special case, the recovery algorithm can then be re-written as

$$\mathscr{P}_1^{\omega,2}: \quad \begin{aligned} \underset{x}{\text{minimize}} \quad & \|\boldsymbol{x}\|_{\ell_1} + (\frac{\omega_2}{\omega_1} - 1)\|\boldsymbol{x}_2\|_{\ell_1} \\ \text{subject to} \quad & \|\mathcal{A}\boldsymbol{x} - \boldsymbol{y}\|_{\ell_2} \leq \epsilon. \end{aligned} \tag{3.7}$$

Since we are minimizing the ℓ_1-norm of $\boldsymbol{x}$ and the ℓ_1-norm of $\boldsymbol{x}_2$, this can be interpreted as ensuring that the vector $\boldsymbol{x}$ is sparse while ensuring that the portion $\boldsymbol{x}_2$ of $\boldsymbol{x}$ is also sparse (since $\frac{\omega_2}{\omega_1} - 1 > 0$). This means that all solutions that are sparse as a whole but somehow dense in their second portion are eliminated.

Remark 2. *Weights design*

The proposed scheme exploits the per-block average occupancy to improve recovery accuracy. From a practical viewpoint, the per-block average occupancy can be acquired by monitoring the occupancy of each band within the block and averaging them over time [49, 26]. It can also be acquired through prediction approaches, which can provide good estimates. That is said, even when the average occupancy is not determined on a per-block basis; i.e., the entire wideband spectrum is considered as one block, our proposed algorithm becomes equivalent to the classical ℓ_1-minimization approach (LASSO) (i.e., $\mathscr{P}_1$). In other words, our algorithm performs similarly to LASSO when average block occupancies are unavailable and outperforms it otherwise.

In the remaining of this section, we show that our proposed recovery algorithm out-

performs existing approaches by 1) incurring smaller errors and 2) requiring lesser measurements.

3.3.3 Mean Square Error Analysis

The following theorem shows that our algorithm incurs lesser errors than LASSO [6].

Theorem 1. *Letting $\boldsymbol{x}^{\sharp}$ be the optimal solution for $\mathscr{P}_1^{\omega}$, $\boldsymbol{x}^{\dagger}$ the optimal solution for $\mathscr{P}_1$ and $\boldsymbol{y} = \mathcal{A}\boldsymbol{x}_0 + \boldsymbol{\eta}$, we have*

$$\|\boldsymbol{x}^{\sharp} - \boldsymbol{x}_0\|_{\ell_2} \leq \|\boldsymbol{x}^{\dagger} - \boldsymbol{x}_0\|_{\ell_2}.$$

with a probability exceeding

$$1 \quad - \sum_{i=1}^{g-1} \sum_{j=i+1}^{g} \sum_{k=1}^{\min(n_i, n_j)} \sum_{l=0}^{k-1} \binom{n_i}{l} q_i^l (1 - q_i)^{n_i - l}$$
$$\binom{n_j}{k} q_j^k (1 - q_j)^{n_j - k} \tag{3.8}$$

assuming $n_1 q_1 \geq ... \geq n_g q_g$.

Proof. The proof is provided in Appendix 3.6.1. ∎

The theorem says that the solution to the proposed $\mathscr{P}_1^{\omega}$ is at least as good as the solution to $\mathscr{P}_1$ (i.e., LASSO [6]). Also as done by design, the more heterogeneous the wideband spectrum is, the higher the error gap between our proposed algorithm and LASSO is.

Now, we assess the stability and robustness of the proposed scheme.

Definition 1. *Stable and Robust Recovery [6]*
For $\boldsymbol{y} = \mathcal{A}\boldsymbol{x} + \boldsymbol{w}$ such that $\|\boldsymbol{w}\|_{\ell_2} \leq \epsilon$, a recovery algorithm, Δ, and a sensing matrix, $\mathcal{A}$, are said to achieve a stable and robust recovery if there exist C_0 and C_1 such that

$$\|\Delta \boldsymbol{y} - \boldsymbol{x}\|_{\ell_2} \leq C_0 \epsilon + C_1 \frac{\sigma_k(\boldsymbol{x}, \|.\|_{\ell_p})}{\sqrt{k}}. \tag{3.9}$$

Note that the stability implies that small perturbations of the observation lead to a small perturbation of the recovered signal. Robustness, on the other hand, is relative to noise; for instance, if the measurement vector is corrupted by noise with a bounded energy, then the error is also bounded [6]. We now state the following result, which follows directly from Theorem 1.

Proposition 2. *Our proposed algorithm, $\mathscr{P}_1^\omega$, achieves a stable and robust recovery.*

Proof. The proof is provided in Appendix 3.6.2. ∎

The proposition gives a bound on the error by means of two quantities. The first is an error of the order of the noise variance while the second is of the order of the sparsity index of $\boldsymbol{x}$.

Remark 3. Effect of time-variability

We want to iterate that our proposed algorithm is guaranteed to outperform existing approaches on the average, and not on a per-sensing step basis. This is because although the performance improvement achieved by our technique stems from the fact that blocks with higher average sparsity levels are given lower weights—which is true on the average, it is not unlikely that, at some sensing step, the actual sparsity level of a block with a higher average could be smaller than that of a block with a lower average. When this happens, our algorithm won't be guaranteed to achieve the best performance during that specific sensing step. The good news is that first what matters is the average over longer periods of sensing time, and second, depending on the gap between the block sparsity averages, this scenario happens with very low probability.

To illustrate, let us assume that the wideband spectrum contains two blocks with average sparsity $\bar{k}_1 = \sum_{j \in \mathcal{G}_1} p_j \approx n_1 p_1$ and $\bar{k}_2 = \sum_{j \in \mathcal{G}_2} p_j \approx n_2 p_2$ with $\bar{k}_2 < \bar{k}_1$, where again $|\mathcal{G}_1| = n_1$ and $|\mathcal{G}_2| = n_2$. Here, the occupancy probabilities of all bands in each of these two blocks are assumed to be close to one another. Our approach encourages to find more occupied bands in the first block than in the second block. However, since band occupancy is time varying, then at some given time we may have a lesser number of non-zero components in the first block than in the second. This unlikely event, in this scenario, happens with probability

$$\sum_{k=1}^{\min(n_1,n_2)} \sum_{l=0}^{k-1} \binom{n_1}{l} q_1^l (1-q_1)^{n_1-l} \binom{n_2}{k} q_2^k (1-q_2)^{n_2-k}$$

For a sufficiently different average sparsity levels (e.g. having $\bar{k}_1 > 2\bar{k}_2$), this probability is smaller than 0.02. Finally, it is worth mentioning that our proposed scheme can achieve further performance improvement by adopting advanced estimation approaches, such as those that are based on machine learning [47]. However, this additional performance improvement comes at the price of additional computational complexity that is accompanied with these estimators.

Having investigated the design of the recovery algorithm, now we turn our attention to the design of the sensing matrix. The number of measurements, m, to be taken determines the size of the sensing matrix and hence the sensing overhead of the recovery approach. Therefore, we aim to exploit the structure of the solution to reduce the required number of measurements as much as possible, so that the sensing overhead is reduced as much as possible.

3.3.4 Number of Required Measurements

The sensing matrix is usually designed with two major design criteria/goals in mind: reducing the number of measurements and satisfying the RIP property, defined as follows.

Definition 2. *Restricted Isometry Property (RIP)* [11]
A matrix $\mathcal{A}$ is said to satisfy the RIP of order k if there exists $\delta_k \in (0,1)$ such that for $\boldsymbol{x} \in \Sigma_k$

$$(1 - \delta_k)\|\boldsymbol{x}\|_{\ell_2}^2 \leq \|\mathcal{A}\boldsymbol{x}\|_{\ell_2}^2 \leq (1 + \delta_k)\|\boldsymbol{x}\|_{\ell_2}^2. \tag{3.10}$$

Broadly speaking, the RIP ensures that every k columns of $\mathcal{A}$ are nearly orthogonal.

We now present one of our main results derived in this paper, which provides a lower bound on the number of required measurements.

Theorem 3. *Let $\mathcal{A} = [\mathcal{A}_1...\mathcal{A}_g]$ be the sensing matrix such that $\mathcal{A}_i$ satisfies the RIP of order $2\bar{k}_i$ with $\{\delta_{2\bar{k}_1},...,\delta_{2\bar{k}_g}\} \in (0, 1/2]$. Then, the number of measurements m must satisfy*

$$m \geq \frac{1}{2\log\left(\frac{\sum_{i=1}^{g}\sqrt{2\bar{k}_i(1+\delta_{\bar{k}_i})}+\max_i(\sqrt{\bar{k}_i(1-\delta_{\bar{k}_i})/8})}{\min_i(\sqrt{\bar{k}_i(1-\delta_{\bar{k}_i})/8})}\right)}\bar{k}\log\left(\frac{n}{\bar{k}}\right) \tag{3.11}$$

Proof. The proof is provided in Appendix 3.6.3. ∎

Theorem 3 given above provides a lower bound on the required number of measurements needed to recover the signal. As shown later in the result section, this bound is tighter than existing approaches in that with the same number of measurements, our proposed framework can recover signals with better accuracy than those obtained via existing approaches. Alternatively, we can also say that our framework can recover signals with an accuracy equal to those obtained with existing approaches, but while requiring lesser numbers of measurements, m. The derived lower bound exhibits an asymptotic behavior similar to that of the classic bound (i.e., $\mathcal{O}(\bar{k} \log(n/\bar{k}))$), but with a smaller constant. By setting $g = 1$, we get the bound provided in [11, Theorem 1.4]. So our derived bound could be viewed as a generalization of that of [11], in that it applies to wideband spectrum with heterogeneous block occupancies; setting $g = 1$ corresponds to the special case of the homogeneous wideband spectrum.

Existing approaches determine the required number of measurements by setting the sparsity level to the average number of occupied bands (e.g., $m \geq \bar{k} \log(n/\bar{k})$). However, as mentioned earlier, in wideband spectrum sensing, the number of occupied bands changes over time, and can easily exceed the average number. Every time this happens, it leads to an inaccurate signal recovery (it yields a solution with high error). To address this issue, in our proposed framework, we do not base the selection of the number of measurements on the average sparsity. Instead, the sparsity level that we use in Theorem 3 to determine m is chosen in such a way that the likelihood that the number of occupied bands exceeds that number is small. The analysis needed to help us determine such a sparsity level is provided in the next section.

3.3.5 PU Traffic Characterization

Based on the model of occupancy of the wideband provided in the system model, the following lemma gives the probability mass distribution of the number of occupied bands.

Lemma 1. *The number of occupied bands across the entire wideband has the following probability mass function*

$$Pr(X = k) = \sum_{\Lambda \in \mathcal{S}_k} \left[\prod_{i \in \Lambda} p_i \right] \left[\prod_{j \in \Lambda^c} (1 - p_j) \right] \tag{3.12}$$

where $\mathcal{S}_k = \{\Lambda : \Lambda \subseteq \{1, ..., n\}, |\Lambda| = k\}$, and Λ^c is the complementary set of Λ.

Proof. Let Λ the support such that its ith component is equal to one when there is a PU using the ith band. Then, the probability that there is exactly k occupied bands is $\left[\prod_{i \in \Lambda} p_i\right]\left[\prod_{j \in \Lambda^c} (1 - p_j)\right]$ such that $|\Lambda| = k$. Now, considering all the supports with a cardinality k gives the expression of the mass distribution. ∎

Given this distribution, the average number of occupied bands across the entire wideband spectrum is $\bar{p} = \sum_{i=1}^{n} p_i$. In the following theorem, we provide a lower bound on the probability that the number of occupied bands is below an arbitrary sparsity level.

Theorem 4. *The probability that the number of occupied bands is below a sparsity level k_0 is lower-bounded by*

$$
\begin{aligned}
Pr(X \leq k_0) &= \sum_{k=0}^{k_0} \sum_{\Lambda \in \mathcal{S}_k} \left[\prod_{i \in \Lambda} p_i\right]\left[\prod_{j \in \Lambda^c} (1 - p_j)\right] \\
&\geq 1 - \frac{e^{k_0 - \sum_i^n p_i}}{(k_0 / \sum_i^n p_i)^{k_0}}
\end{aligned}
\tag{3.13}
$$

Proof. The proof is provided in Appendix 3.6.4. ∎

Since the sparsity level is a time-varying process, this theorem gives a probabilistic bound on how to choose a sparsity level such that the level will be exceeded only with a certain probability. Now depending on the allowed fraction, α, of instances in which the actual number of occupied bands exceeds the sparsity level, Theorem 4 can be used to determine the sparsity level, k_0, that can be used in Theorem 3 to determine the required number of measurements, m. In other words, α is the probability that the actual number of occupied bands is above the defined sparsity level k_0. If α is set to 5%, then it means that only about 5% of the time the actual number of occupied bands exceeds k_0. As expected, there is a clear tradeoff between α and k_0. Smaller values of α requires higher values of k_0, and vice-versa. In our numerical evaluations given in the next section, α is set to 4%.

3.4   Numerical Evaluation

In this section, we evaluate our proposed wideband spectrum sensing approach and we compare its performance to the state-of-the-art approaches. Consider a primary system operating over a wideband consisting of $n = 256$ bands. We assume that the wideband contains $g = 4$ blocks with equal sizes. The average probabilities of occupancy in each block are as follows: $\bar{k}_1 = 0.1 \times 64$, $\bar{k}_2 = 0.01 \times 64$, $\bar{k}_3 = 0.1 \times 64$, $\bar{k}_4 = 0.01 \times 64$. To model the signals coming from the active users, we generate them in the frequency domain with random magnitudes (which captures the effect of the different channel SNRs that every operating PU has with the SU). At the SU side, the sensing matrix Ψ is generated according to a Bernoulli distribution with zero mean and $1/m$ variance. We opted for a sub-Gaussian distribution since it guarantees the RIP with high probability [11]. Here, the number of measurements is generated first according to $m = \mathcal{O}(k_0 \log(n/k_0))$. We fix k_0 to 25, which ensures that the probability that the actual number of occupied bands is below k_0 exceeds 0.96%, as determined by Theorem 4 and plotted in Fig. 3.4. In the same figure, for completeness, we also show the tightness of the lower bound derived in Theorem 4. Now assuming an RIP constant $\delta_{2k_i} \leq 1/2$ and replacing k_0 and the RIP constant with their values in Theorem 3 yields that the number of measurements should be at least 29. We use CVX for the solving of the optimization problem [15].

A first performance that we look at is the mean square error $\|\boldsymbol{x}^\sharp - \boldsymbol{x}_0\|_{\ell_2}$ as a function of the sensing SNR defined as SNR $= \frac{\|\mathcal{A}\boldsymbol{x}\|_{\ell_2}^2}{\|\boldsymbol{\eta}\|_{\ell_2}^2}$, where $\|\mathcal{A}\boldsymbol{x}\|_{\ell_2}^2 = (\mathcal{A}\boldsymbol{x})^T \mathcal{A}\boldsymbol{x}$ and $\|\boldsymbol{\eta}\|_{\ell_2}^2 = \boldsymbol{\eta}^T \boldsymbol{\eta}$. In Fig. 3.5, we compare our proposed technique to the existing approaches. Compared to LASSO [6], CoSaMP [30], and (OMP) [44], our proposed approach achieves a lesser error when fixing the number of measurement m to 27. This is because we account for the average sparsity levels in each block, thereby favoring the search on the first and third block rather than the two others. Also, observe that as the sensing SNR gets better, not only does the error of the proposed technique decrease, but also the error gap between our technique and that of the other ones increases. This is because the noise effect becomes limited. Furthermore, OMP has the worst performance as it requires a higher number of measurements to perform well. In Fig. 3.6, we look at the performance of the recovery scheme as a function of the average received SNR defined as the ratio between the received signal power and the noise power; i.e., $\|\boldsymbol{x}\|_{\ell_0}^2 / \|\boldsymbol{\eta}\|_{\ell_2}^2$. We observe a similar behavior as in Fig. 3.5.
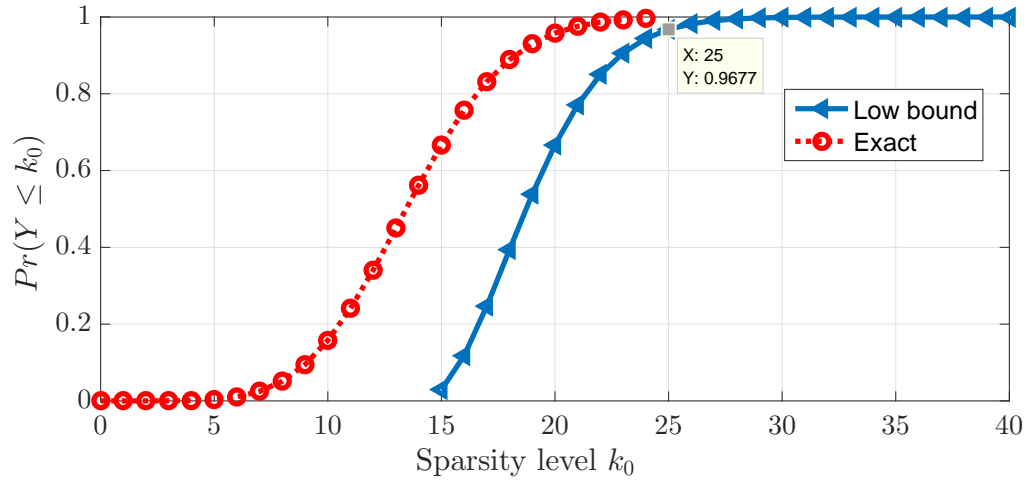
Figure 3.4: Lower bound and exact expression of $\Pr(X < k_0)$ as a function of the sparsity level k_0, as derived in Theorem 4.
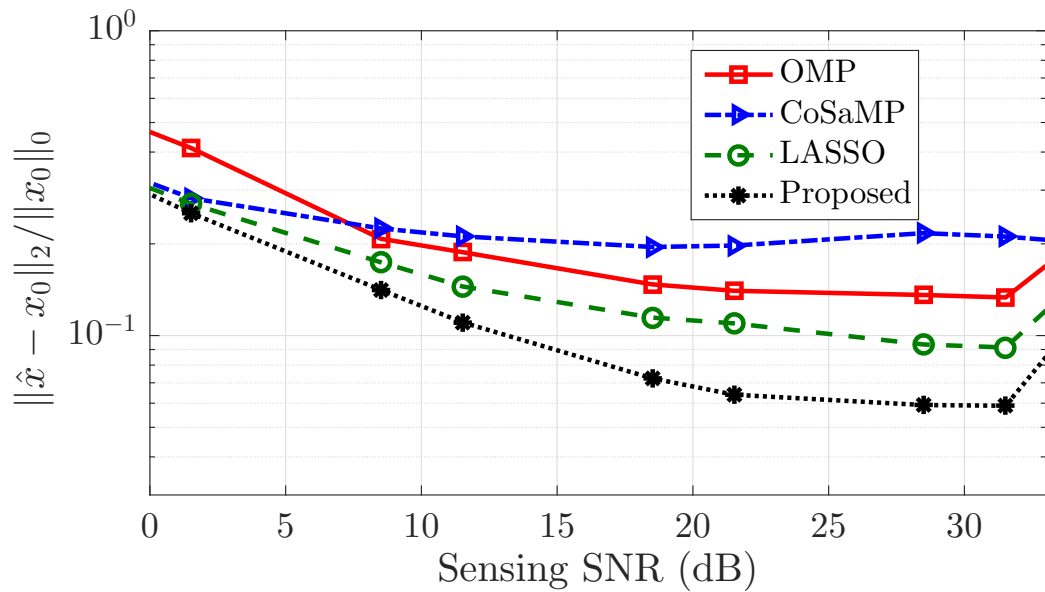
Figure 3.5: Comparison between the recovery approaches in terms of mean square error as a function of the sensing SNR ($m = 27$).
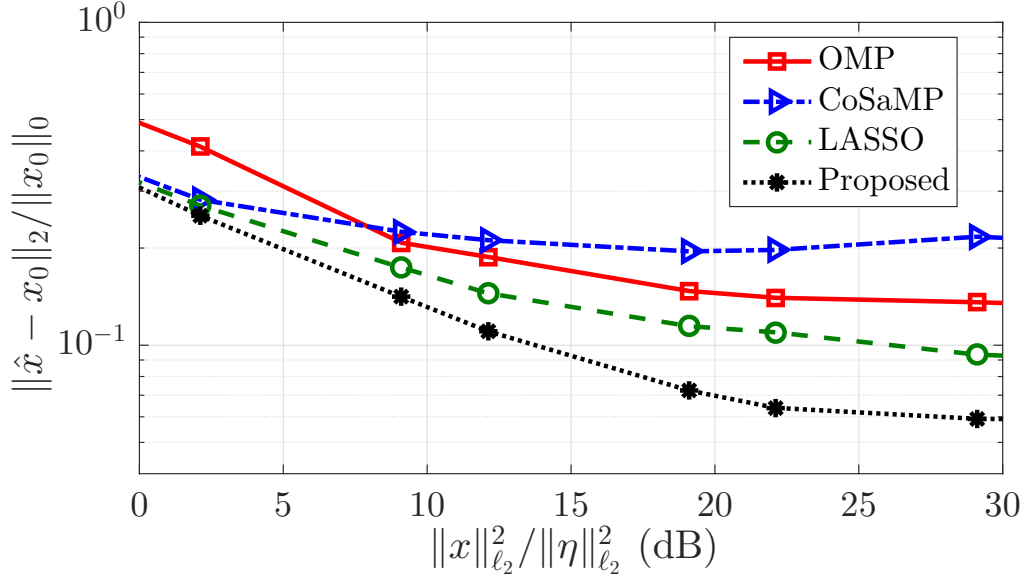
Figure 3.6: Comparison between the recovery approaches in terms of mean square error as a function of received signal SNR ($m = 27$).

In Fig. 3.7, in addition to the random sensing matrix, we show the normalized mean square error of the proposed recovery approach under the Circulant [34] and Toeplitz [36] matrices. Here the elements of the first row of the Circulant matrix and the elements of the first row and first column of the Toeplitz matrix are drawn from a Gaussian distribution with zero mean and $1/m$ variance. The figure shows that random (Bernoulli) matrices outperform Circulant and Toeplitz matrices [50] in terms of achieved errors. This is because Circulant/Toeplitz matrices have lesser incoherent projections than random matrices. In other words, to achieve a robust recovery, the rows of the sensing matrix should have low cross-correlation which is achieved more with a fully random matrix. This superior performance gain comes, however, at the price of a slower recovery compared to Circulant/Toeplitz matrices as shown in the literature [50, 36].

In Fig. 3.8, we investigate the error percentage gain (EPG) achieved by our technique when compared to the other schemes under various different numbers of measurements.
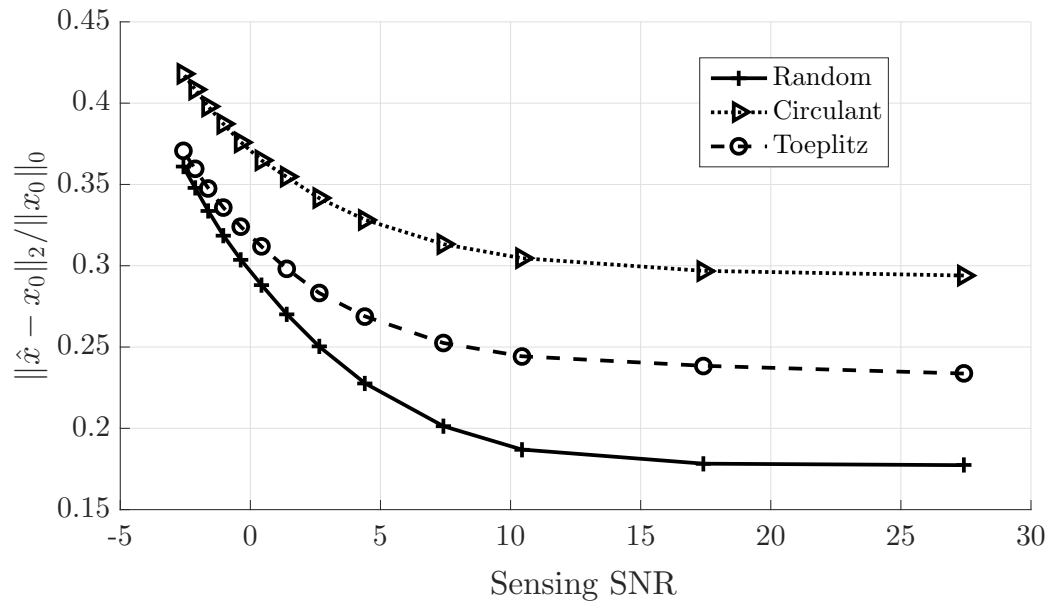
Figure 3.7: The proposed recovery approach in terms of mean square error for different sensing matrices as a function of the sensing SNR ($m = 27$).
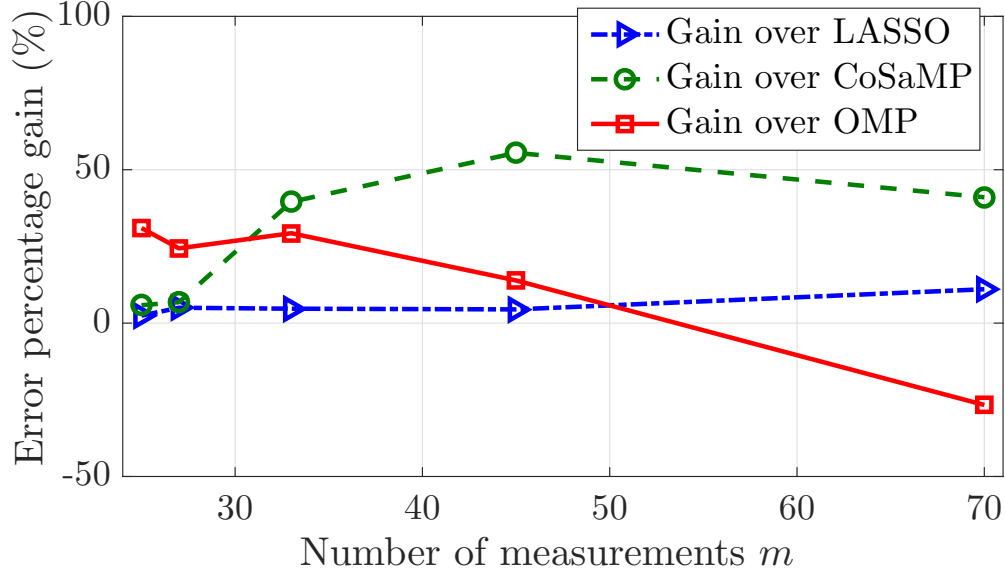
Figure 3.8: Error gain comparison with LASSO [6], CoSaMP [30], and (OMP) [44] for SNR= $20dB$.

We define the error gain of our approach over an existing approach i as

$$\text{EPG}(\%) = \frac{\|\boldsymbol{x}_i^\sharp - \boldsymbol{x}_0\|_{\ell_2} - \|\boldsymbol{x}_{\text{Proposed}}^\sharp - \boldsymbol{x}_0\|_{\ell_2}}{\|\boldsymbol{x}_i^\sharp - \boldsymbol{x}_0\|_{\ell_2}} 100\% \tag{3.14}$$

Observe that when the number of measurements is low, our proposed technique outperforms the other three techniques. But when the number of measurements m is relatively high, our technique still performs better than CoSaMP and LASSO, but worse than OMP. However, OMP achieves this superior performance only under a high number of measurements, a range that is not of interest due to its high incurred overhead.

After recovering the signal and in order to decide on the availability of the different bands, we compare the energy of the recovered signal in every band with the threshold [12], $\lambda = \frac{\mathbb{E}(\|\boldsymbol{\eta}\|_{\ell_2}^2)}{m}\left(1 + \frac{Q^{-1}(P_f)}{\sqrt{1/2}}\right)$, where P_f is a user-defined threshold for the false alarm probability. It is defined as the probability that a vacant band is detected as
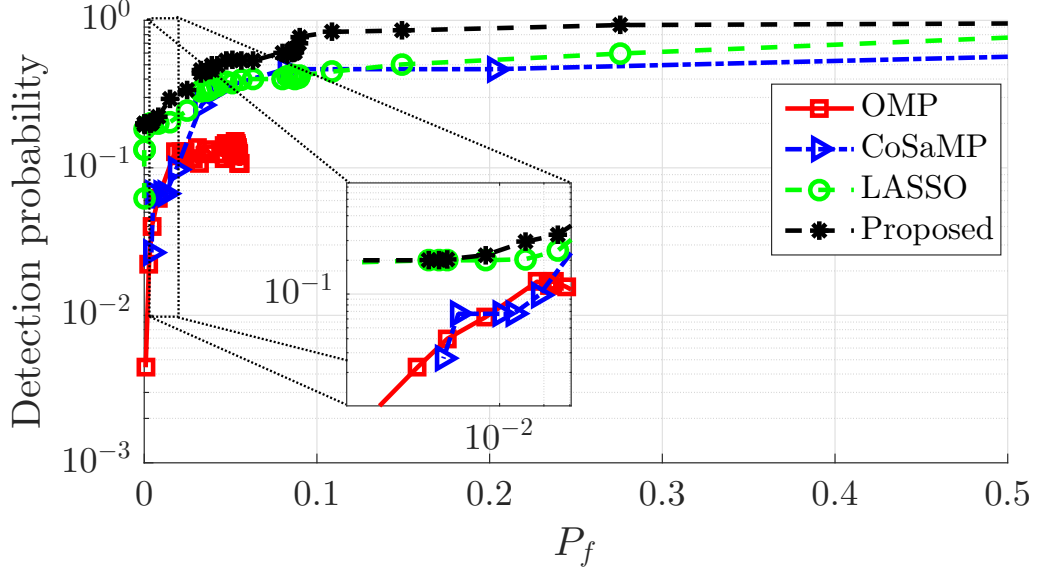
Figure 3.9: Probability of detection as a function of the probability of false alarm with number of measurements $m = 27$ and sensing SNR= 33 dB.

occupied, and is expressed as

$$P_f = \frac{1}{\sum_{i=1}^{n} (1 - H_i)} \sum_{i=1}^{n} Pr(|x_i|^2 \geq \lambda | \mathcal{H}_i = 0). \tag{3.15}$$

Q^{-1} is the inverse of the $Q-$function. In Fig. 3.9, we plot this detection probability as a function of the false probability for a fixed average sensing SNR, where the detection probability is computed as

$$P_d = \frac{1}{\sum_{i=1}^{n} \mathcal{H}_i} \sum_{i=1}^{n} Pr(|x_i|^2 \geq \lambda | \mathcal{H}_i = 1) \tag{3.16}$$

Although the number of measurements is less than what is required, our proposed technique has the best detection capability among all other approaches. This also confirms the result of Fig. 3.8.

3.5   Conclusion

We proposed an efficient wideband spectrum sensing technique based on compressive sampling. Our proposed technique is a weighted ℓ_1-minimization recovery approach that accounts for the block-like structure inherent to the heterogeneous nature of wideband spectrum allocation. We showed that the proposed approach outperforms existing approaches by achieving lower mean square errors, enabling higher detection probability, and requiring lesser numbers of measurements when compared to the-state-of-the-art approaches.

3.6   Appendix

3.6.1   Proof of Theorem 1

Let us consider the average sparsity level in every block to be $\bar{k}_i = p_i.n_i$ and define the weights as $\omega_i = \frac{1}{\bar{k}_i}$ (and then we normalize it, as in Equation (3.6), as $\omega_i = \omega_i / \sum_{j=1}^{n} \omega_j$). Without loss of generality, we assume that $\omega_1 \leq \omega_2 \leq ... \leq \omega_g$. First, let us assume to have only knowledge of $\bar{k}_1$ to have the highest sparsity level in all the blocks. Then, we can consider the recovery problem as

$$\mathscr{P}_1^{\omega_1,1} : \underset{x}{\text{minimize}} \quad \omega_1 \|\boldsymbol{x}_1\|_{\ell_1} + \sum_{l=2}^{g} \|\boldsymbol{x}_l\|_{\ell_1}$$

$$\text{subject to} \qquad \|\mathcal{A}\boldsymbol{x} - \boldsymbol{y}\|_{\ell_2} \leq \epsilon.$$

Since we have $\omega_1 \leq 1$, this means we encourage the search of more components of $\boldsymbol{x}$ in the first than in the second block. We know that the set of solutions are given by $\boldsymbol{x}_0 + \mathcal{N}ull(\mathcal{A})$. Ideally, its intersection with the ℓ_1-ball gives the minimizer of $\mathscr{P}_1$. Now by introducing the weight in the first block, the weighted norm ball will be pinched towards the axis containing $\boldsymbol{x}_1$ which has, in average, lot of non-zero components. Therefore, the recovered vector from $\mathscr{P}_1^{\omega_1,1}$ is going to be more accurate than the recovered vector from $\mathscr{P}_1$.

Now, assume to have the knowledge of $1 \leq i < g$ sparsity level of i blocks. Then, the

optimization can be written as

$$\mathscr{P}_1^{\omega_1,\omega_2,\ldots,\omega_i,1} : \underset{x}{\text{minimize}} \quad \sum_{l=1}^{i} \omega_l \|\boldsymbol{x}_l\|_{\ell_1} + \sum_{l=i+1}^{g} \|\boldsymbol{x}_l\|_{\ell_1}$$

$$\text{subject to} \qquad \|\mathcal{A}\boldsymbol{x} - \boldsymbol{y}\|_{\ell_2} \leq \epsilon.$$

Applying the same observation, the weighted norm ball is pinched more towards the components of the denser blocks. Therefore, the performance should be at least the performance of $\mathscr{P}_1$. Setting $l = g$, we get $\|\boldsymbol{x}^\sharp - \boldsymbol{x}_0\|_{\ell_2} \leq \|\boldsymbol{x}^\dagger - \boldsymbol{x}_0\|_{\ell_2}$. On the other hand, the bands' occupation is a random process following the bernoulli, then at some given time we may have a lesser number of non-zero components in the ith block than in the jth block with $(j > i)$, the event can be quantified as

$$\sum_{k=1}^{\min(n_i,n_j)} \sum_{l=0}^{k-1} \binom{n_i}{l} q_i^l (1-q_i)^{n_i-l} \binom{n_j}{k} q_j^k (1-q_j)^{n_j-k}. \tag{3.17}$$

Examining all the cases and taking the complementary, we get Equation (3.8).

3.6.2 Proof of Proposition 2

Our proposed approach achieves a stable and robust recovery if we can find C_0 and C_1 such that

$$\|\boldsymbol{x}^\sharp - \boldsymbol{x}_0\|_{\ell_2} \leq C_0 \epsilon + C_1 \frac{\sigma_k(\boldsymbol{x}, \|.\|_{\ell_p})}{\sqrt{k}}. \tag{3.18}$$

Combining Theorem 1 and [6, Theorem 2], we get (with a probability exceeding (3.8))

$$\begin{aligned} \|\boldsymbol{x}^\sharp - \boldsymbol{x}_0\|_{\ell_2} &\leq \|\boldsymbol{x}^\dagger - \boldsymbol{x}_0\|_{\ell_2} \\ &\leq C_0.\epsilon + C_1.\frac{\sigma_k(\boldsymbol{x}_0, \|.\|_{\ell_1})}{\sqrt{k}} \end{aligned} \tag{3.19}$$

where

$$C_0 = \frac{2(1 + 1/\sqrt{a})}{\sqrt{1 - \delta_{(a+1)k}} - \sqrt{1 + \delta_{ak}}/\sqrt{a}} \tag{3.20}$$

and

$$C_1 = \frac{2\sqrt{1 - \delta_{(a+1)k}} + \sqrt{1 + \delta_{ak}}/\sqrt{a}}{\sqrt{a}\sqrt{1 - \delta_{(a+1)k}} - \sqrt{1 + \delta_{ak}}} \tag{3.21}$$

with a and b such that $\delta_{ak} + a\delta_{(a+1)k} < a - 1$. Therefore, our approach is stable and robust.

3.6.3 Proof of Theorem 3

Prior to give the proof of the theorem, we start by providing the following lemma.

Lemma 2. *Let* $\bar{k} = \sum_{i=1}^g \bar{k}_i$ *and* $n = \sum_{i=1}^g n_i$ *with* $\bar{k}_i \leq n_i/2$. *There exists a set* $X = \bigcup_{i=1}^g X_i \subset \Sigma_{\bar{k}}$ *such that for any* $x = [x_1^T x_2^T ... x_g^T]$ *with* $x_i \in X_i$ *for* $i = 1, \ldots, g$, *we have:*
(1) $\|x_i\|_{\ell_2} \leq \sqrt{\bar{k}_i}$
(2) for any $x, y \in X$ *with* $x \neq y$, $\|x_i - y_i\|_{\ell_2} \geq \sqrt{\bar{k}_i/2}$ *and* $\log |X| \geq \frac{k}{2} \log \left(\frac{n}{k}\right)$.

Proof. The proof of the lemma is similar to [11, Lemma A.1]. It is omitted here for brevity. ■

The proof of the theorem is inspired from the proof in [11] and based on Lemma 2. First, we have $x = \sum_{i=1}^g x_i$ with $\|x_i\|_{\ell_0} \leq \bar{k}_i$. Then, for any x_i and $y_i \in \Sigma_{2\bar{k}_i}$, we have according to the RIP property

$$
\begin{aligned}
\sqrt{1 - \delta_{\bar{k}_i}}\|x_i - y_i\|_{\ell_2} &\leq \|\mathcal{A}_i x_i - \mathcal{A}_i y_i\|_{\ell_2} \\
\|\mathcal{A}_i x_i - \mathcal{A}_i y_i\|_{\ell_2} &\leq \sqrt{1 + \delta_{\bar{k}_i}}\|x_i - y_i\|_{\ell_2}
\end{aligned}
\tag{3.22}
$$

Combining the above property with Lemma 2, we get

$$\sqrt{\bar{k}_i(1 - \delta_{\bar{k}_i})/2} \leq \|\mathcal{A}_i x_i - \mathcal{A}_i y_i\|_{\ell_2} \leq \sqrt{2\bar{k}_i(1 + \delta_{\bar{k}_i})}. \tag{3.23}$$

By considering the balls with radius τ_i such that $\tau_i = \sqrt{\bar{k}_i(1 - \delta_{\bar{k}_i})/2}/2 = \sqrt{\bar{k}_i(1 - \delta_{\bar{k}_i})/8}$ centered at $\mathcal{A}_i x_i$, then these balls are disjoint. On the other hand, we have for any x

and $y \in \Sigma_{\bar{k}}$,

$$\|\mathcal{A}x - \mathcal{A}y\|_{\ell_2} \leq \sum_{i=1}^{g} \|\mathcal{A}_i x_i - \mathcal{A}_i y_i\|_{\ell_2} \leq \sum_{i=1}^{g} \sqrt{2\bar{k}_i(1 + \delta_{\bar{k}_i})} \qquad (3.24)$$

The upper bound gives an idea about the maximum distance between the centers of any pair of balls which is $d^{\max} = \sum_{i=1}^{g} \sqrt{2\bar{k}_i(1 + \delta_{\bar{k}_i})}$. Therefore, all the balls are contained in the ball of radius $\tau = d^{\max} + \max_i(\tau_i)$. Thus, we have

$$\text{Vol}\Big(B^m(\tau)\Big) \geq |X| \text{Vol}\Big(B^m(\min_i \tau_i)\Big), \qquad (3.25)$$

where $\text{Vol}(B^m(\tau))$ is the volume of the ball which is given by $\text{Vol}(B^m(\tau)) = \frac{\pi^{m/2}}{\Gamma(m/2+1)} \tau^m$ and $\Gamma(.)$ is the Euler Gamma function. This yields

$$\left(\frac{d^{\max} + \max_i(\tau_i)}{\min_i \tau_i}\right)^m \geq |X| \qquad (3.26)$$

Therefore, after applying log, we get

$$m \geq \frac{1}{\log\left(\frac{d^{\max} + \max_i(\tau_i)}{\min_i \tau_i}\right)} \log(|X|) \qquad (3.27)$$

Now recalling Lemma 2, we get $m \geq C_{\delta_{\bar{k}_1}, \ldots, \delta_{\bar{k}_g}} \bar{k} \log(n/\bar{k})$ where

$$C_{\delta_{\bar{k}_1}, \ldots, \delta_{\bar{k}_g}} = \frac{1}{2\log\left(\frac{\sum_{i=1}^{g} \sqrt{2\bar{k}_i(1+\delta_{\bar{k}_i})} + \max_i(\sqrt{\bar{k}_i(1-\delta_{\bar{k}_i})/8})}{\min_i(\sqrt{\bar{k}_i(1-\delta_{\bar{k}_i})/8})}\right)}. \qquad (3.28)$$

which ends the proof.

3.6.4   Proof of Theorem 4

Let $Y = \sum_{i=1}^{n} \mathcal{H}_i$ be the random variable that contains the number of occupied bands. Since the occupation of the band is independent, then the moment generating function of Y is given by

$$\mathcal{M}_Y(t) = \prod_{i=1}^{n} (e^t p_i + 1 - p_i). \qquad (3.29)$$

Now using the Chernoff bound, we have

$$
\begin{aligned}
\Pr(Y \geq k_0) \ &\leq \ \inf_{t \geq 0} \left\{ e^{-k_0 t} \mathcal{M}_Y(t) \right\} \\
&= \ \inf_{t \geq 0} \left\{ e^{-k_0 t} \prod_{i=1}^{n} \left((e^t - 1)p_i + 1 \right) \right\} \tag{3.30}
\end{aligned}
$$

Using the fact that $e^x \geq 1 + x$, we get

$$
\begin{aligned}
\Pr(Y \geq k_0) \ &\leq \ \inf_{t \geq 0} \left\{ e^{-k_0 t} \prod_{i=1}^{n} e^{(e^t - 1)p_i} \right\} \\
&= \ \inf_{t \geq 0} \left\{ e^{-k_0 t} e^{(e^t - 1) \sum_{i=1}^{n} p_i} \right\} \\
&= \ \inf_{t \geq 0} \left\{ \left[\underbrace{e^{(e^t - 1)} e^{-t k_0 / \sum_{i=1}^{n} p_i}}_{(*)} \right]^{\sum_{i=1}^{n} p_i} \right\} \tag{3.31}
\end{aligned}
$$

To optimize $(*)$, we take the derivative over t which yields to $t^* = \log(k_0 / \sum_{i=1}^{n} p_i)$. Now substituting t^*, we get

$$
\Pr(Y \geq k_0) \ \leq \ \frac{e^{k_0 - \sum_{i=1}^{n} p_i}}{(k_0 / \sum_{i=1}^{n} p_i)^{k_0}} \tag{3.32}
$$

Now since $\Pr(Y \geq k_0) = 1 - \Pr(Y \leq k_0)$, we get

$$
1 - \Pr(Y \leq k_0) \ \leq \ \frac{e^{k_0 - \sum_{i=1}^{n} p_i}}{(k_0 / \sum_{i=1}^{n} p_i)^{k_0}} \tag{3.33}
$$

which gives the result of the theorem.

Acknowledgement

Bibliography

[1] FCC: GN docket no: 14-177, report and order and further notice of proposed rule-

making, July 2016.

[2] Omid Abari, Fabian Lim, Fred Chen, and Vladimir Stojanović. Why analog-to-information converters suffer in high-bandwidth sparse signal applications. *IEEE Trans. on Circuits and Systems I: Regular Papers*, 60(9):2273–2284, 2013.

[3] M Eren Ahsen and M Vidyasagar. Error bounds for compressed sensing algorithms with group sparsity: A unified approach. *Applied and Computational Harmonic Analysis*, 2015.

[4] Ian F. Akyildiz, Brandon F. Lo, and Ravikumar Balakrishnan. Cooperative spectrum sensing in cognitive radio networks: A survey. *Physical Communication*, 4:40–62, 2011.

[5] Fadi M Al-Turjman. Information-centric sensor networks for cognitive iot: an overview. *Annals of Telecommunications*, pages 1–16, 2016.

[6] Emmanuel J Candes, Justin K Romberg, and Terence Tao. Stable signal recovery from incomplete and inaccurate measurements. *Communications on pure and applied mathematics*, 59(8):1207–1223, 2006.

[7] Emmanuel J Candes and Terence Tao. Decoding by linear programming. *IEEE Trans. on information theory*, 51(12):4203–4215, 2005.

[8] Emmanuel J Candes, Michael B Wakin, and Stephen P Boyd. Enhancing sparsity by reweighted ℓ_1-minimization. *Journal of Fourier analysis and applications*, 14(5-6):877–905, 2008.

[9] Yunfei Chen and Hee-Seok Oh. A survey of measurement-based spectrum occupancy modeling for cognitive radios. *IEEE Communications Surveys & Tutorials*, 18(1):848–859, 2014.

[10] Mark A Davenport, Petros T Boufounos, Michael B Wakin, and Richard G Baraniuk. Signal processing with compressive measurements. *IEEE Journal of Selected Topics in Signal Processing*, 4(2):445–460, 2010.

[11] Mark A Davenport, Marco F Duarte, Yonina C Eldar, and Gitta Kutyniok. Introduction to compressed sensing. *Preprint*, 93(1):2, 2011.

[12] Fadel F Digham, Mohamed-Slim Alouini, and Marvin K Simon. On the energy detection of unknown signals over fading channels. *IEEE Trans. on communications*, 55(1):21–24, 2007.

[13] Michael P Friedlander, Hassan Mansour, Rayan Saab, and Oezguer Yilmaz. Recovering compressively sampled signals using partial support information. *IEEE Trans. on Information Theory*, 58(2):1122–1134, 2012.

[14] Asvin Gohil, Hardik Modi, and Shobhit K Patel. 5G technology of mobile communication: A survey. In *Intelligent Systems and Signal Processing (ISSP), 2013 International Conference on*, pages 288–292. IEEE, 2013.

[15] Michael Grant, Stephen Boyd, and Yinyu Ye. Cvx: Matlab software for disciplined convex programming, 2008.

[16] Mohsen Guizani, Bassem Khalfi, Mahdi Ben Ghorbel, and Bechir Hamdaoui. Large-scale cognitive cellular systems: resource management overview. *IEEE Communications Magazine*, 53(5):44–51, 2015.

[17] Z-C Hao and J-S Hong. Highly selective ultra wideband bandpass filters with quasi-elliptic function response. *IET microwaves, antennas & propagation*, 5(9):1103–1108, 2011.

[18] Timothy Harrold, Rafael Cepeda, and Mark Beach. Long-term measurements of spectrum occupancy characteristics. In *Proc. of IEEE Symposium on New Frontiers in Dynamic Spectrum Access Networks (DySPAN)*, pages 83–89, 2011.

[19] Steven Siying Hong and Sachin Rajsekhar Katti. Dof: a local wireless information plane. In *ACM SIGCOMM Computer Communication Review*, volume 41, pages 230–241, 2011.

[20] Jing Jiang, Hongjian Sun, David Baglee, and H Vincent Poor. Achieving autonomous compressive spectrum sensing for cognitive radios. *IEEE Trans. on Vehicular Technology*, 65(3):1281–1291, 2016.

[21] M Amin Khajehnejad, Weiyu Xu, A Salman Avestimehr, and Babak Hassibi. Analyzing weighted minimization for sparse recovery with nonuniform sparse models. *IEEE Trans. on Signal Processing*, 59(5):1985–2001, 2011.

[22] Sami Kirolos, Jason Laska, Michael Wakin, Marco Duarte, Dror Baron, Tamer Ragheb, Yehia Massoud, and Richard Baraniuk. Analog-to-information conversion via random demodulation. In *Proc. of IEEE Dallas/CAS Workshop on Design, Applications, Integration and Software*, pages 71–74, 2006.

[23] Eva Lagunas, Shree Krishna Sharma, Symeon Chatzinotas, and Björn Ottersten. Compressive sensing based energy detector. In *Proc. of IEEE European Signal Processing Conference*, pages 1678–1682, 2016.

[24] Eva Lagunas, Shree Krishna Sharma, Symeon Chatzinotas, and Björn Ottersten. Compressive sensing based target counting and localization exploiting joint sparsity. In *Proc. of IEEE Acoustics, Speech and Signal Processing*, pages 3231–3235, 2016.

[25] Miles Lopes. Estimating unknown sparsity in compressed sensing. In *Proc. of Int. Conf. on Machine Learning*, pages 217–225, 2013.

[26] M Mehdawi, NG Riley, M Ammar, A Fanan, and M Zolfaghari. Spectrum occupancy measurements and lessons learned in the context of cognitive radio. In *Proc. of IEEE Telecommunications Forum Telfor (TELFOR)*, pages 196–199, 2015.

[27] M. Mishali and Y. C. Eldar. From theory to practice: Sub-Nyquist sampling of sparse wideband analog signals. *IEEE Journal of Selected Topics in Signal Processing*, 4(2):375–391, Apr. 2010.

[28] D. Needell and R. Vershynin. Signal recovery from incomplete and inaccurate measurements via regularized orthogonal matching pursuit. *IEEE Journal of Selected Topics in Signal Processing*, 4(2):310–316, Apr. 2010.

[29] Deanna Needell, Rayan Saab, and Tina Woolf. Weighted ℓ_1-minimization for sparse recovery under arbitrary prior information. *arXiv preprint arXiv:1606.01295*, 2016.

[30] Deanna Needell and Joel A Tropp. Cosamp: Iterative signal recovery from incomplete and inaccurate samples. *Applied and Computational Harmonic Analysis*, 26(3):301–321, 2009.

[31] Vilaskumar M Patil and Siddarama R Patil. A survey on spectrum sensing algorithms for cognitive radio. In *2016 International Conference on Advances in Human Machine Interaction (HMI)*, pages 1–5. IEEE, 2016.

[32] Z. Qin, Y. Gao, M. D. Plumbley, and C. G. Parini. Wideband spectrum sensing on real-time signals at sub-Nyquist sampling rates in single and cooperative multiple nodes. *IEEE Trans. on Signal Processing*, 64(12):3106–3117, Jun. 2016.

[33] Zhijin Qin, Yue Gao, and Clive G Parini. Data-assisted low complexity compressive spectrum sensing on real-time signals under sub-Nyquist rate. *IEEE Trans. on Wireless Communications*, 15(2):1174–1185, 2016.

[34] Fatima Salahdine, Naima Kaabouch, and Hassan El Ghazi. Bayesian compressive sensing with circulant matrix for spectrum sensing in cognitive radio networks. In *Proc. of IEEE Annual Ubiquitous Computing, Electronics & Mobile Communication Conference (UEMCON)*, pages 1–6, 2016.

[35] Fatima Salahdine, Naima Kaabouch, and Hassan El Ghazi. A survey on compressive sensing techniques for cognitive radio networks. *Physical Communication*, 20:61–73, 2016.

[36] Fatima Salahdine, Naima Kaabouch, and Hassan El Ghazi. A bayesian recovery technique with toeplitz matrix for compressive spectrum sensing in cognitive radio networks. *International Journal of Communication Systems*, 2017.

[37] S. K. Sharma, E. Lagunas, S. Chatzinotas, and B. Ottersten. Application of compressive sensing in cognitive radio communications: A survey. *IEEE Communications Surveys & Tutorials*, 18(03):1838–1860, 2016.

[38] Shree Krishna Sharma, Symeon Chatzinotas, and Björn Ottersten. Compressive sparsity order estimation for wideband cognitive radio receiver. *IEEE Trans. on Signal Processing*, 62(19):4984–4996, 2014.

[39] Hongjian Sun, Arumugam Nallanathan, Shuguang Cui, and Cheng-Xiang Wang. Cooperative wideband spectrum sensing over fading channels. *IEEE Trans. on Vehicular Technology*, 65(3):1382–1394, 2016.

[40] Hongjian Sun, Arumugam Nallanathan, Cheng-Xiang Wang, and Yunfei Chen. Wideband spectrum sensing for cognitive radio networks: a survey. *IEEE Wireless Communications*, 20(2):74–81, 2013.

[41] Z. Sun and J. N. Laneman. Performance metrics, sampling schemes, and detection algorithms for wideband spectrum sensing. *IEEE Trans. on Signal Processing*, 62(19):5107–5118, Oct. 2014.

[42] Zhi Tian and Georgios B Giannakis. Compressed sensing for wideband cognitive radios. In *Acoustics, Speech and Signal Processing, 2007. ICASSP 2007. IEEE International Conference on*, volume 4, pages IV–1357. IEEE, 2007.

[43] Zhi Tian, Yohannes Tafesse, and Brian M Sadler. Cyclic feature detection with sub-Nyquist sampling for wideband spectrum sensing. *IEEE Journal of Selected topics in signal processing*, 6(1):58–69, 2012.

[44] Joel A Tropp and Anna C Gilbert. Signal recovery from random measurements via orthogonal matching pursuit. *IEEE Trans. on information theory*, 53(12):4655–4666, 2007.

[45] Joel A Tropp, Jason N Laska, Marco F Duarte, Justin K Romberg, and Richard G Baraniuk. Beyond nyquist: Efficient sampling of sparse bandlimited signals. *IEEE Trans. on Information Theory*, 56(1):520–544, 2010.

[46] Namrata Vaswani and Wei Lu. Modified-CS: Modifying compressive sensing for problems with partially known support. *IEEE Trans. on Signal Processing*, 58(9):4595–4607, 2010.

[47] Yue Wang, Zhi Tian, and Chunyan Feng. Sparsity order estimation and its application in compressive spectrum sensing for cognitive radios. *IEEE Trans. on wireless communications*, 11(6):2116–2125, 2012.

[48] Weiyu Xu, M Amin Khajehnejad, A Salman Avestimehr, and Babak Hassibi. Breaking through the thresholds: an analysis for iterative reweighted ℓ_1- minimization via the grassmann angle framework. In *Proc. of IEEE Int. Conf. on Acoustics, Speech and Signal Processing*, pages 5498–5501, 2010.

[49] Mümtaz Yılmaz, Damla Gürkan Kuntalp, and Akan Fidan. Determination of spectrum utilization profiles for 30 MHz–3 GHz frequency band. In *Proc. of IEEE International Conference on Communications (COMM)*, pages 499–502, 2016.

[50] Wotao Yin, Simon Morgan, Junfeng Yang, and Yin Zhang. Practical compressive sensing with toeplitz and circulant matrices. In *Proc. of SPIE*, volume 7744, page 77440K, 2010.

[51] M-H Yoon, Y Shin, H-K Ryu, and J-M Woo. Ultra-wideband loop antenna. *Electronics letters*, 46(18):1249–1251, 2010.

When Machine Learning Meets Compressive Sampling for Wideband Spectrum Sensing

Bassem Khalfi, Adem Zaid, and Bechir Hamdaoui

Chapter 4: Manuscript 3: When Machine Learning Meets Compressive Sampling for Wideband Spectrum Sensing

Bassem Khalfi, Adem Zaid, Bechir Hamdaoui

Oregon State University, Oregon, USA

{khalfib,zaida,hamdaoui}@oregonstate.edu

Abstract

This paper proposes a novel technique that exploits spectrum occupancy behaviors inherent to wideband spectrum access to enable efficient cooperative wideband spectrum sensing. Our technique requires lesser number of sensing measurements while still recovering spectrum occupancy information accurately. It does so by leveraging compressive sampling theory to exploit the block-like occupancy structure of wideband spectrum access. Our technique is also adaptive in that it accounts for the variability of spectrum occupancy over time. It exploits supervised learning to provide and use accurate realtime estimates of the spectrum occupancy. Using simulations, we show that our proposed technique outperforms existing approaches by making accurate spectrum occupancy decisions with lesser sensing communication and energy overheads.

Index terms— Cooperative wideband spectrum sensing; compressive sampling; supervised learning.

4.1   Introduction

Spectrum availability presents a major challenge that fifth-generation (5G) networks need to overcome in order to support the massive number of emerging 5G devices. In an effort to overcome this foreseen challenge, spectrum regulators have started to create service rules and policies for allowing high frequency band use. For example, as recently as July 2016, FCC established new rules for opening up mmWave band use for wireless broadband devices in frequencies above 24 GHz [1]. With these new rules, 5G networks will be forced to operate in a wide range of spectrum bands with diverse characteristics and limitations (e.g. propagation condition, transmission power limits, etc.). These

new spectrum access policies call for innovative techniques that enable the access of this wideband spectrum in an efficient manner.

On the other hand, despite the rapidly increasing number of users, recent measurement studies [33] reveal that the allocated spectrum still suffers from under-utilization. As a result, dynamic spectrum access (DSA) has been adopted by 5G as the key solution for addressing this spectrum access inefficiency [14, 19, 17, 16, 15]. The core idea of DSA is to rely on spectrum sensing techniques to locate unoccupied bands that can be exploited opportunistically by secondary users (SUs) [24, 32, 9, 10, 6, 21, 8].

Many techniques have already been proposed with the aim of improving spectrum sensing, but mostly for single-band DSA [25, 13, 12, 11]. Wideband spectrum sensing has, however, received lesser attention [27]. Most of wideband spectrum sensing techniques leverage compressive sampling theory [5] to exploit the inherent sparsity nature of wideband occupancy, thus allowing for spectrum occupancy information recovery at sub-Nyquist sampling rates. Applying compressive sampling requires the estimation of the sparsity level which reflects the spectrum occupancy [5]. In the literature, this sparsity level has usually been set to the average occupancy across the entire wideband spectrum [27, 28]. However, spectrum occupancy is a time-varying process, and hence, setting it to a fixed average makes these compressive sampling based techniques inefficient. More specifically, when the actual sparsity level is higher than this used average, compressive spectrum sensing techniques fail to recover the spectrum occupancy information, and when it is below the average, SUs end up taking more measurements than needed, which leads to wasting energy and bandwidth resources.

In this paper, we propose a novel technique that enables efficient cooperative spectrum sensing in wideband DSA. The novelty of our proposed technique lies in the key observations that spectrum occupancy (i) changes over time and (ii) varies considerably from one spectrum block to another [33]. Our technique accounts for the time variability by leveraging supervised learning [30] to provide and use estimates of the sparsity levels, and exploits the block-like spectrum occupancy structure by leveraging compressive sampling [5] to reduce the number of measurements needed to recover spectrum occupancy information. Our technique tracks and provides a sparsity level estimate in realtime for each spectrum block separately to exploit the observed block-like occupancy behavior and to account for time variability of these occupancies. The tracking and incorporation of this adaptive, fine-grained spectrum occupancy is the key behind the performance

improvement that our proposed technique achieves. To this end, our contributions in this paper are:

- We propose an efficient spectrum sensing technique for cooperative wideband spectrum access that overcomes the shortcomings of conventional approaches. It combines machine learning with weighted compressive sampling to accurately estimate wideband spectrum occupancy.

- We propose prediction approaches that rely on regression to provide accurate estimates of the sparsity levels, thereby allowing efficient spectrum occupancy information recovery.

- We propose a weighted compressive sampling approach that exploits the block-like, inherent structure of spectrum occupancy to enable efficient recovery of wideband occupancy information.

The remainder of the paper is structured as follows. In Section 4.2, we present our system model. In Section 4.3, we describe our proposed scheme. In Section 4.4, we present the performance evaluation of the proposed technique. Related works are presented in Section 4.5. Finally, we present our conclusion and future works in Section 4.6.

4.2   System Model

4.2.1   Primary System Model

We consider a heterogeneous wideband spectrum access system containing n frequency bands. We assume that wideband spectrum accommodates multiple types of user applications, where applications of the same type are allocated frequency bands within the same block. Therefore, we consider that wideband spectrum has a block-like occupation structure, where each block (accommodating applications of similar type) has different occupancy behavioral characteristics (as observed in [33]). The wideband spectrum can then be grouped into g disjoint contiguous blocks, $\mathcal{G}_i, i = 1, ..., g$, with $\mathcal{G}_i \bigcap \mathcal{G}_j = \emptyset$ for $i \neq j$. Each block, $\mathcal{G}_i$, is a set of n_i contiguous bands. We assume that within each block $\mathcal{G}_i$ of frequency, the number of primary users (PU)s' arrivals within a time slot T

and the service time/duration of each PU, each follows some probabilistic distribution. Therefore, our system can be seen as g $G/G/n_i/n_i$ independent queueing systems.

4.2.2   Secondary System Model

We consider a set of SUs co-located in the same cell as the PUs, and assume that a subset of SUs perform the wideband spectrum sensing task cooperatively, as illustrated by Fig. 4.1, and report their sensing measurements to a fusion center (FC), which uses them to determine whether the spectrum is occupied. The FC then relies on this spectrum occupancy information to assign spectrum to the SUs requesting spectrum access. Further details on the cooperative sensing protocol are given in Section 4.3.

The time-domain signal $\boldsymbol{r}_i(t)$ received by the ith SU can be expressed as

$$\boldsymbol{r}_i(t) = \boldsymbol{h}_i(t) \otimes \boldsymbol{s}(t) + \boldsymbol{w}_i(t), \tag{4.1}$$

where $\boldsymbol{h}_i(t)$ is the channel impulse between the primary transmitters and the SU_i, $\boldsymbol{s}(t)$ is the PUs' signal, $\otimes$ stands for the convolution operator, and $\boldsymbol{w}_i(t)$ is an additive white Gaussian noise with mean 0 and variance σ^2. Ideally, the SU should take samples at a rate of at least twice the maximum frequency, $f_{\max}$, of the signal in order to ensure complete signal recovery. Let the sensing window be $[0, mT_0]$ with $T_0 = 1/(2f_{\max})$. Assuming a normalized number of wideband Nyquist samples per band, then the vector of the taken samples is $\boldsymbol{r}_i(t) = [r_i(0), ..., r_i((m_0 - 1)T_0)]^T$ where $r_i(j) = r_i(t)|_{t=jT_0}$, for $j = 0, ..., m_0$, and $m_0 = n$. Note that a reasonable assumption that we make is that the sensing window length is assumed to be sufficiently small when compared to the time it takes a band state to change. That is, each band's occupancy is assumed to remain constant during each sensing time window.

To reveal which bands are occupied, the SU performs a discrete Fourier transform of the received signal $\boldsymbol{r}_i(t)$; i.e.,

$$\boldsymbol{r}_{f,i} = \boldsymbol{h}_{f,i}\boldsymbol{s}_f + \boldsymbol{w}_{f,i} = \boldsymbol{x}_i + \boldsymbol{w}_{f,i}, \tag{4.2}$$

where $\boldsymbol{h}_{f,i}$, $\boldsymbol{s}_f$, and $\boldsymbol{w}_{f,i}$ are the Fourier transforms of $\boldsymbol{h}_i(t)$, $\boldsymbol{s}(t)$, and $\boldsymbol{w}_i(t)$, respectively. The vector $\boldsymbol{x}_i$ contains a faded version of the PUs' signals operating in the different bands. Given the occupancy of the bands by their PUs and in the absence of fading
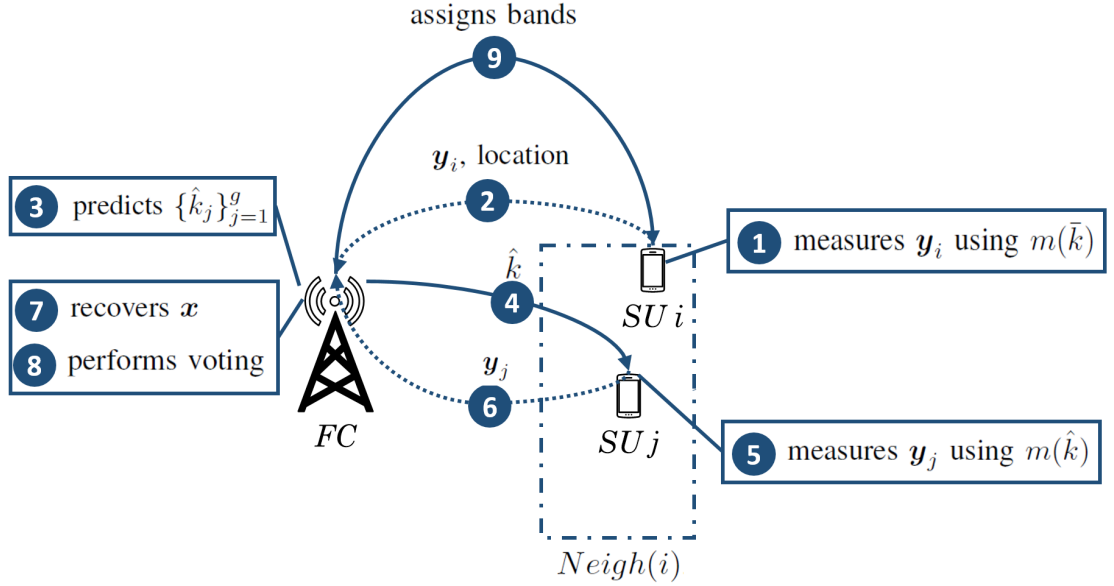
Figure 4.1: Illustration of the cooperative spectrum sensing task.

and interference, the vector $\boldsymbol{x}_i$ is *sparse*. Formally, a vector $\boldsymbol{x} \in \mathbb{R}^n$ is said *k-sparse* if it has (or after performing a basis change) at most k non-zero elements [5]. That is, $supp(\boldsymbol{x}) = \|\boldsymbol{x}\|_{\ell_0} = |\{i : x_i \neq 0\}| \leq k$. But since, in practice, there will likely be interference coming from other nearby cells and users, the vector $\boldsymbol{x}_i$ could rather be *nearly sparse* than sparse. Mathematically, a vector $\boldsymbol{x} \in \mathbb{R}^n$ is said *nearly sparse* (called also compressible [5]) if most of its components obey a fast power law decay.

Sampling the wideband signal at the Nyquist rate is prohibitively costly, and goes beyond the hardware capabilities of the SUs. Compressive sampling has been used to overcome this issue by reducing the number of measurements significantly given that the signal is nearly sparse [5]. Hence, the measured signal can be written as

$$\begin{aligned} \boldsymbol{y}_i &= \Psi \mathcal{F}^{-1}(\boldsymbol{x}_i + \boldsymbol{w}_{f,i}) \\ &= \mathcal{A}\boldsymbol{x}_i + \boldsymbol{\eta}, \end{aligned} \quad (4.3)$$

where $\boldsymbol{y}_i \in \mathbb{R}^m$ is the measurement vector, $\mathcal{F}^{-1}$ is the inverse discrete Fourier transform, and Ψ is the sensing matrix assumed to have a full rank, i.e. $rank(\Psi) = m$. The sensing noise $\boldsymbol{\eta}$ is equal to $\Psi \mathcal{F}^{-1} \boldsymbol{w}_f$. These measurements $\boldsymbol{y}_i$ are then sent to FC to perform

the spectrum recovery and decide on the occupancy of each band in that given region.

4.3   The Proposed Cooperative Wideband Spectrum Sensing Scheme

In this section, we present our technique. We begin by describing the proposed sensing protocol. Then, we investigate the different approaches used for predicting the spectrum occupancy, and describe our prediction-based scheme proposed for enabling efficient spectrum occupancy information recovery.

4.3.1   The Proposed Scheme

Acquiring accurate and consistent spectrum occupancy information across the entire cell requires that all SUs perform wideband spectrum sensing and at every time slot. However, this is prohibitively costly, as it incurs excessive overhead (energy, communication, etc.), and is not efficient either, as not all SUs will be needing access to the spectrum. To address this, we therefore propose that the sensing task is performed only by and within the region whose SUs need spectrum access.

The proposed cooperative sensing scheme is described as shown in Fig. 4.1. First, we assume that FC computes over time the average occupancy $\bar{k}$ of the wideband spectrum and shares it with all SUs. Now, if a particular SU_i wants to access the spectrum, it takes $m(\bar{k})$ measurements such that $m(\bar{k}) = O(\bar{k} \log(n/\bar{k}))$ as described by Equation (4.3). Then, SU i reports the measurement vector $\boldsymbol{y}_i$ and its location to FC. After receiving the measurements and exploiting the other features (as described later), FC predicts the actual sparsity level in each block $\{\hat{k}_j\}_{j=1}^g$, as will be explained in Section 4.3.2. Then, FC communicates $\hat{k} = \sum_{j=1}^g \hat{k}_i$ to the recent neighbors of SU_i, denoted as $Neigh(i)$. Next, each SU of $Neigh(i)$ takes $m(\hat{k}) = \mathcal{O}(\hat{k} \log(n/\hat{k}))$ measurements. Then, these measurements are reported to FC which exploits the predicted sparsity levels to perform an efficient recovery, as explained in Section 4.3.3. Having recovered the spectrum occupancy information, the energy level of each band is compared to a threshold λ, and then used to decide, using voting, on the band occupancy. This is summarized in Algorithm 1.

Using Step 2, FC uses the measurements $\boldsymbol{y}_i$ and the location to determine the features used to predict the sparsity levels in each block, $\{\hat{k}_j\}_{j=1}^g$. In Steps 4-5, the main intuition

---
Algorithm 1 Cooperative Wideband Spectrum Sensing

1: SU_i performs wideband spectrum sensing using $\bar{k}$.
2: SU_i reports $\boldsymbol{y}_i$ and its location to FC.
3: FC predicts $\{\hat{k}_j\}_{j=1}^g$.
4: FC multicasts $\hat{k}$ to $Neigh(i)$.
5: $Neigh(i)$ performs wideband spectrum sensing.
6: $Neigh(i)$ reports their measurements to FC.
7: FC recovers spectrum occupancy as seen by each SU.
8: FC uses voting to decide on the occupancy.
9: FC assigns some bands to SU i.

---

behind requesting the measurements only from the neighbors of SU_i is twofold. First, users which are near-by SU_i are most likely to observe the same occupancy of the spectrum, and therefore, combining the observations of $Neigh(i)$ would lead to a more accurate decision which is the benefit of the cooperation. Here, SUs which are far from SU_i are most likely to have a different observation of the spectrum occupancy, and hence, it is better to discard their contributions. Second, reducing the number of contributing SUs has a direct implication on reducing the total network overhead, as well as the sensing energy at these devices. In Step 7, the spectrum recovery is performed at FC since this entity has more computing capability and has no constraint on the energy consumption. In Step 8, any voting technique can still be applied once the spectrum decision is performed for every band. We use the majority voting [21].

Remark 4. During the sensing process initiated by SU_i, if one of $Neigh(i)$ requested to access the spectrum, FC does not need to re-initiate the sensing protocol. Spectrum bands are directly assigned to it from the set of available bands.

4.3.2   Spectrum Occupancy Prediction

Recall that having accurate, realtime estimates of the sparsity level $k = \sum_{i=1}^g k_i$ is vital for determining the exact number, $m = O(k \log(n/k))$, of measurements required to accurately recover the spectrum occupancy information [5]. In fact, because k varies with time, not having accurate values of k may lead to over- or under-sampling, which may in turn result either in having inaccurate recovery or in taking unnecessary measurements. In this work, we investigated the use of regression models, a class of supervised learning

algorithms, to derive prediction approaches that can provide accurate estimates of the sparsity levels. These regression models require having historical training dataset that connects the set of observed features with the occupancy level of each spectrum block (labels). The training per-block dataset consists of N training samples $\{(\boldsymbol{z}_i^{(j)}, k_i^{(j)})\}_{j=1}^N$ where j is the sample index, i is the block index, $\boldsymbol{z}_i^{(j)} = \left[z_i^{(j)}[1], \ldots, z_i^{(j)}[d]\right]$ is the vector of d features with $k_i^{(j)}$ representing the number of occupied bands in the ith block. For ease of presentation, we drop the subscript i of the ith block as the prediction is performed on a per-block basis. Next, we present the regression techniques along with the considered features for predicting the sparsity level in each block.

4.3.2.1 Proposed Features

- *PUs' activities:* Spectrum occupancy is correlated with the activities of PUs. Therefore, PUs' average service times and their inter-arrival rates are considered as features in the used regression models.

- *SUs' neighbors:* Our scheme leverages SU cooperation to improve spectrum occupancy detection accuracy. Hence, since FC uses voting when deciding about spectrum availability, a greater number of neighboring SUs means a higher decision accuracy [21]. We, therefore, consider the number of neighbors as a feature.

- *Correlation of spectrum occupancy over time:* The sparsity level of a given block at time slot t is dependent on (and highly correlated to) that at the previous time slot $t-1$. Therefore, we use this feature in the regression models to capture such a dependency.

4.3.2.2 Regression Techniques

Using these proposed features, we consider different regression models to design our prediction technique. We provide next a brief description of each of the considered models.

Linear regression using batch gradient descent We model the spectrum occupancy of each block as $k = \boldsymbol{w}^T \boldsymbol{z} = \sum_{i=0}^d w[i]z[i]$ where $d = m(\bar{k}) + 4$ and the parameter

$\boldsymbol{w}$ is searched using the batch gradient descent, which consists of adaptively determining $\boldsymbol{w} = [w_0, ..., w_d]^T$ that minimizes a loss function. We use as a loss function the mean square error defined as $\mathcal{J}(\boldsymbol{w}) = \frac{1}{2N} \sum_{j=1}^{N} \left(\boldsymbol{w}^T \boldsymbol{z}^{(j)} - k^{(j)} \right)^2$.

Support vector regression (SVR) The objective of SVR is to find the function $\boldsymbol{g}(\boldsymbol{z})$ that predicts k with at most ε error where $\boldsymbol{g}(\boldsymbol{z}) = \langle \boldsymbol{w}, \boldsymbol{z} \rangle + b, b \in \mathbb{R}$; $\langle \cdot, \cdot \rangle$ represents the dot product and b represents the intercept [29]. The optimal $\boldsymbol{w}$ is the solution to:

$$
\begin{aligned}
\min_{\boldsymbol{w}} \quad & \frac{1}{2} \|\boldsymbol{w}\|_2 + C \sum_{j=1}^{N} (\zeta^j + \zeta^{j^*}), \\
\text{s.t.} \quad & k^{(j)} - \boldsymbol{w}^T \boldsymbol{z}^{(j)} - b \leq \varepsilon + \zeta^j, \\
& \boldsymbol{w}^T \boldsymbol{z}^{(j)} + b - k^{(j)} \leq \varepsilon + \zeta^{j^*}, \\
& \zeta^j, \zeta^{j*} \geq 0.
\end{aligned}
\tag{4.4}
$$

The slack variables ζ^j and ζ^{j*} are introduced to tolerate some errors whenever the optimization is not feasible [29].

In this work, we consider linear SVR; i.e.,

$$
k = \sum_{j=1}^{N} (\alpha^{(j)} - \alpha^{(j)^*}) \langle \boldsymbol{z}^{(j)}, \boldsymbol{z} \rangle + b,
\tag{4.5}
$$

where $\alpha^{(j)}$ and $\alpha^{(j)^*}$ are the Lagrangian multipliers [29]. In general, when the data set is linearly inseparable, linear SVR may fail to achieve the optimal regression. Hence, kernel functions are used in this context to transform data set to high dimensional spaces to perform the linear separation [29]. In this case, nonlinear SVR is written as

$$
k = \sum_{j=1}^{N} (\alpha_j - \alpha_j^*) . \mathcal{K}(\boldsymbol{z}^{(j)}, \boldsymbol{z}) + b,
\tag{4.6}
$$

where $\mathcal{K}(\boldsymbol{z}^i, \boldsymbol{z}) = \langle \phi(\boldsymbol{z}^i), \phi(\boldsymbol{z}) \rangle$ and ϕ_i are mapping functions. In this work, we also considered a nonlinear SVR as the regression approach, which uses the Gaussian kernel function [29].

(a) Block 1. (b) Block 2. (c) Block 3. (d) Block 4.
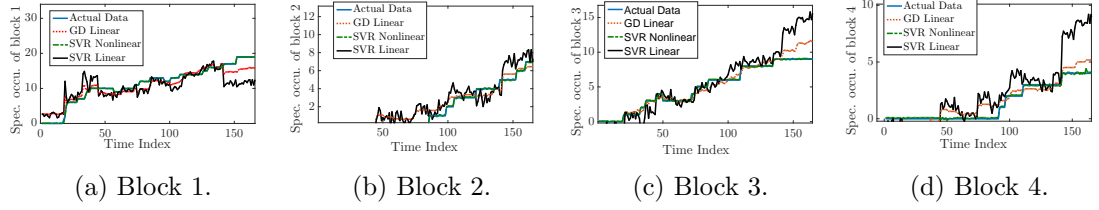
Figure 4.2: Performance of the regression techniques applied to the training data.

4.3.3 Spectrum Occupancy Information Recovery Approach

The proposed recovery scheme exploits the predicted estimates of the per-block spectrum occupancy to improve the recovery accuracy. We propose a weighted ℓ_1-minimization compressive sampling technique that favors the search in the unoccupied bands in the blocks with higher band occupancy.

Given the occupancy is different from one block to another, we propose to set the weights inversely proportional to the estimated block occupancy levels. Formally, the weights can be written as

$$\omega_i = \frac{1}{\hat{k}_i} / \sum_{j=1}^{g} \frac{1}{\hat{k}_j} \ \forall \ i = [1, ..., g] \tag{4.7}$$

and hence, our proposed recovery approach can be formulated as

$$\mathscr{P}(\boldsymbol{x}; \boldsymbol{\omega}) \quad \min_{x} \quad \sum_{l=1}^{g} \omega_l \|\boldsymbol{x}_l\|_{\ell_1}$$
$$\text{s.t.} \quad \|\mathcal{A}\boldsymbol{x} - \boldsymbol{y}\|_{\ell_2} \leq \epsilon. \tag{4.8}$$

where $\boldsymbol{x} = [\boldsymbol{x}_1^T, ..., \boldsymbol{x}_g^T]^T$, $\boldsymbol{x}_l^T$ is a $n_l \times 1$ vector for $l \in \{1, ..., g\}$. The intuition behind this approach is to down-weigh the effect of the heavy-loaded blocks so that the search focuses on blocks with more unoccupied bands [20].

4.4 Performance Evaluation

Our proposed technique is implemented using Matlab and python. We consider 500 SUs randomly deployed in a region of 1 km^2. The wireless transmission of SUs and PUs

(a) Block 1.　　(b) Block 2.　　(c) Block 3.　　(d) Block 4.
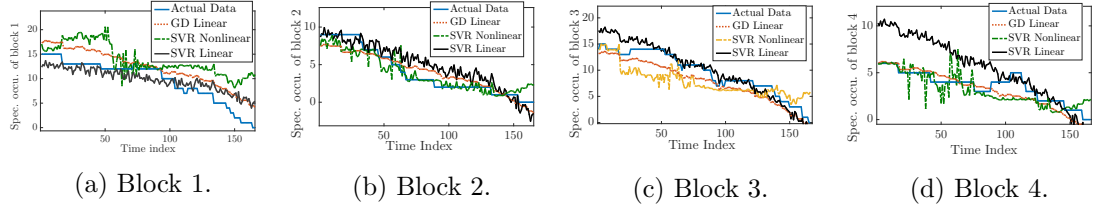
Figure 4.3: Performance of the regression techniques applied to the testing data.

is mainly impacted by the path loss defined as $L_{dB} = 20\log(dist) + 20\log(f_i) - 27.55$ where $dist$ is the distance between the transmitting PU and the sensing SU and f_i is the carrier frequency over which users are operating. The used system parameters are summarized in Table 4.1. FC stores the features defined in Section 4.3.2.1 as well as

Table 4.1: System parameters.

System Parameters	
SU Transmit Power	33 dBm
PU Transmit Power	33 dBm
Coverage Area	$1\ km^2$
Number of Channels n	256
Number of Blocks g	4
Decision Threshold λ	-100 dBm
Receiver Sensitivity	-100 dBm

the occupancy of the blocks over a period of two hours resulting in more than 500 data samples. The 2/3 of resulted data set is served as the training set while 1/3 as a testing set. Then, we used scikit-learn package library in python[26] to implement the three regression models explained in Section 4.3.2.2.

4.4.1　Evaluation of the Regression Techniques

Fig. 4.2a-4.2d show the predicted spectrum occupancy against the actual spectrum occupancy of each block using the training set. Observe that the models follow closely the behavior of the actual data which seems to have a random behavior across the different spectrum blocks. A second observation that we make is that the overall spectrum occupancy is sparse, time varying, and different from one block to another. Further-

more, we notice that the nonlinear SVR is the regression technique that achieves the best performance. Now, we assess the performance against the testing set as shown in Fig. 4.3a-4.3d. Overall, the regression techniques still follow the same behavior of the actual occupancy of every block. We observe that batch linear regression has a superior performance compared to the other in this case. We also observe that nonlinear SVR still behaves somehow better than the linear models. This is mainly because it gives more accurate support vectors and it deals better with data that is linearly inseparable.

4.4.2 Evaluation of the Proposed Sensing Scheme

Having assessed the performance of the prediction of the occupancy of every block, we look at the overall performance of our proposed scheme and the effectiveness of the recovery algorithm. We studied the false alarm and the miss-detection probabilities as measures of the effectiveness of our scheme. We compared the results against the traditional cooperative wideband spectrum sensing algorithm where measurements are taken based on the average spectrum occupancy $\bar{k}$. Here, a false alarm occurs when a band is declared occupied while it is not, whereas a miss-detection occurs when an occupied band is not detected. We take $m = 1.8k \log(n/k)$.

Fig. 4.4 shows the miss-detection performance achieved under our proposed technique using the three studied learning approaches, and compares it to that achieved under the conventional approach. We observe that gradient descent and linear SVR achieve superior performances when compared to that achieved under the nonlinear SVR. Surprisingly compared to the previous results, linear regressions achieve better performance. This is because these techniques over-predict the sparsity levels, and hence results in more taken measurements that help achieve better accuracy. Similar conclusions can be drawn with the false alarm results shown in Fig. 4.5.

4.5 Related Works

The application of machine learning techniques in the context of cognitive radio networks is not new [4, 30, 3]. Authors in [4] surveyed the use of machine learning in spectrum sensing. Authors in [30] have discussed the use of unsupervised and supervised learning techniques for cooperative spectrum sensing. The vector of energy is treated as the
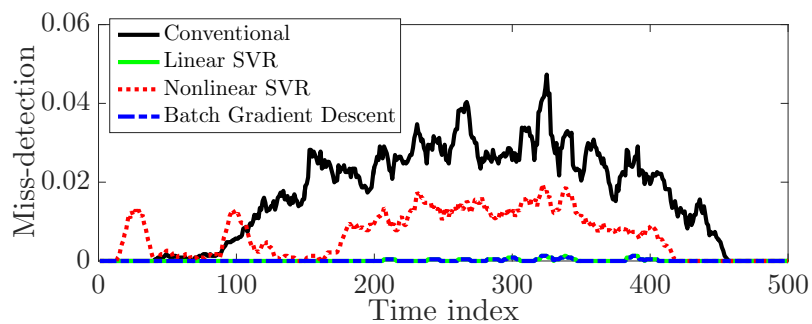
Figure 4.4: Miss-detection probability of the proposed scheme under the different studied regression techniques compared to conventional approach [27].
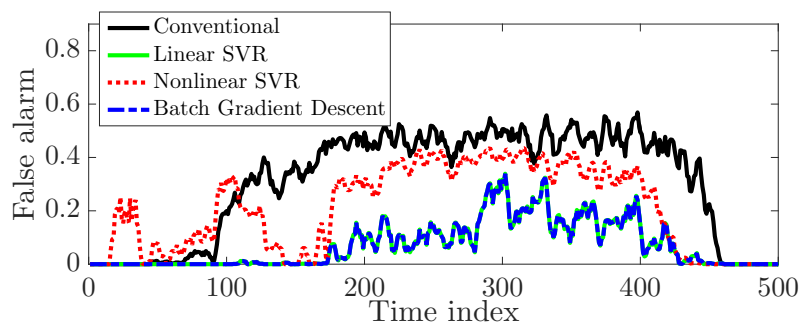
Figure 4.5: False alarm probability of the proposed scheme under the different studied regression techniques compared to conventional approach [27].

feature vector to be fed to the classifier. Although a good number of techniques has been tested, the main shortcoming of this work is that it is designed for single band spectrum sensing. Similar approaches using k-means and SVM are considered in [22]. Authors in [3] considered the case of multiband spectrum where the features are the status of the bands while authors in [2] used a multi-class support vector machine for cooperative wideband spectrum sensing. However, these approaches did not account for the heterogeneity of spectrum allocation nor did they consider wideband spectrum sensing. On the other hand, compressive sampling received recently more research attention for cooperative wideband spectrum [28, 27]. Nevertheless, these works did not exploit the additional knowledge about the spectrum although there has been some works that aimed on exploiting additional knowledge about the signal in general frameworks but not in spectrum sampling [31, 7, 23, 18]. This work aims at leveraging regression models to improve the performance of the cooperative sensing task while not incurring excessive energy and communication overheads.

4.6   Conclusion

We proposed an efficient cooperative wideband spectrum technique that exploits regression techniques as well compressive sampling to improve the sensing performance. We applied supervised learning to provide accurate estimates of the wideband spectrum occupancy, and compressive sampling theory to reduce the number of needed sensing measurements. We proposed an efficient spectrum occupancy information recovery scheme, and showed that our scheme makes great performance enhancements in terms of sensing overhead, sensing energy, and spectrum decision accuracy.

Acknowledgment

Bibliography

[1] FCC: GN docket no: 14-177, report and order and further notice of proposed rule-

making, July 2016.

[2] Olusegun Peter Awe and Sangarapillai Lambotharan. Cooperative spectrum sensing in cognitive radio networks using multi-class support vector machine algorithms. In *Proc. of International Conference on Signal Processing and Communication Systems (ICSPCS),*, pages 1–7. IEEE, 2015.

[3] F. Azmat, Y. Chen, and N. Stocks. Analysis of spectrum occupancy using machine learning algorithms. *IEEE Trans. on Vehicular Technology*, 65(9):6853–6860, Sept 2016.

[4] Mario Bkassiny, Yang Li, and Sudharman K Jayaweera. A survey on machine-learning techniques in cognitive radios. *IEEE Communications Surveys & Tutorials*, 15(3):1136–1159, 2013.

[5] Mark A Davenport, Marco F Duarte, Yonina C Eldar, and Gitta Kutyniok. Introduction to compressed sensing. *Preprint*, 93(1):2, 2011.

[6] Samina Ehsan, Bechir Hamdaoui, and Mohsen Guizani. Radio and medium access contention aware routing for lifetime maximization in multichannel sensor networks. *IEEE Trans. on Wireless Communications*, 11(9):3058–3067, 2012.

[7] Michael P Friedlander, Hassan Mansour, Rayan Saab, and Oezguer Yilmaz. Recovering compressively sampled signals using partial support information. *IEEE Trans. on Information Theory*, 58(2):1122–1134, 2012.

[8] Mahdi Ben Ghorbel, Bechir Hamdaoui, Mohsen Guizani, and Bassem Khalfi. Distributed learning-based cross-layer technique for energy-efficient multicarrier dynamic spectrum access with adaptive power allocation. *IEEE Trans. on Wireless Communications*, 15(3):1665–1674, 2016.

[9] Mahdi Ben Ghorbel, Bassem Khalfi, Bechir Hamdaoui, and Mohsen Guizani. Resources allocation for large-scale dynamic spectrum access system using particle filtering. In *proc. of Globecom Workshops*, pages 219–224. IEEE, 2014.

[10] Mahdi Ben Ghorbel, Bassem Khalfi, Bechir Hamdaoui, and Mohsen Guizani. Power allocation analysis for dynamic power utility in cognitive radio systems. In *Com-

munications (ICC), IEEE International Conference on, pages 3732–3737. IEEE, 2015.

[11] Mohamed Grissa, Attila Yavuz, and Bechir Hamdaoui. Lpos: Location privacy for optimal sensing in cognitive radio networks. In *proc. of IEEE GLOBECOM*, pages 1–6. IEEE, 2015.

[12] Mohamed Grissa, Attila Yavuz, and Bechir Hamdaoui. An efficient technique for protecting location privacy of cooperative spectrum sensing users. In *proc of IEEE INFOCOM WKSHPS*, pages 915–920, 2016.

[13] Mohamed Grissa, Attila A Yavuz, and Bechir Hamdaoui. Preserving the location privacy of secondary users in cooperative spectrum sensing. *IEEE Trans. on Information Forensics and Security*, 12(2):418–431, 2017.

[14] Mohsen Guizani, Bassem Khalfi, Mahdi Ben Ghorbel, and Bechir Hamdaoui. Large-scale cognitive cellular systems: resource management overview. *IEEE Communications Magazine*, 53(5):44–51, 2015.

[15] Bechir Hamdaoui. Adaptive spectrum assessment for opportunistic access in cognitive radio networks. *IEEE Trans. on Wireless Communications*, 8(2):922–930, 2009.

[16] Bechir Hamdaoui and Kang G Shin. Os-mac: An efficient mac protocol for spectrum-agile wireless networks. *IEEE Transactions on Mobile Computing*, 7(8):915–930, 2008.

[17] Rami Hamdi, Mahdi Ben Ghorbel, Bechir Hamdaoui, Mohsen Guizani, and Bassem Khalfi. Implementation and analysis of reward functions under different traffic models for distributed dsa systems. *IEEE Transactions on Wireless Communications*, 14(9):5147–5155, 2015.

[18] M Amin Khajehnejad, Weiyu Xu, A Salman Avestimehr, and Babak Hassibi. Analyzing weighted minimization for sparse recovery with nonuniform sparse models. *IEEE Trans. on Signal Processing*, 59(5):1985–2001, 2011.

[19] Bassem Khalfi, Mahdi Ben Ghorbel, Bechir Hamdaoui, and Mohsen Guizani. Dynamic power pricing using distributed resource allocation for large-scale dsa systems. In *Wireless Communications and Networking Conference (WCNC)*, pages 1090–1094. IEEE, 2015.

[20] Bassem Khalfi, Bechir Hamdaoui, Mohsen Guizani, and Nizar Zorba. Exploiting wideband spectrum occupancy heterogeneity for weighted compressive spectrum sensing. In *Computer Communications Workshops (INFOCOM WKSHPS), IEEE Conference on*, pages 1–6, 2017.

[21] Khaled Ben Letaief and Wei Zhang. Cooperative communications for cognitive radio networks. *Proc. of the IEEE*, 97(5):878–893, 2009.

[22] Yingqi Lu, Pai Zhu, Donglin Wang, and Michel Fattouche. Machine learning techniques with probability vector for cooperative spectrum sensing in cognitive radio networks. In *Proc. of Wireless Communications and Networking Conference (WCNC)*, pages 1–6. IEEE, 2016.

[23] Deanna Needell, Rayan Saab, and Tina Woolf. Weighted ℓ_1-minimization for sparse recovery under arbitrary prior information. *arXiv preprint arXiv:1606.01295*, 2016.

[24] MohammadJavad NoroozOliaee, Bechir Hamdaoui, and Kagan Tumer. Efficient objective functions for coordinated learning in large-scale distributed osa systems. *IEEE Trans. on Mobile Computing*, 12(5):931–944, 2013.

[25] Vilaskumar M Patil and Siddarama R Patil. A survey on spectrum sensing algorithms for cognitive radio. In *2016 International Conference on Advances in Human Machine Interaction (HMI)*, pages 1–5. IEEE, 2016.

[26] Fabian Pedregosa, Gaël Varoquaux, Alexandre Gramfort, Vincent Michel, Bertrand Thirion, Olivier Grisel, Mathieu Blondel, Peter Prettenhofer, Ron Weiss, Vincent Dubourg, et al. Scikit-learn: Machine learning in python. *Journal of Machine Learning Research*, 12(Oct):2825–2830, 2011.

[27] Z. Qin, Y. Gao, M. D. Plumbley, and C. G. Parini. Wideband spectrum sensing on real-time signals at sub-Nyquist sampling rates in single and cooperative multiple nodes. *IEEE Trans. on Signal Processing*, 64(12):3106–3117, Jun. 2016.

[28] Zhijin Qin, Yue Gao, and Clive G Parini. Data-assisted low complexity compressive spectrum sensing on real-time signals under sub-Nyquist rate. *IEEE Trans. on Wireless Communications*, 15(2):1174–1185, 2016.

[29] Alex J Smola and Bernhard Schölkopf. A tutorial on support vector regression. *Statistics and computing*, 14(3):199–222, 2004.

[30] Karaputugala Madushan Thilina, Kae Won Choi, Nazmus Saquib, and Ekram Hossain. Machine learning techniques for cooperative spectrum sensing in cognitive radio networks. *IEEE JSAC*, 31(11):2209–2221, 2013.

[31] Namrata Vaswani and Wei Lu. Modified-CS: Modifying compressive sensing for problems with partially known support. *IEEE Trans. on Signal Processing*, 58(9):4595–4607, 2010.

[32] Pavithra Venkatraman, Bechir Hamdaoui, and Mohsen Guizani. Opportunistic bandwidth sharing through reinforcement learning. *IEEE Trans. on Vehicular Technology*, 59(6):3148–3153, 2010.

[33] Mümtaz Yılmaz, Damla Gürkan Kuntalp, and Akan Fidan. Determination of spectrum utilization profiles for 30 MHz–3 GHz frequency band. In *Proc. of IEEE International Conference on Communications (COMM)*, pages 499–502, 2016.

Distributed Wideband Sensing for Faded Dynamic Spectrum Access with Changing Occupancy

Bassem Khalfi, Abdurrahman Elmaghbub, and Bechir Hamdaoui

Chapter 5: Manuscript 4: Distributed Wideband Sensing for Faded Dynamic Spectrum Access with Changing Occupancy

Bassem Khalfi, Abdurrahman Elmaghbub, Bechir Hamdaoui

Oregon State University

{khalfib,elmaghba,hamdaoui}@eecs.oregonstate.edu

Abstract

We propose a distributed compressive sampling technique for cooperative wideband spectrum sensing that requires lesser numbers of measurements while overcoming time-variability of spectrum occupancy and the hidden terminal problem. First, we prove that the wideband spectrum occupancy information can almost surely be recovered with reduced numbers of spectrum measurements. Second, we propose non-uniform sensing matrices design that exploits the heterogeneity in the wideband spectrum access to further improve the spectrum sensing recovery accuracy. Using simulations, we confirm our theoretic results and show that cooperation leads to high detection probability, even with each SU taking only a small number of measurements. We also show that it is sufficient to consider a subset of close-by SUs to obtain comparable performances.

Index terms— Heterogeneous wideband access; distributed compressive sampling; cooperative spectrum sensing.

5.1 Introduction

Dynamic spectrum access (DSA) emerges as a key technology for overcoming spectrum shortage problems [7]. Due to its great potential, DSA has already found its way to standardization—e.g., IEEE 802.22 [5] for enabling opportunistic access in the TV bands and 3GPP's Licensed-Assisted Access (LAA) and LTE-U [4] for enabling spectrum access in the unlicensed 5 GHz band. Spectrum sensing is vital to enabling successful DSA, and as a result, has been studied thoroughly in the literature. Most of the sensing technique development effort, however, has been focused on narrow band access, and

not until recently, has it attracted some attention for the wideband spectrum access case [16, 8, 15].

Performing wideband spectrum sensing (WSS) through traditional methods has been shown ineffective, by incurring excessive delays, costly hardware, and/or high energy consumption; for instance, sequential sensing approaches require cheap hardware, but incur high sensing delays, whereas, parallel sensing approaches overcome delay issues, but require more hardware [19]. Frequency-domain analysis methods, on the other hand, require sampling rates that are excessively high for the case of wideband, which can be feasible only through complex hardware circuitry and processing algorithms. More insights into the limitations of traditional sensing methods when applied to WSS can be found in [19].

Motivated by the sparsity feature inherent to spectrum occupancy and in an effort to address the high sampling rate limitation, researchers have resorted to exploiting compressive sampling (CS) theory to make WSS possible at reasonable sampling rates (e.g. [16, 13, 8]). In essence, these CS-based sensing approaches require a number of measurements that is much smaller than what traditional non-CS-based approaches require [6]. Despite the ability of these CS-based approaches to overcome the high sampling rate limitation, there remains a number of key challenges that limit their applicability in practice. These challenges are:

- *Limited receiver hardware:* The number of measurements that receiver hardware designs are able to perform is practically way smaller than the number of measurements required by the CS-based sensing approaches. Therefore, multiple sequential sensing scans are often required to enable CS-based spectrum occupancy recovery, which leads to excessive recovery delays, making these CS-based approaches unsuitable for realtime applications.

- *Uncertain and time-varying spectrum occupancy:* The number of measurements required by the CS-based sensing approaches depends on the number of occupied bands (i.e., sparsity level). However, the sparsity level is often unknown in advance and changes over time, making it more challenging for CS-based sensing approaches to achieve accurate and robust recovery without incurring unreasonable amounts of overhead.

- *Measurement inconsistency across the different SU s:* Due to impairments of the

wireless channel, different secondary users (SUs) may observe different spectrum occupancy, leading to inconsistent measurements across the users. This poses a challenge when using CS-based approaches for cooperative occupancy recovery.

This paper combines user cooperation with compressive sampling to propose a practical WSS technique that overcomes these three aforementioned challenges. In addition, unlike most previous approaches in which the entire wideband is considered as one single block with a fixed, global sparsity level, our work considers a more realistic, *non-homogeneous* WSS. In practice indeed, the wideband spectrum occupancy is rather *heterogeneous*, with different frequency blocks exhibiting different occupancy behaviors and statistics [20, 12, 10]. This is mainly because applications of similar types (cellular, TV, etc.) are often assigned spectrum bands within the same (or nearby) frequency block, and different application types show different occupancy patterns, resulting in a non-homogeneous wideband spectrum occupancy. Unlike previous works, our proposed technique exploits the heterogeneity information in wideband spectrum occupancy to provide further improvement of the spectrum recovery efficiency. To this end, the main contributions of this paper are:

- We propose a distributed, cooperative CS-based sensing technique for wideband access in faded environments, and prove that the proposed technique recovers the occupancy information with fewer spectrum measurements.

- We show that the number of required measurements can be reduced even further while maintaining a high recovery accuracy by exploiting user closeness.

- We design efficient sensing matrices that capture and leverage prior knowledge about the spectrum occupancy heterogeneity to improve the occupancy recovery accuracy of the CS-based sensing approaches.

The rest of this paper is organized as follows. Section 5.2 describes the system model. Section 5.3 presents current CS-based sensing approaches along with their challenges. Section 5.4 presents the proposed techniques. Section 5.5 presents the numerical evaluations. Section 5.6 concludes the paper.

5.2   Wideband Spectrum Sensing Model

We consider a heterogeneous WSS system with N frequency bands and denote the support of the occupied bands by Ω. We assume that the wideband spectrum accommodates multiple different types of user applications, where applications of the same type are allocated frequency bands within the same block. That is, the N narrow bands are grouped into g disjoint contiguous blocks, with each block, $\mathtt{G_i}$, consisting of $\mathtt{N}_i$ contiguous bands, being assigned to one application type. For simplicity, we model the state of each band i using a Bernoulli(p_i) with parameter $p_i \in [0, 1]$ where p_i is the probability that band i is occupied by some primary user (PU). We assume every PU can only occupy one band. Let $\bar{\mathtt{K}}_j = \sum_{i \in \mathtt{G_j}} p_i$ be the average number of bands occupied within block j (assuming independence across band occupancies). As observed via real measurement studies [20, 12, 10], the band occupancy statistics (e.g., $\bar{\mathtt{K}}_j$) vary from one block to another; that is, the spectrum occupancy in wideband access exhibits a *block-like occupancy behavior* where the spectrum occupancy can vary significantly from one block to another.

We also consider that the WSS system has J SUs that are able and willing to perform the sensing task. The time-domain signal $\boldsymbol{r}(t)$ received by each SU can be expressed as

$$\boldsymbol{r}(t) = \sum_{i=1}^{\mathtt{N}_{sig}} h_i(t) \otimes s_i(t) + w(t), \tag{5.1}$$

where $h_i(t)$ is the channel impulse response between the PUs and the SU, $s(t)$ is the primary user's signal with power P, $w(t)$ is an Additive White Gaussian Noise with mean 0 and variance $\mathtt{NN_0}$, $\otimes$ is the convolution operator, and $\mathtt{N}_{sig}$ is the number of active primary users (PUs) (for simplicity $\mathtt{N}_{sig}$ is assumed to be equal to the number of occupied bands).

The discrete Fourier transform of the received signal $\boldsymbol{r}(t)$ can be expressed as

$$\boldsymbol{r}_f = \boldsymbol{h}_f \boldsymbol{s}_f + \boldsymbol{w}_f = \mathtt{x} + \boldsymbol{w}_f, \tag{5.2}$$

where $\boldsymbol{h}_f$, $\boldsymbol{s}_f$, and $\boldsymbol{w}_f$ are the Fourier transforms of $\boldsymbol{h}(t)$, $\boldsymbol{s}(t)$, and $\boldsymbol{w}(t)$, respectively. Here, we assume that $\mathbb{E}(\boldsymbol{s}(t)) = 0$. The vector $\mathtt{x}$ in Eq. (5.2) represents the faded version of the PUs' signals being sent on the different bands. Since $\boldsymbol{s}_f$ is independent of $\boldsymbol{h}_f$, $\mathbb{E}(\mathtt{x}) = 0$. The vector $\boldsymbol{r}_f$ is nearly sparse with energy levels in the unoccupied bands

being equal to $\mathbb{E}(\boldsymbol{w}_f^2) = \mathtt{N_0}$.

5.3 Compressive Sampling-based Sensing: Current Approaches and their Limitations

Recall that the number of samples needed to recover the occupancy information through classical frequency-domain analysis methods can be excessively large, especially when the spectrum is wideband, making such methods unpractical. To overcome this issue, compressive sampling (CS) theory has been leveraged to take advantage of the sparsity nature of the spectrum occupancy vector $\mathtt{x}$ to reduce the number of required samples [6]. More specifically, the signal resulting from applying CS theory can be written as [8]:

$$\mathtt{y} \;=\; \Phi\mathtt{F}^{-1}(\mathtt{x} + \boldsymbol{w}_f) = \Psi\mathtt{x} + \eta, \tag{5.3}$$

where $\mathtt{y} \in \mathbb{R}^{\mathtt{M}}$ is the measurement vector, $\mathtt{F}^{-1}$ is the inverse discrete Fourier transform (as $\mathtt{x}$ is sparse in the Fourier basis), Φ is the $\mathtt{M} \times \mathtt{N}$ sensing matrix assumed to be full rank, i.e. $\mathtt{rank}(\Phi) = \mathtt{M}$, and $\mathtt{M} = \mathcal{O}(\mathtt{K}\log(\mathtt{N/K})$ [6]. The coefficients of Φ are drawn from a Bernoulli distribution $\{\frac{\pm 1}{\sqrt{\mathtt{M}}}\}$ and the sensing noise η is equal to $\Phi\mathtt{F}^{-1}\boldsymbol{w}_f$. From a hardware perspective, the number of measurements $\mathtt{M} = \mathcal{O}(\mathtt{K}\log(\mathtt{N/K})$ corresponds to the number of hardware branches each SU device needs to have to be able to perform the CS-based sensing, with each branch using a pseudo-random sequence mixer corresponding to a raw of Φ [13, 19].

5.3.1 CS-Based Wideband Spectrum Sensing

Broadly speaking, there are two classes of CS-based approaches that can be used to recover the spectrum occupancy vector $\mathtt{x}$ from the measurement vector $\mathtt{y}$ (Eq. (5.3)). These are (i) heuristic approaches, such as BP [2] and OMP [17], which are fast and easy to implement, but may not be very accurate, and (ii) convex relaxation approaches which allow for more robust and accurate recovery, but require more computation. One widely known approach of the latter class is LASSO [3, 6], which recovers the occupancy vector $\mathtt{x}$ by solving

$$\mathscr{P}_{\mathtt{LASSO}} : \min_{\mathtt{z}} \|\mathtt{z}\|_{\ell_1} \quad \text{s.t.} \quad \|\Psi\mathtt{z} - \mathtt{y}\|_{\ell_2} \leq \epsilon \tag{5.4}$$

where ϵ is a pre-defined error threshold parameter. `wLASSO` (or weighted LASSO) [11] is another convex relaxation approach which exploits the spectrum occupancy variability observed across the different frequency blocks to allow for a more efficient solution search, thereby requiring lesser numbers of measurements and/or incurring smaller errors when compared to LASSO [11]. Formally, by referring to $\mathscr{P}_{\texttt{LASSO}}$ (Eq. (5.4)), re-writing the vector variable $\mathbf{z}$ as $\mathbf{z} = [\mathbf{z}_1^T, \mathbf{z}_2^T, \ldots, \mathbf{z}_{\mathbf{g}}^T]^T$ where $\mathbf{z}_i$ is the $\mathbf{N}_i \times 1$ vector corresponding to block i for $i = 1, 2, \ldots, \mathbf{g}$, and assigning for each block i a weight $\omega_{\mathbf{i}}$ such that $\omega_{\mathbf{i}} > \omega_{\mathbf{j}}$ when $\bar{\mathbf{K}}_i < \bar{\mathbf{K}}_j$ for all blocks i, j, `wLASSO` recovers $\mathbf{x}$ by solving

$$\mathscr{P}_{\texttt{wLASSO}} : \min_{\mathbf{z}} \ \sum_{i=1}^{\mathbf{g}} \omega_{\mathbf{i}} \|\mathbf{z}_{\mathbf{i}}\|_{\ell_1} \ \ \text{s.t.} \ \ \|\Psi\mathbf{z} - \mathbf{y}\|_{\ell_2} \leq \epsilon \tag{5.5}$$

Here, the weights are chosen such that a block with a higher sparsity level is assigned a smaller weight; one way of meeting this requirement is to set $\omega_{\mathbf{i}} = (1/\bar{\mathbf{K}}_{\mathbf{i}})/\sum_{\mathbf{j}=1}^{\mathbf{g}}(1/\bar{\mathbf{K}}_{\mathbf{j}})$.

5.3.2 Challenges with Current CS-Based Sensing Approaches

Recall that the number of measurements needed for the CS-based sensing approaches to successfully recovery the occupancy is $\mathbf{M} = \mathcal{O}(\mathbf{K}\log(\mathbf{N}/\mathbf{K}))$ [13, 19], which depends on the total number of bands, $\mathbf{N}$, and the sparsity level of spectrum occupancy, $\mathbf{K}$. This gives rise to the following two challenges.

- **Challenge 1: Hardware limitation.** The number of hardware branches needed to enable the CS-based recovery can be high and unpractical. For example, even when the number of occupied bands is as small as $K = 6$, the number of needed branches for a total number of bands $N = 50$ can be as high as $\mathbf{M} = 16$ [19]. In practice, however, the number of branches that reasonable receiver designs have is typically in the order of 4 to 8 [18], a number that is much smaller than the number of measurements, $\mathbf{M}$, required by the CS-based approaches. Therefore, hardware presents a major limitation on the applicability of such CS-based approaches.

- **Challenge 2: Uncertain and time-varying sparsity.** The second challenge that these CS-based approaches also face is that the number of occupied bands (i.e., the sparsity level) is time-varying. Most CS-based approaches, however, assume that the sparsity level, $\mathbf{K}$, is fixed, often done by setting it to the overall average

occupancy of the spectrum [16, 9]. Therefore, the time variability of the sparsity of the wideband occupancy makes existing approaches either inaccurate or incur high overhead.

In general, from a practical viewpoint, cooperative spectrum sensing approaches are more effective than non-cooperative approaches, since they are designed with the aim of providing spectrum availability information not only to just one SU, but to multiple SU s, often located in different geographic locations. Clearly, having each SU perform the CS-based spectrum sensing task on its own can be costly and redundant, as it might suffice for one SU to perform sensing and share it with other SUs, thereby saving SUs' energy and computation resources. Despite all the known benefits of cooperation, there is another major challenge that needs to be addressed to enable cooperative CS-based sensing.

- **Challenge 3: Inconsistent observations.** In practice, different SUs may observe different spectrum occupancy due to wireless channel impairments (e.g., fading, multipath, etc.), leading to inconsistent measurements across the different users. This presents a challenge when it comes to using CS-based sensed measurements to collaboratively recover spectrum occupancy information. This problem captures the hidden terminal problem as a special case.

5.4   The Proposed WSS Technique

In this work, we propose a cooperative, distributed compressed sensing technique for wideband spectrum access that overcomes the three above challenges. In addition, our proposed technique allows exploiting any prior knowledge about the spectrum occupancy statistics to improve the recovery accuracy further.

5.4.1   The Proposed Spectrum Recovery Approach

Although, due to fading, each SU observes a different spectrum occupancy vector $\mathbf{x}$, most SUs observe the same support of the (nearly) sparse occupancy vector. Hence, to be able to detect the support, we propose to compute, for every SU j, the contribution $\xi_{j,n}$ of every column of SU j's sensing matrix, Ψ_j, to $\mathbf{y}_j$ on each band n; i.e., $\xi_{j,n} =$

$\langle \mathbf{y}_j, \psi_{j,n} \rangle^2 = (\mathbf{y}_j^T \psi_{j,n})^2$ for $n = 1..\mathtt{N}$. Based on this, we define the sample mean in every bands n as

$$\xi_n = \frac{1}{\mathtt{J}} \sum_{j=1}^{\mathtt{J}} \xi_{j,n} = \frac{1}{\mathtt{J}} \sum_{j=1}^{\mathtt{J}} \langle \mathbf{y}_j, \psi_{j,n} \rangle^2 \text{ for } n = 1..\mathtt{N} \tag{5.6}$$

Once ξ_n is computed, the indexes corresponding to the $\mathtt{K}$ highest values among the $\mathtt{N}$ statistics are selected iteratively. We refer to this technique as *spectrum occupancy recovery*. Although inspired by the approach proposed in [1], our proposed recovery approach differs in the following aspects: in our work, (i) the signal occupying each band is not Gaussian, but rather follows a mixed Rayleigh and Gaussian distribution in the occupied bands that depends on the distance between each SU and the active PU, and Gaussian with mean 0 and variance $\mathtt{N_0}$ in the unoccupied bands (nearly sparse signal); (ii) the sensing matrices are non-uniform Bernoulli, where elements in column i have mean 0 and variance $\frac{1}{\omega_i^2}$; and (iii) the sensing matrices contain a very small number of measurements $\mathtt{M}$, making their columns highly correlated (orthogonality between columns is hard to meet). Algorithm 2 presents our proposed iterative approach for recovering the occupied support. Recall that we are only interested in detecting the support rather than actual signal values in every band.

Algorithm 2 Spectrum Occupancy Recovery

Require: $\mathbf{y}_j$, Ψ_j, $\mathbf{r}_{j,0} = \mathbf{y}_j$, $j = 1..J$, $k = 1$

1: **while** $\|\mathbf{r}_{j,k}\|_{\ell_2} \geq \epsilon \|\mathbf{y}_j\|_{\ell_2}$, $j = 1..\mathtt{N}$ **do**

2:     $n_k = \arg\max_{n \in \{1..\mathtt{N}\}} \frac{1}{J} \sum_{j=1}^{\mathtt{J}} |\langle \mathbf{r}_{j,k-1}, \psi_{j,n} \rangle|^2$

3:     $\Omega = \Omega \bigcup \{n_k\}$

4:     $\mathbf{r}_{j,k} = \mathbf{r}_{j,k-1} - \frac{\langle \mathbf{r}_{j,k-1}, \psi_{j,n_k} \rangle}{\|\psi_{j,n_k}\|_{\ell_2}^2} \psi_{j,n_k}$

5:     $k = k + 1$

6: **end while**

7: **return** Ω

Now that we presented an algorithm that leverages cooperation to recover the occupied support of a wideband spectrum from only a very small number of measurements per SU, in the next section, we focus on studying the correctness of such an algorithm by proving that indeed it recovers the true support Ω with an overwhelming probability.

5.4.2 Correctness of the Proposed Spectrum Recovery Approach

The following theorem states that by considering a large number of SUs, Ω can almost surely be recovered from only a small number of measurements per SU.

Theorem 5. *Consider* $\mathtt{J}$ *SUs, and let the measurement matrix* Ψ_j *of SU j contain independent Bernoulli elements, with column i's elements being set to* $\{\frac{\pm 1}{\omega_i}\}$. *The vector* $\mathbf{x}$ *is nearly sparse such that* $\mathbf{x}_\ell$ *is i.i.d. Gaussian with zero mean and variance* $\mathtt{N_0}$ *if* $\ell \notin \Omega$ *and zero mean and variance* $\mathbb{E}(x_\ell^2) > \mathtt{N_0}$, *if* $\ell \in \Omega$. *With* $\mathtt{M} > 1$ *measurements per SU,* **Algorithm 2** *recovers* Ω *with a probability approaching one as* $\mathtt{J} \to \infty$.

Remark 5. Observe that our proposed sensing matrix is by design chosen to non-uniformly distributed; this is done so that to allow the exploitation of any prior knowledge about the spectrum occupancy statistics to improve recovery accuracy. This will be shown later in Section 5.4.4.

Proof. The proof is based on Kolmogorov's Strong Law of Large Numbers (SLLN) [14], following the same line of argument as in [1]. The main idea is to show that ξ_n in an occupied band n when $\mathtt{J}$ increases is sufficiently high compared to when the band n is not occupied. Due to space limitation, some of the details in the proof are omitted. However, we provide all that is required to guide the reader to the complete proof.

SLLN [14] states that the sample mean $\bar{\mathtt{X}}_n = \frac{1}{n}\sum_{i=1}^{n} \mathtt{X}_i$ of n independent random variables, $\mathtt{X}_1$, $\mathtt{X}_2$, $\cdots$, $\mathtt{X}_n$, with finite expectations $(\mathbb{E}(\mathtt{X}_n) < \infty$ for $n \geq 1)$ converges almost surely to $\mathbb{E}(\mathtt{X}_n)$; i.e., $\mathbb{P}(\lim_{n\to\infty} \bar{\mathtt{X}}_n = \mathbb{E}(\mathtt{X}_n)) = 1$,

and that SLLN holds if one of the following conditions is satisfied:

1. $\mathtt{X}_1$, $\mathtt{X}_2$, $\cdots$, $\mathtt{X}_n$ are identically distributed.

2. $\mathbb{V}ar[\mathtt{X}_n] < \infty$ and $\sum_{n=1}^{\infty} \frac{\mathbb{V}ar[\mathtt{X}_n]}{n^2} < \infty$ for all n.

Considering $\xi_{j,n} = \langle \mathbf{y}_j, \boldsymbol{\psi}_{j,n} \rangle^2$, first we need to prove that these $\xi_{j,n}$ have finite expectations. Then, since $\xi_{j,n}$ are not identically distributed (due to the presence of fading), we have to prove the second part of Kolmogorov's theorem. Therefore, we start by computing the mean and variance of $\xi_{j,n}$ for every band n to show that both are finite. Without loss of generality, we will assume that the first $\mathtt{K}$ bands are the ones that are occupied and the rest are not (contain only noise). The means and variances are given by the following proposition.

$$
\mathbb{V}ar(\xi_{j,n}) = \begin{cases}
\sum_{\ell=1}^{\text{K}} \dfrac{\mathbb{E}(x_\ell^4)\text{M}(3\text{M}-2)}{\omega_\ell^4 \omega_\text{n}^4} + 2\sum_{\ell=1}^{\text{K}}\sum_{\substack{m=1 \\ m \neq \ell}}^{\text{K}} \dfrac{\mathbb{E}(x_\ell^2)\mathbb{E}(x_m^2)}{\omega_\ell^2 \omega_\text{m}^2 \omega_\text{n}^4} + \dfrac{\text{N}_0{}^2\text{M}^4}{\omega_\text{n}^8} \\[2ex]
+6\left[\sum_{\ell=1}^{\text{K}} \dfrac{\mathbb{E}(x_\ell^2)\text{M}}{\omega_\ell^2\omega_\text{n}^2}\right]\left[\sum_{\substack{\ell=\text{K}+1 \\ \ell \neq n}}^{\text{N}} \dfrac{\text{N}_0\text{M}}{\omega_\ell^2\omega_\text{n}^2} + \dfrac{\text{N}_0\text{M}^2}{\omega_\text{n}^4}\right] + \sum_{\substack{\ell=\text{K}+1 \\ \ell \neq n}}^{\text{N}} \dfrac{\text{N}_0{}^2\text{M}(3\text{M}-2)}{\omega_\ell^4\omega_\text{n}^4} \\[2ex]
+2\sum_{\substack{\ell=\text{K}+1 \\ \ell\neq n}}^{\text{N}}\sum_{\substack{m=\text{K}+1 \\ m\neq\ell \\ m\neq n}}^{\text{N}} \dfrac{\text{N}_0{}^2\text{M}^2}{\omega_\ell^2\omega_\text{m}^2\omega_\text{n}^4} + 6\dfrac{\text{N}_0\text{M}^2}{\omega_\text{n}^4}\left[\sum_{\substack{\ell=\text{K}+1 \\ \ell\neq n}}^{\text{N}} \dfrac{\text{N}_0\text{M}}{\omega_\text{n}^2\omega_\ell^2} + \dfrac{\text{N}_0\text{M}^2}{\omega_\text{n}}\right], & \text{if } n \notin \Omega \\[3ex]
\sum_{\substack{\ell=1 \\ \ell\neq n}}^{\text{K}} \dfrac{\mathbb{E}(x_\ell^4)\text{M}(3\text{M}-2)}{\omega_\text{n}^4\omega_\ell^4} + 2\sum_{\substack{\ell=1 \\ \ell\neq n}}^{\text{K}}\sum_{\substack{p=1 \\ p\neq\ell \\ p\neq n}}^{\text{K}} \dfrac{\mathbb{E}(x_p^2)\mathbb{E}(x_\ell^2)\text{M}^2}{\omega_\text{n}^4\omega_\ell^4\omega_\text{p}^2} \\[2ex]
+6\left[\sum_{\substack{\ell=1 \\ \ell\neq n}}^{\text{K}} \dfrac{\mathbb{E}(x_\ell^2)\text{M}}{\omega_\text{n}^2\omega_\ell^2} + \dfrac{\mathbb{E}(x_\ell^2)\text{M}^2}{\omega_\text{n}^4}\right]\left[\sum_{\ell=\text{K}+1}^{\text{N}} \dfrac{\mathbb{E}(x_\ell^2)\text{M}}{\omega_\text{n}^2\omega_\ell^2}\right] \\[2ex]
+4\sum_{\substack{\ell=1 \\ \ell\neq n}}^{\text{K}} \dfrac{\mathbb{E}(x_p^2)\mathbb{E}(x_\ell^2)\text{M}^3}{\omega_\text{n}^6\omega_\ell^2} + \dfrac{\mathbb{E}(x_n^4)}{\omega_\text{n}^8} + \sum_{\ell=\text{K}+1}^{\text{N}} \dfrac{\mathbb{E}(x_\ell^4)\text{M}(3\text{M}-2)}{\omega_\text{n}^4\omega_\ell^4} \\[2ex]
+2\sum_{\ell=\text{K}+1}^{\text{N}}\sum_{\substack{p=\text{K}+1 \\ p\neq\ell}}^{\text{N}} \dfrac{\mathbb{E}(x_\ell^2)\mathbb{E}(x_p^2)\text{M}^2}{\omega_\text{n}^4\omega_\text{p}^2\omega_\ell^2}, & \text{if } n \in \Omega
\end{cases}
\tag{5.7}
$$

Proposition 6. *Consider the nth band. The mean of $\xi_{j,n}$ is*

$$
\mathbb{E}(\xi_{j,n}) = \begin{cases}
\sum_{\ell=1}^{\text{K}} \dfrac{\mathbb{E}(x_\ell^2)\text{M}}{\omega_\ell^2\omega_\text{n}^2} + \sum_{\substack{\ell=\text{K}+1 \\ \ell\neq n}}^{\text{N}} \dfrac{\text{N}_0\text{M}}{\omega_\ell^2\omega_\text{n}^2} + \dfrac{\text{N}_0\text{M}^2}{\omega_\text{n}^4}, & if\, n \notin \Omega \\[3ex]
\dfrac{\mathbb{E}(x_n^2)\text{M}^2}{\omega_\text{n}^4} + \sum_{\substack{\ell=1 \\ \ell\neq n}}^{\text{K}} \dfrac{\mathbb{E}(x_\ell^2)\text{M}}{\omega_\ell^2\omega_\text{n}^2} + \sum_{\ell=\text{K}+1}^{\text{N}} \dfrac{\text{N}_0\text{M}}{\omega_\ell^2\omega_\text{n}^2}, & if\, n \in \Omega
\end{cases}
$$

and the variance of $\xi_{j,n}$, $\mathbb{V}ar(\xi_{j,n})$, is given by Eq. (5.7).

To prove Proposition 6, we use the definitions of mean and variance and the following Lemma. However, we did not provide the complete proofs as well as the proof of the lemma due to space limitation.

Lemma 3. *Let ψ_n be the nth column of the sensing matrix Ψ whose elements are Bernoulli with zero mean and variance $\frac{1}{\omega_n^2}$. Then, we have the following results.*

$$\mathbb{E}(\langle \psi_n, \psi_\ell \rangle^2) = \frac{M}{\omega_n^2 \omega_\ell^2} \tag{5.8}$$

$$\mathbb{E}(\langle \psi_n, \psi_\ell \rangle^4) = \frac{M(3M-2)}{\omega_n^4 \omega_\ell^4} \tag{5.9}$$

$$\mathbb{E}(\langle \psi_n, \psi_\ell \rangle^2 \langle \psi_n, \psi_p \rangle^2) = \frac{M^2}{\omega_n^4 \omega_p^2 \omega_\ell^2} \tag{5.10}$$

$$\mathbb{E}(\|\psi_\ell\|^4 \langle \psi_n, \psi_\ell \rangle^2) = \frac{M^3}{\omega_n^2 \omega_\ell^6} \tag{5.11}$$

$$\mathbb{E}(\|\psi_\ell\|^4) = \frac{M^2}{\omega_\ell^4} \tag{5.12}$$

$$\mathbb{E}(\|\psi_\ell\|^8) = \frac{M^4}{\omega_\ell^8} \tag{5.13}$$

First, we need to show that both the means and the variances of $\xi_{j,n}$ for $n = 1..N$ are finite. It is sufficient to see that $\mathbb{E}(x_\ell^2)$ and $\mathbb{E}(x_\ell^4)$ are finite (upper bounded by the transmit power P and P^2) since in practice PUs are sending with finite powers. Moreover, $\sum_{j=1}^\infty \frac{\mathbb{V}ar(\xi_{j,n})}{j^2}$ is finite (upper bounded by $\max_j \mathbb{V}ar(\xi_{j,n}) \sum_{j=1}^\infty \frac{1}{j^2}$) which according to Kolmogorov's theorem is sufficient to prove that ξ_n almost surely converges to the mean given by Proposition 6. Finally, we have $\frac{1}{J} \sum_{j=1}^J \xi_{j,n}$ converge to $\mathbb{E}(\xi_{j,n})$ for $n = 1..N$. To finish the proof, we only need to show that the two means are sufficiently different. Even with uniform distribution for the sensing matrix, we still have a clear distinction between the two cases. This distinction is more important with non-uniform sensing matrix. For the sake of illustration, we show in Fig. 5.1 the ratio between the two means: when band n is occupied and when band n is not occupied for different SNRs and different values of M. ∎
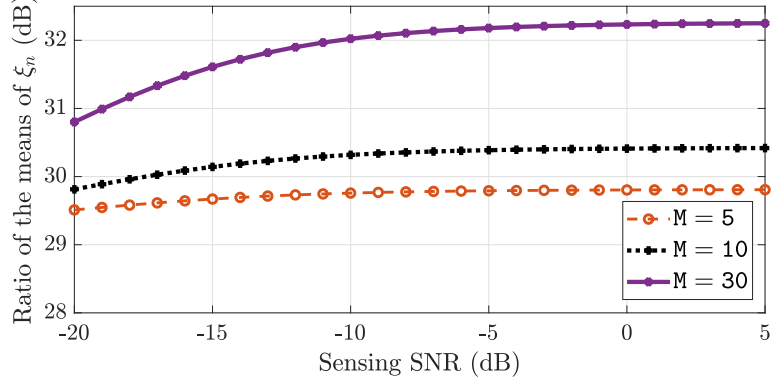
Figure 5.1: The ratio between $\mathbb{E}(\xi_n)$ when n is an occupied band and when it is not as a function of the sensing SNR and for a different number of measurements in dB. $\mathtt{N} = 256$, $\mathtt{K} = 29$, weights in the occupied bands $\omega_{\mathtt{in}} = 1/\mathtt{K}$, weights in the unoccupied bands $\omega_{\mathtt{out}} = 1$, $\mathtt{N_0} = -120dBm$.

5.4.3 Exploiting User Closeness

While the previous result brings forth the power of cooperation for overcoming the hardware limitation along with the hidden terminal problem, a large number of SUs is needed to do so. In this section, we show that by exploiting the closeness between SUs, the number of required SUs can be significantly reduced. To illustrate this further, consider two SUs with measurement vectors $\mathbf{y}_1 = \boldsymbol{\Psi}_1 \mathbf{x}_1 + \eta_1$ and $\mathbf{y}_2 = \boldsymbol{\Psi}_2 \mathbf{x}_2 + \eta_2$. When the received signals at the SUs are quite similar, say $\mathbf{x}_2 = \mathbf{x}_1 + \delta\mathbf{x}$, $\mathbf{y}_2$ can be rewritten as $\mathbf{y}_2 = \boldsymbol{\Psi}_2 \mathbf{x}_1 + \eta_2 + \boldsymbol{\Psi}_2 \delta\mathbf{x}$. This is equivalent to having one SU takes twice the number of measurements, i.e., $\mathbf{y}_c = [\mathbf{y}_1^T\ \mathbf{y}_2^T]^T$, $\boldsymbol{\Psi}_c = [\boldsymbol{\Psi}_1^T\ \boldsymbol{\Psi}_2^T]^T$, and $\eta = [\eta_1^T\ \eta_2^T + (\boldsymbol{\Psi}_2 \delta\mathbf{x})^T]^T$. With a higher number of measurements, conventional recovery approaches such as LASSO [2] and OMP [17] can be used. Clearly, as the two received signals at the SUs start to differ, it corresponds to the case of having higher noise variance, which yields a worse recovery. This approach will be evaluated in Section 5.5.

5.4.4 Non-uniform Sensing Matrix Design

So far we discussed how cooperation could be exploited to overcome the hardware limitation and the hidden terminal problem. We now propose an efficient design of the sensing
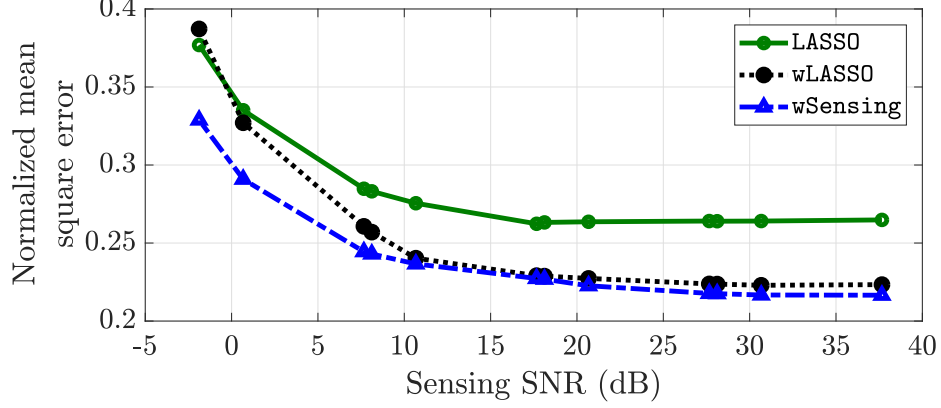
Figure 5.2: Recovery performance under nonuniform sensing matrix and weighted recovery using same parameters as in [11]. ($N = 256$, $M = 27$)

matrices that leverages prior knowledge about the spectrum occupancy to improve the recovery accuracy. We show that capturing and exploiting the heterogeneity in spectrum occupancy, which is inherent to wideband spectrum access, in the sensing matrix can indeed yield a comparable performance gain to $\mathscr{P}_{\texttt{wLASSO}}$. Recalling $\mathscr{P}_{\texttt{wLASSO}}$ given in Eq. (5.5) and letting $\texttt{p} = \texttt{Wz}$ where $\texttt{W} = \text{diag}(\underbrace{\omega_1, \cdots, \omega_1}_{N_1}, \underbrace{\omega_2, \cdots, \omega_2}_{N_2}, \cdots, \underbrace{\omega_g, \cdots, \omega_g}_{N_g})$, $\mathscr{P}_{\texttt{wLASSO}}$ could also be reformulated as

$$\mathscr{P}_{\texttt{wSensing}} : \min_{\texttt{p}} \|\texttt{p}\|_{\ell_1} \quad \text{s.t.} \quad \|\Psi\texttt{W}^{-1}\texttt{p} - \texttt{y}\|_{\ell_2} \leq \epsilon \tag{5.14}$$

The new matrix $\texttt{W}^{-1}$ magnifies the columns of the sensing matrix Ψ that correspond to high average sparsity levels (low weights), and diminishes the columns that correspond to low average sparsity levels. By doing so, the sensing energy is better allocated, and more importantly, the error achievable under Algorithm 2 is reduced. Fig. 5.2 shows the equivalence in terms of performance between the two formulations. To ensure fair comparison under the two scenarios, the elements in the sensing matrix Ψ have variance $\frac{\beta}{M}$, with $\beta = \frac{N}{(M \sum_{j=1}^{N} \frac{1}{\omega_j^2})}$. To avoid confusion, we set $\omega_i = \omega_i / \sqrt{\beta}$. The figure also shows that the new formulation is more robust to noise (better performance at low sensing SNR, with SNR defined as $\frac{\|\Psi\texttt{x}\|^2}{\|\eta\|^2}$).

5.5 Performance Evaluation Results

Consider a primary system operating over a wideband consisting of $N = 128$ bands grouped into $\mathtt{g} = 4$ blocks with equal sizes. The average probabilities of occupancy in each block are as follows: $\bar{\mathtt{K}}_1 = p_1 \times 32$, $\bar{\mathtt{K}}_2 = p_2 \times 32$, $\bar{\mathtt{K}}_3 = p_3 \times 32$, $\bar{\mathtt{K}}_4 = p_4 \times 32$, where $p_1 = p_3 = 0.1$ and $p_2 = p_4 = 0.001$. The PUs are randomly deployed in a cell and for simplicity, we assume that the number of active PUs are equal to the number of occupied bands. We assume all PUs are transmitting with constant power $\mathtt{P} = 10$ W, and the received signal in each band is affected by a Rayleigh distributed channel impulse response with mean $1/d^{\alpha/2}$. We also consider Gaussian noise, with each band experiencing Gaussian signal with zero mean and variance $N_0 = -120dBm$.

In Fig. 5.3, we plot the detection probability as a function of the number of cooperating SUs, $\mathtt{J}$. First, we observe that as the number of cooperating SUs increases, a high detection probability is achieved regardless of the number of measurements each SU is taking, thus confirming our main theorem result. This is mainly because as $\mathtt{J}$ increases, $\xi_{j,n}$ converges to its expectation $\mathbb{E}(\xi_{j,n})$, and hence, a better distinction between the bands is achieved. Second, we also observe that for a fixed $\mathtt{J}$, a high detection probability is achieved when each SU is talking a higher number of measurements.
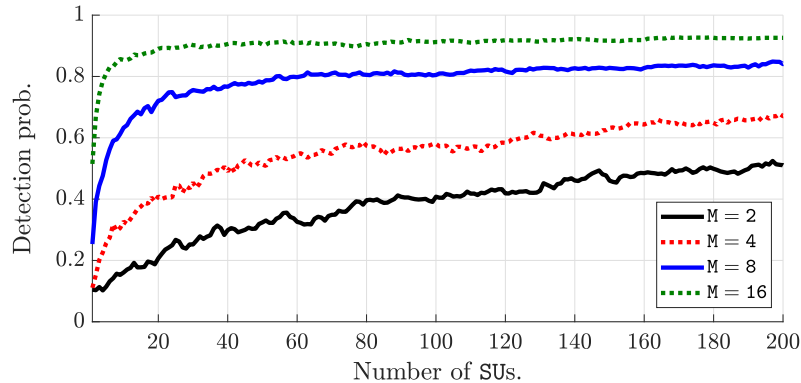
Figure 5.3: The detection probability for $\mathtt{M} = 8$ and $N = 128$.

To overcome the need for high numbers of SUs, we investigate the effect of considering only a subset of close-by SUs when performing detection using OMP and LASSO, and compare that to the previous approach. Fig. 5.4 shows that when considering close-by

SUs (6 SUs), the achieved detection probability is close to the one achieved with a high number of SUs, which confirms our observation. Second, our proposed approaches outperform sequential sensing approach proposed in [18], mainly because of their ability to overcome the hidden terminal problem.
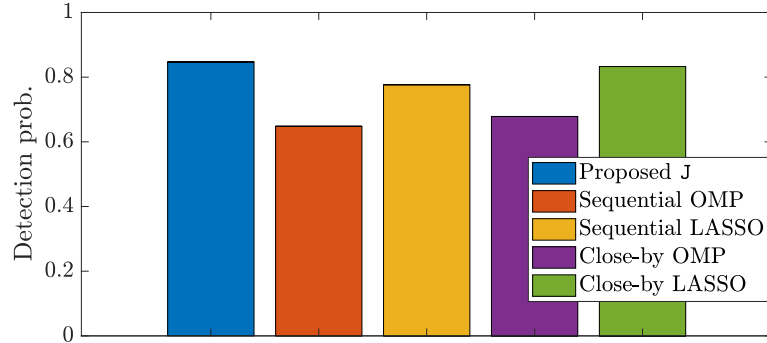
Figure 5.4: The detection probability for $M = 8$ and $N = 128$.

5.6   Conclusions

We leverage user cooperation to overcome receiver hardware limitations as well as time variability of band occupancy during wideband spectrum sensing. We show that cooperation overcomes these issues by enabling distributed compressive sampling-based spectrum sensing, and does so by requiring smaller numbers of measurements by each user only. Also, we consider heterogenous wideband spectrum access environment and design efficient non-uniform sensing matrices suitable for such an environment. Finally, we show that when the impact of fading is not so significant (for instance by considering close-by SUs), comparable performance can still be achieved from a smaller number of SUs.

Acknowledgment

Bibliography

[1] Dror Baron, Marco F Duarte, Michael B Wakin, Shriram Sarvotham, and Richard G Baraniuk. Distributed compressive sensing. *arXiv preprint arXiv:0901.3403*, 2009.

[2] Emmanuel J Candès, Justin Romberg, and Terence Tao. Robust uncertainty principles: Exact signal reconstruction from highly incomplete frequency information. *IEEE Trans. on inf. theory*, 52(2):489–509, 2006.

[3] Emmanuel J Candes, Justin K Romberg, and Terence Tao. Stable signal recovery from incomplete and inaccurate measurements. *Communications on pure and applied mathematics*, 59(8):1207–1223, 2006.

[4] Bolin Chen, Jiming Chen, Yuan Gao, and Jie Zhang. Coexistence of LTE-LAA and Wi-Fi on 5 GHz with corresponding deployment scenarios: A survey. *IEEE Comm. Surveys & Tutorials*, 19(1):7–32, 2017.

[5] Carlos Cordeiro, Kiran Challapali, Dagnachew Birru, and Sai Shankar. Ieee 802.22: the first worldwide wireless standard based on cognitive radios. In *New Frontiers in Dynamic Spectrum Access Networks, 2005. DySPAN 2005. 2005 First IEEE International Symposium on*, pages 328–337. Ieee, 2005.

[6] David L Donoho. Compressed sensing. *IEEE Trans. on information theory*, 52(4):1289–1306, 2006.

[7] Bechir Hamdaoui. Adaptive spectrum assessment for opportunistic access in cognitive radio networks. *IEEE Trans. on Wireless Communications*, 8(2):922–930, 2009.

[8] Bechir Hamdaoui, Bassem Khalfi, and Mohsen Guizani. Compressed wideband spectrum sensing: Concept, challenges and enablers.

[9] Tanbir Haque, Rabia Tugce Yazicigil, Kyle Jung-Lin Pan, John Wright, and Peter R Kinget. Theory and design of a quadrature analog-to-information converter for energy-efficient wideband spectrum sensing. *IEEE Trans. on Circuits and Systems I: Regular Papers*, 62(2):527–535, 2015.

[10] Timothy Harrold, Rafael Cepeda, and Mark Beach. Long-term measurements of spectrum occupancy characteristics. In *Proc. of IEEE Symposium on New Frontiers in Dynamic Spectrum Access Networks (DySPAN)*, pages 83–89, 2011.

[11] Bassem Khalfi, Bechir Hamdaoui, Mohsen Guizani, and Nizar Zorba. Efficient spectrum availability information recovery for wideband DSA networks: A weighted compressive sampling approach. *IEEE Trans. on Wireless Communications*, 17(4), April 2018.

[12] M Mehdawi, NG Riley, M Ammar, A Fanan, and M Zolfaghari. Spectrum occupancy measurements and lessons learned in the context of cognitive radio. In *Proc. of IEEE Telecommunications Forum Telfor (TELFOR)*, pages 196–199, 2015.

[13] M. Mishali and Y. C. Eldar. From theory to practice: Sub-Nyquist sampling of sparse wideband analog signals. *IEEE Journal of Selected Topics in Signal Processing*, 4(2):375–391, Apr. 2010.

[14] Valentin V Petrov. Limit theorems of probability theory: sequences of independent random variables. Technical report, Oxford, New York, 1995.

[15] Zhijin Qin, Yue Gao, and Clive G Parini. Data-assisted low complexity compressive spectrum sensing on real-time signals under sub-Nyquist rate. *IEEE Trans. on Wireless Communications*, 15(2):1174–1185, 2016.

[16] S. K. Sharma, E. Lagunas, S. Chatzinotas, and B. Ottersten. Application of compressive sensing in cognitive radio communications: A survey. *IEEE Communications Surveys & Tutorials*, 18(03):1838–1860, 2016.

[17] Joel A Tropp and Anna C Gilbert. Signal recovery from random measurements via orthogonal matching pursuit. *IEEE Trans. on information theory*, 53(12):4655–4666, 2007.

[18] R. T. Yazicigil, T. Haque, M. Kumar, J. Yuan, J. Wright, and P. R. Kinget. How to make analog-to-information converters work in dynamic spectrum environments with changing sparsity conditions. *IEEE Trans. on Circuits and Systems I: Regular Papers*, PP(99):1–10, 2017.

[19] Rabia Tugce Yazicigil, Tanbir Haque, Michael R Whalen, Jeffrey Yuan, John Wright, and Peter R Kinget. Wideband rapid interferer detector exploiting compressed sampling with a quadrature analog-to-information converter. *IEEE Journal of Solid-State Circuits*, 50(12):3047–3064, 2015.

[20] Mümtaz Yılmaz, Damla Gürkan Kuntalp, and Akan Fidan. Determination of spectrum utilization profiles for 30 MHz–3 GHz frequency band. In *Proc. of IEEE International Conference on Communications (COMM)*, pages 499–502, 2016.

AirMap: Scalable Spectrum Occupancy Recovery Using Local Low-Rank Matrix Approximation

Bassem Khalfi, Bechir Hamdaoui, and Mohsen Guizani

Chapter 6: Manuscript 5: AIRMAP: Scalable Spectrum Occupancy Recovery Using Local Low-Rank Matrix Approximation

Bassem Khalfi, Bechir Hamdaoui, and [†]Mohsen Guizani

Oregon State University, [†]University of Idaho

{khalfib,hamdaoui}@eecs.oregonstate.edu, [†]mguizani@ieee.org

Abstract

We propose AIRMAP, a framework for enabling scalable database-driven dynamic spectrum access and sharing. We bring together the merits of compressive sensing and collaborative filtering to provide accurate radio occupancy map while reducing the network overhead cost and overcome the scalability issue with conventional approaches. We start from an observation that close-by users have a highly correlated spectrum observation and we propose to recover the spectrum occupancy matrix in the borough of each sensing node by minimizing the rank of local submatrices. Then, we combine the recovered matrix entries using a similarity criterion to get the global spectrum occupancy map. Through simulations, we show that the proposed framework minimizes the error while reducing the network overhead. We also show that the proposed framework is scalable when considering high frequencies.

Index terms— Wideband spectrum sensing; compressive sampling; local low rank matrix completion; collaborative filtering.

6.1 Introduction

Opportunistic spectrum access has great potential for overcoming radio resource shortage challenges that wireless systems are currently facing [12]. Broadly speaking, spectrum sensing techniques that have been proposed for spectrum awareness can be categorized into two classes: sensing-based approaches [9, 13, 18, 21] and database-driven approaches [19, 7, 17, 6, 25, 22]. While the former class allows users to identify unused spectrum portions on their own via local measurements, the latter provides users with radio occupancy databases, which users can query to acquire spectrum occupancy information in their vicinity. These databases can, for example, be constructed by relying on

observations collected from sensing nodes (SNs) that are deployed specifically for this sensing task. Database-driven approaches are more attractive due to their practical appeal [19], and as a result, have recently been adopted and embraced by industries (e.g., Google [6], Spectrum Bridge [25], RadioSoft [22]), standard organizations (e.g., 5G), and government agencies (e.g., FCC [4]).

However, current spectrum database-driven approaches suffer from several shortcomings. For instance, they are primarily designed for TV white spaces [19], which represent only a small portion of the wideband spectrum that can potentially be shared. In addition, TV carrier frequencies are mostly below 1 GHz, and hence, these signals can propagate long distances, requiring only a small number of SNs to get the spectrum occupancy in a relatively wide region. Therefore, to extend spectrum databases to cover wider spectrum ranges, say 10 GHz bandwidth or more, a higher number of SNs must be deployed to be able to obtain a complete radio occupancy map covering the entire wideband spectrum, as well as to overcome the hidden terminal problem, where due to, for example, fading, different SNs may observe different primary signals, thereby leading to different occupancy decisions. Fortunately, by exploiting spectrum occupancy sparsity that is inherent to spectrum usage, compressive sensing theory [9] has been leveraged to sense widebands (e.g., 1 GHz bandwidth) at lower sensing overheads (e.g. [8]). Now given that within the same region, the spectrum occupancy seen by the different SNs can roughly be the same for some set of bands, the *occupancy matrix*[1] has a low-rank property. The aim of this work is to exploit this low rank property to construct the occupancy matrix from smaller numbers of observations/sensors [18, 21].

Let us illustrate this further with a simple example. Consider the spectrum occupancy matrix whose columns again represent the occupancy decisions taken by SNs for each band of the wideband spectrum. If the SNs are close to each other, then they roughly observe the same wideband spectrum occupancy, resulting in a low-rank spectrum occupancy matrix. Therefore, one can estimate all the entries of the spectrum matrix by only taking and relying on a small number of measurements [2, 21]. This can be done by means of the low-rank matrix theory which consists of formulating an optimization problem whose objective is to minimize the rank of the matrix, as will be detailed later. This approach is often referred to as collaborative filtering in the machine

---

[1]It is the matrix whose columns each corresponds to the occupancies of the different bands as seen by the corresponding SN.

learning community [16].

Although collaborative filtering reduces the network overhead, it fails to scale well with the number of bands. This limitation comes from the propagation nature of signals at different spectrum frequencies, and especially at high frequencies (e.g. millimeter waves) that is being adopted in 5G systems [23]. Note that SNs at different locations tend to observe a completely different spectrum occupancy, which can result in losing the low-rank property of the spectrum occupancy matrix. However, *close-by SNs do observe a similar occupancy*, which means if close-by SNs are re-arranged in the spectrum occupancy matrix based on their neighborhoods, then the low-rank property is preserved but only locally; i.e., although the entire occupancy matrix may not be low-rank, sub-matrices preserve their low-rank property. We will refer to this as *local low-rank property*. Hence, to maintain the merits of collaborative filtering in reducing network overhead while taking advantage of the cooperation, this local low-rank property can be exploited to design efficient sensing techniques suitable for database-driven wideband spectrum access.

In summary, compressive sensing and collaborative filtering are found to be useful theories for enabling cooperative wideband spectrum sensing at reduced sensing overhead. However, they suffer from a scalability issue when it comes to considering wideband spectrum (a few GHz). In this work, we propose a sensing framework that exploits the local low-rank property mentioned above to enable scalable occupancy matrix construction suitable for wideband spectrum.

Methodology and Contributions. In this paper, we present AirMap, a framework that provides accurate wideband spectrum occupancy recovery for database-driven spectrum systems. Our key motivation is to build a radio occupancy map for the wideband spectrum (e.g. 10 GHz or wider) to enable spectrum sharing. We propose to combine the merits of compressive sensing and low-rank matrix theories to reduce the sensing and network overhead while accurately acquiring the spectrum occupancy in the borough of each SN. Unlike previous works, our work relies on *local low-rank matrix approximation* to get the complete spectrum occupancy in the neighborhood of each SN. That is, instead of completing the spectrum occupancy matrix such that it has a low-rank property, we propose to focus on exploiting the local low-rank property. This stems from the fact that neighboring SNs tend to observe the same spectrum occupancies.

The main contributions of this work are:

- We propose an efficient sensing framework that enables scalable construction of the spectrum occupancy matrix for wideband spectrum access and sharing.

- To the best of our knowledge, we are the first to use and combine local low-rank matrix approximation theory with compressive sampling to enable scalable wideband spectrum occupancy recovery at low overhead.

- We construct the spectrum sub-matrices using propagation models suitable for wideband spectrum. This allows to improve the estimation of the observations reported in edges of the regions, thereby enhancing the accuracy of the proposed recovery approach.

The proposed framework can be combined with existing signal classification approaches (e.g., [11]) to help identify signal types. This can be very useful in applications such as spectrum monitoring and enforcement [11].

The rest of this paper is organized as follows. Section 6.2 describes the proposed framework and the intuition behind it. Section 6.3 discusses the proposed local low rank based spectrum occupancy matrix recovery as well as its performance. Section 6.4 presents the numerical evaluation. Section 6.5 reviews the related works. This work is concluded in Section 6.6.

6.2   Wideband Spectrum Occupancy Recovery Framework

6.2.1   Framework Overview

We propose AIRMAP, a scalable sensing framework that is suitable for database-driven wideband spectrum access and sharing. AIRMAP relies on a set of J *SN*s deployed on a region of interest to construct and update the database (*DB*) with accurate occupancy information of I bands in the borough of these *SN*s. Here, we assume that the entire wideband spectrum is composed of I bands. The different components of AIRMAP are illustrated in Fig. 6.1. First, it is important to mention that our focus in this work is on a *DB* covering very wideband spectrum, e.g. more than 10 GHz. We assume that the *SN*s leverage compressive sampling theory that exploits spectrum occupancy sparsity to enable sub-Nyquist spectrum sampling rates (e.g., [14]). However, even with sub-Nyquist sampling rates, each *SN* is assumed not to able to sense the entire spectrum of interest
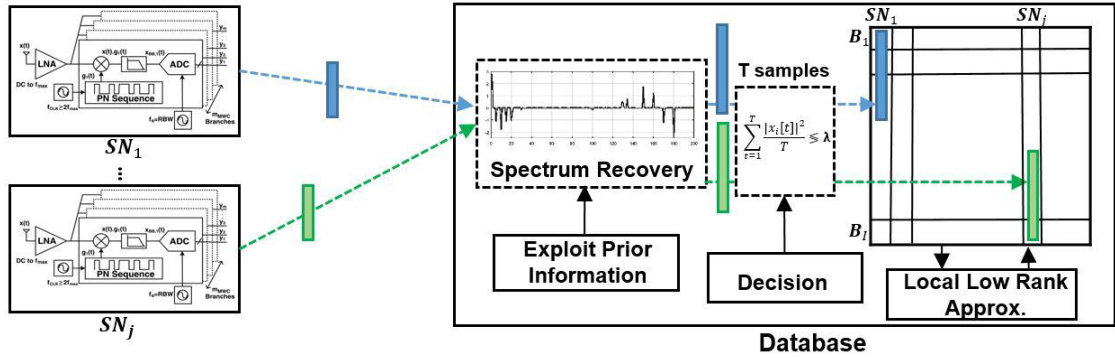
Figure 6.1: An overview of the different components of AirMap.

due to its wideness, but rather senses a portion of it; say 1 GHz bandwidth as done in [9]. To reduce the computation and the reporting overheads, the compressed measurements are reported to the *DB* which recovers the spectrum occupancy of the portion sensed by each *SN* by exploiting prior information about the spectrum occupancy. Typically, different spectrum portions are assigned to different types of applications, each with a different occupancy statistics [5]. The *DB* exploits this occupancy heterogeneity across the different spectrum portions, as proposed in [13], to recover occupancies of the entire spectrum.

A major problem in spectrum sensing is the hidden terminal problem, which we address in this framework by relying on multiple *SN*s deployed across the entire region of interest to provide redundant sensing of each portion of the spectrum. Now since having each *SN* sense all portions of the entire spectrum is impractical, we propose to use *local low-rank approximation* to efficiently recover the spectrum occupancy in the borough of each of the J *SN*s.

To sum up, AirMap consists of: (*i*) having each *SN* sense a small portion of the wideband spectrum of interest, (*ii*) recovery of band occupancies of all the portions at the *DB* by exploiting a priori information about the spectrum occupancy statistics, and (*iii*) completion of the occupancy matrix by using low-rank approximation theory to recover the missing band occupancies. Next, we will detail each of these phases.

6.2.2 Sub-Nyquist Wideband Spectrum Sensing and Recovery

6.2.2.1 Spectrum Occupancy Model

We consider a practical scenario where a wideband spectrum is allocated to multiple applications; e.g., aviation, satellite communications and maritime, wireless communications, TV broadcasting, ISM, etc. [5]. Applications of the same type are typically allocated bands within the same block. Hence, the spectrum is considered to have a block-like occupancy structure, where each block (accommodating applications of a similar type) has different occupancy behavioral characteristics. The wideband spectrum can then be grouped into $\mathtt{g}$ disjoint contiguous blocks, $\mathtt{G}_i, i = 1, \cdots, \mathtt{g}$, with $\mathtt{G}_i \bigcap \mathtt{G}_j = \emptyset$ for $i \neq j$. Each block, $\mathtt{G}_i$, is a set of n_i contiguous bands such that $\mathtt{I} = \sum_{i=1}^{\mathtt{g}} n_i$. Now provided that the actual spectrum occupancy has been observed to be under-utilized; i.e, the total number of occupied bands is small, wideband spectrum sensing can be enabled at sub-Nyquist sampling rates [8, 18]. However, even with sub-Nyquist sampling rates, given that the spectrum of interest is wideband, it is unpractical to assume that each *SN* can sense the entire spectrum. Therefore, in this work, we assume that each *SN* can only sense few, $\mathtt{g}_b$ contiguous spectrum blocks out of the $\mathtt{g}$ blocks.

6.2.2.2 Compressed Wideband Spectrum Sensing

Exploiting the fact that the spectrum is under-utilized, compressive sampling theory allows to sense and recover the n bands using $m < n$ branches [9]. After tuning to the block of bands of interest, each branch uses an independent pseudo-random (PN) sequence mixed with the received signal to yield a measurement vector [8]

$$\boldsymbol{y} \;\; = \;\; \Psi \mathtt{F}^{-1}(\boldsymbol{x} + \boldsymbol{w}_f) = \mathtt{A}\boldsymbol{x} + \boldsymbol{\eta}, \tag{6.1}$$

where $\boldsymbol{y} \in \mathbb{R}^m$ is the measurement vector taken by each *SN*, $\mathtt{F}^{-1}$ is the inverse discrete Fourier transform, and Ψ is the sensing matrix assumed to have a full rank, i.e. $\mathtt{rank}(\Psi) = m$. Here, Ψ contains the m PN sequences generated at the mixer.

After collecting the compressed measurements, and in order to reduce the reporting overhead as well as the computation complexity at the *SN*s, the compressed measurements are sent to the *DB* to recover the different bands' occupancy as observed by each

SN.

6.2.2.3 Heterogeneous Spectrum Occupancy Recovery

In AIRMAP, the *DB* exploits the occupancy variability across the different blocks to recover the spectrum occupancy information [13]. In essence, this approach encourages the search of the occupied bands in the blocks that have higher average sparsity levels. Such a variability in the block sparsity levels can be incorporated in the formulation through carefully designed weights and formulated as the following weighted ℓ_1-minimization recovery scheme

$$\mathscr{P}_1 : \min_{\boldsymbol{x}} \sum_{i=1}^{\mathsf{g}_b} \omega_i \|\boldsymbol{x}_i\|_{\ell_1} \text{ s.t. } \|\mathtt{A}\boldsymbol{x} - \boldsymbol{y}\|_{\ell_2} \le \epsilon \tag{6.2}$$

where $\boldsymbol{x} = [\boldsymbol{x}_1^T, \cdots, \boldsymbol{x}_{\mathsf{g}_b}^T]^T$, $\boldsymbol{x}_l^T$ is a $n_l \times 1$ vector, and ω_i, the weight assigned to block i for $i \in \{1, \cdots, \mathsf{g}_b\}$, can be expressed as [13] $\omega_i = \frac{1/\bar{k}_i}{\sum_{j=1}^{\mathsf{g}_b} 1/\bar{k}_j}$.

6.2.3 Global Spectrum Occupancy Matrix Completion

Having recovered the vector $\boldsymbol{x}$ from the compressed measurement $\boldsymbol{y}$ using (6.2), the energy in each band is compared to a threshold to decide on the occupancy of each band, i.e., $= \frac{1}{T} \sum_{t=1}^{T} |x_i[t]|^2 \lessgtr \lambda$ where λ is a predefined threshold that depends on the noise floor. Then, these spectrum decisions are updated to the spectrum occupancy matrix $\mathtt{R}$. Since each *SN* is sensing only a small portion of the wideband spectrum, most entries of the spectrum occupancy matrix are missing. Conventionally, collaborative filtering is used to recover these missing entries of $\mathtt{R}$ as long as the number of observed decisions in $\mathtt{R}$ is at least $\xi = O(\alpha^{5/4} r \log \alpha)$ with r is the rank of $\mathtt{R}$ and $\alpha = \max(\mathtt{I}, \mathtt{J})$ [2, Theorem 1.1]. That is, the recovery can be formulated as a convex optimization

$$\mathscr{P}_2 : \min_{\mathtt{X}} \mathtt{rank}(\mathtt{X}) \text{ s.t. } \sum_{(i,j) \in \Omega} \left(\mathtt{O}_{ij} - X_{ij} \right)^2 \le \epsilon \tag{6.3}$$

or

$$\mathscr{P}_3 : \min_{\mathtt{X}} \|\mathtt{X}\|_* \text{ s.t. } \sum_{(i,j) \in \Omega} \left(\mathtt{O}_{ij} - X_{ij} \right)^2 \le \epsilon \tag{6.4}$$

where $\|\cdot\|_*$ is the nuclear norm. Note that the main difference between both approaches is that $\mathscr{P}_3$ does not require any knowledge about the rank of R.

When considering high frequencies, this approach fails as the low-rank property is not preserved. This stems from the fact that SNs in different locations observe a completely different spectrum occupancy when the frequencies of interest are relatively high. In this work, we overcome this limitation by proposing an approach that relies on the fact that low-rank property (though is not preserved in the global matrix) is still preserved at the sub-matrix levels, and can therefore be used to complete the global occupancy matrix. This proposed approach is described next.

6.3 AirMap: Proposed Local Low-Rank Approximation Approach

The distance between SNs is an important metric for our proposed framework. We start from the following observation: the portion (sub-matrix) of the spectrum occupancy matrix that contains close-by SNs possesses a low rank property, though the global matrix does not. Therefore, each sub-matrix of the global occupancy matrix can be efficiently completed/constructed using $\mathscr{P}_2$, as described next.

6.3.1 Spectrum Sub-matrices Construction

The spectrum occupancy matrix can be seen as a rating matrix containing zeros and ones, where zeros denote that bands are unoccupied and ones denote that the bands are occupied. First, we scale the values to make the mean equal zero by subtracting 0.5 from each entry of the observed entries in the matrix. This is to distinguish between the observed occupancies (part of Ω) and the ones that need to be recovered (containing zeros). Then, based on the location of the SNs, we split the region of interest into q sub-regions, where the width of each sub-region is decided based on how far the highest carrier frequency can be detected. This can be computed using practical propagation models for high frequencies [23]. After deciding on the number of sub-regions, q, and their anchor points (centers), $\{c_k\}_{k=1}^{q}$, the SNs are clustered such that each user is associated with the closest anchor point. Note that unlike the approaches proposed for recommendation systems, which use local low-rank matrix approximation such as LLORMA [16] and SLOMA [26], the anchor points are constructed independently from

the sensing nodes. These depend only on the highest frequency and the region of interest.

6.3.2 Local Low-rank Spectrum Sub-matrices Recovery

The occupancy of each spectrum sub-matrix $\mathtt{M}^k$ for $k = 1, \ldots, \mathtt{q}$ is the solution to the optimization problem

$$\mathscr{P}_4 : \min_{\mathtt{X}} \|\mathtt{X}\|_* \text{ s.t. } \sum_{(i,j) \in \Omega^k} \left(\mathtt{O}^k_{ij} - X_{ij}\right)^2 \leq \epsilon \tag{6.5}$$

where Ω^k is a subset of Ω containing observations used to complete the matrix $\mathtt{M}^k$. Note that $\mathscr{P}_4$ is similar to $\mathscr{P}_3$ except that it only considers a subset of the observed spectrum occupancies Ω.

6.3.3 Global Recovery via Weighted Decisions

Having recovered the spectrum occupancy in each sub-matrix, a global decision, combining these sub-matrices, is made. This is illustrated in Fig. 6.2. To decide on the observations of the SNs located close to the edges of the regions covered by each of the sub-matrices, we account for the decision of the neighboring SNs. The elements of the global spectrum matrix $\hat{\mathtt{R}}$ is then expressed as

$$\hat{\mathtt{R}}_{ij} = \sum_{k=1}^{\mathtt{q}} \frac{\mathtt{K}^k_{ij}}{\sum_{s=1}^{\mathtt{q}} \mathtt{K}^s_{ij}} \mathtt{M}^k_{ij} \tag{6.6}$$

where $\mathtt{K}^k_{ij}$ is a kernel function applied to the distance, d_{ik}, between $SN\,i$ and an anchor point $\boldsymbol{c}_k$. As the distance increases, $\mathtt{K}^k_{ij}$ converges to zero. We opted for the following kernel (similarity function)

$$\mathtt{K}^k_{ij}(d_{ik}) = \begin{cases} 1, & \text{if } x < d^{th} \\ e^{-\beta d_{ik}}, & \text{otherwise} \end{cases} \tag{6.7}$$

with d^{th} is a distance threshold and β is a decay parameter. This similarity function tends to give constant weight within a given neighborhood. As we get further, the

similarity decays and goes exponentially to zero.

Finally, the final binary matrix is obtained by checking the sign of each element of the matrix R.
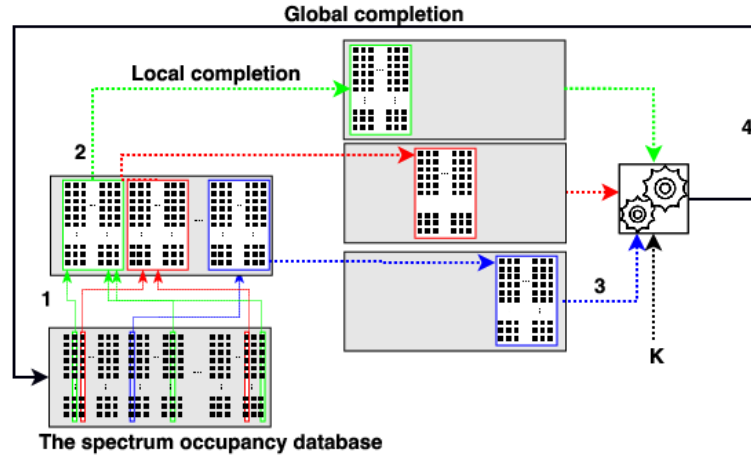
Figure 6.2: The different steps of the local low rank matrix based recovery. (1) Spectrum sub-matrices construction, (2) Local low rank matrix completion of each sub-matrix, (3) and (4) Global matrix completion.

6.3.4 Computational and Communication Overhead

The merit of the proposed framework is that it builds an accurate radio occupancy map to enable database-driven wideband spectrum sharing. The proposed framework does so while ensuring scalability, in terms of network overhead. Conventionally, making occupancy decisions of spectrum in vicinity of a SN incurs a communication overhead that is linear in T, I, and J. When using compressive sensing without collaborative filtering, the incurred communication overhead is linear in T, J, the number of compressed samples m, and $\lfloor I/n \rfloor$. AIRMAP incurs a communication overhead cost that is linear in T, J, and the number of compressed samples m. Therefore, network overhead reduction is achieved with our proposed scheme, which also results in lesser reporting energy. In terms of computational complexity, the weighted recovery results in $O(m^2n^3)$ per SN measurement. Hence, the total computation complexity for spectrum recovery is $O(Jm^2n^3T)$. The complexity of the recovery of the global occupancy is equivalent to

q times the recovery of $\mathscr{P}_4$, or even lesser since this can be excused in parallel.

6.4 Simulation Results

We consider synthetic data to assess the efficiency of AIRMAP. We assume the presence of multiple primary users operating in some of $\mathtt{I} = 250$ bands (this can be in the $5 - 15$ GHz range with 20 MHz bandwidth each) unless specified otherwise. The deployment of the active users follows a Poisson point process (PPP) with density $2/Km^2$ deployed in the 2D plane. To mimic real-world scenario, we assume high-frequency bands are reused more frequently than low-frequency bands. Each SN senses only one fifth of the total bands, using sub-Nyquist sampling [13]. To define the sub-matrices, we first compute how far a signal sent over a frequency f_c with a power $P = 10$ W can go. We adopted the 3GPP TR 38.901 UMa LOS path loss model [23] given by

$$PL_{dB} = 32.4 + 20\log_{10}\big(d(m)\big) + 30\log_{10}\big(f_c(GHz)\big) \tag{6.8}$$

for $0.5 < f_c < 100 GHz$ and the shadow fading standard deviation equal to 7.8 dB. We consider the sensitivity to be -120 dBm, bellow which a signal a considered absent. This allows defining the radii of the circles centered at the anchor points as illustrated in Fig 6.3. The sensing nodes are deployed according to a uniform PPP with density $10/Km^2$ deployed in the 2D plane. The SNs are linked to the closest anchor point forming the sub-matrices. To assess the performance of AIRMAP, we generate the entire spectrum occupancy matrix to compare the final recovery matrix with it. Since our focus is on the spectrum occupancy matrix completion, we consider the wideband spectrum recovery of the observed portion from each SN to be error free. The spectrum matrix completion is done using [1]. First, we observed from the generated spectrum occupancy matrix that the low-rank property for the sub-matrices is confirmed while the global matrix has no low-rank property ($rank > 50$ for the case of having 250 bands).

Fig. 6.4 shows the recovery error (computed as the Frobenius norm) as a function of the number of frequency bands. First, observe that our proposed framework allows to achieve a high reduction gain in the error (about 10 times) compared to classical approach. This is thanks to the observation of the local rank property (confirmed through simulations). Second, we observe that as the number of bands increases, the error de-
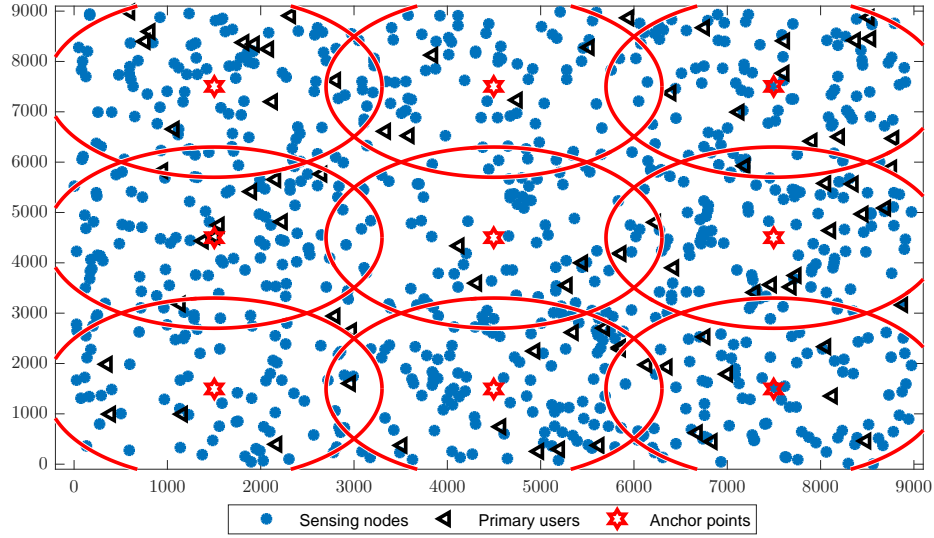
Figure 6.3: Example of deployment of the sensing nodes.

creases for both classical and proposed approaches. This is because as the number of bands increases, the global low rank property tends to hold more, and hence, a lower matrix recovery error is achieved.

In Fig. 6.5, we study the effect of the proposed similarity function used for the global recovery. When d^{th} is small, the user observation is given more weight with respect to the closest anchor point decision and lesser weight as the SN gets further. This helps mainly build an accurate decision for users located at the edges of the sub-matrices. As this parameter increases beyond a certain distance threshold, the performance drops and becomes similar to that of the classical recovery, as we no longer favor the decision with respect to the closest anchor point.

Fig. 6.6 studies the effect of the number of anchor points. Overall, we observe that as the number of anchor points increases, a reduction in the error is achieved which confirms the same observation made in Fig. 6.4.

6.5   Related works

Spectrum awareness. The proposed framework combines advances in both wideband
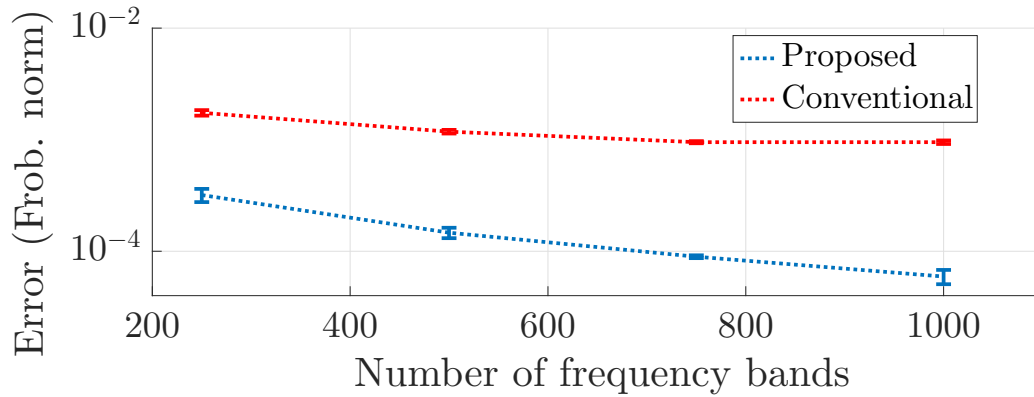
Figure 6.4: Error: proposed approach vs traditional approach.
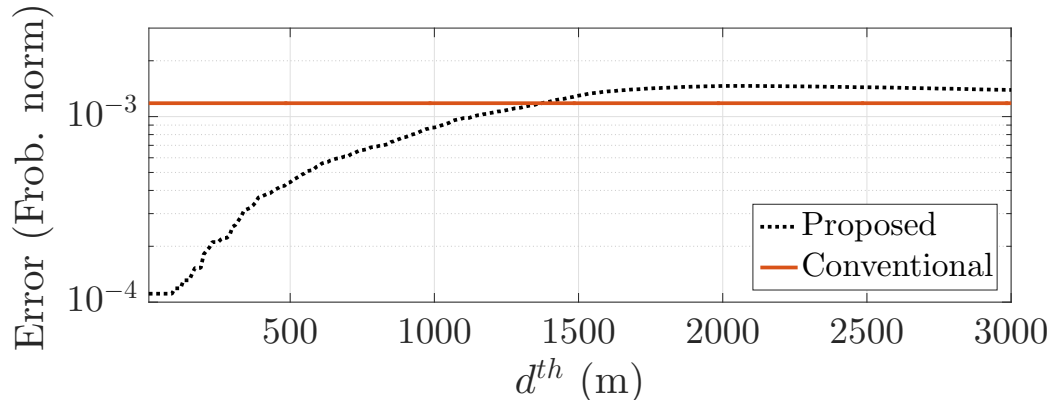
Figure 6.5: Error: proposed approach vs traditional approach as a function of dth.

spectrum sensing [13, 9, 18, 21, 20, 19, 24, 3] and recommendation systems [16, 26]. Authors in [19] proposed SenseLess, a trustworthy database to provide the spectrum availability of TV wideband spectrum. However, this database is only restricted to TV bands. To be able to get the occupancy of wider bandwidth, authors in [9] made a proof of concept for a 1 GHz wide bandwidth scanner. There are also some efforts towards applying machine learning and compressive sampling theories for spectrum sensing [27, 24, 10, 18]. Authors in [27] proposed Rxminer which uses a mixed Gaussian and Rayleigh models to identify spectrum occupancy. Authors in [18] proposed to exploit the low-rank property of the measurement matrix to recover the unreported measurements. The proposed approach assumes that all sensing nodes use the same sensing
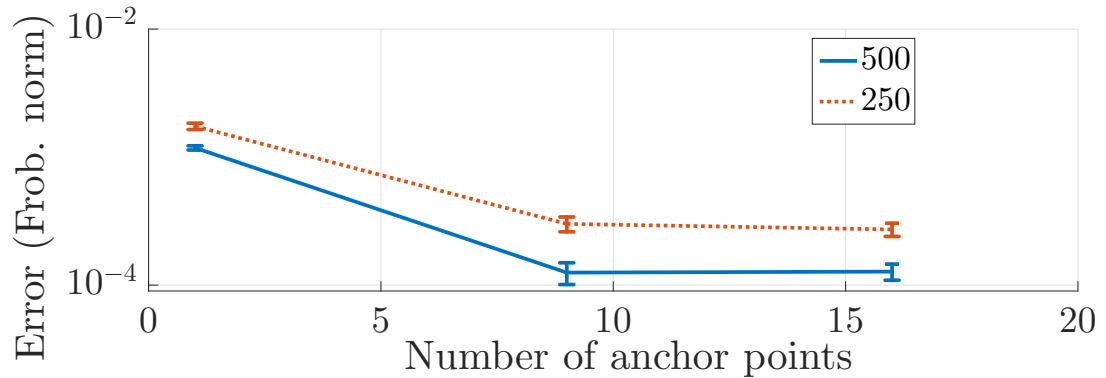
Figure 6.6: Effect of the number of submatrices.

matrix, which makes the approach unpractical. Moreover, the proposed modeling fails to capture frequency reuse, which is crucial in high-frequency bands. This has also been extended to detect malicious users in [20].

Collaborative filtering. Collaborative filtering was introduced in recommendation systems to handle the information overhead. The main approach uses matrix factorization, which is shown to achieve great performance while being scalable [15]. This is based on the fact that the users' preference for a particular item is only controlled by a small number of latent factors, which translates to a low-rank rating matrix. This assumption does not hold true in real-world applications as shown by [16]. Authors in [16] showed through experiments that when considering the global matrix having a number of low-rank matrices, better performance is achieved, making this approach, LLROMA, attractive to other fields such as multi-label classification, documents, etc. The main concern with LLROMA is the construction of the sub-matrices which is done by first randomly selecting a number of anchor points, and then, using distance metrics, points are connected to the closest anchor point. Besides, it suffers from high computation and storage cost. Recently, SLOMA [26] has been proposed to overcome LLORMA weaknesses by incorporating the social connections among users. However, the chosen number of anchor points was not justified for both approaches.

6.6   Conclusions

We proposed AirMap, a framework that builds an accurate spectrum occupancy map for wideband spectrum sharing. AirMap exploits the under-utilization of the wideband spectrum, the heterogeneity in the spectrum occupancy, and the spatial correlation between sensing nodes to achieve scalable decisions for the spectrum occupancy while incurring small network communication overhead. The proposed framework can be extended to other applications, such as spectrum enforcement and monitoring, which can help recognize the type of signals occupying the wideband spectrum.

Acknowledgment

Bibliography

[1] S Becker, EJ Candes, and M Grant. TFOCS: Templates for first-order conic solvers, version 1.3. 1, 2014.

[2] Emmanuel J Candès and Benjamin Recht. Exact matrix completion via convex optimization. *Foundations of Computational mathematics*, 9(6):717, 2009.

[3] Ayon Chakraborty, Md Shaifur Rahman, Himanshu Gupta, and Samir R Das. Specsense: Crowdsensing for efficient querying of spectrum occupancy. In *Proc. of IEEE INFOCOM*, pages 1–9, May 2017.

[4] Federal Communications Commission. Tv white space.

[5] Federal Communications Commission et al. Fcc online table of frequency allocations. *Online:[https://transition.fcc.gov/oet/spectrum/table/fcctable.pdf]*, 2017.

[6] Inc. Google. Google spectrum database.

[7] Mohamed Grissa, Attila A Yavuz, and Bechir Hamdaoui. When the hammer meets the nail: Multi-server pir for database-driven crn with location privacy assurance. *arXiv preprint arXiv:1705.01085*, 2017.

[8] Bechir Hamdaoui, Bassem Khalfi, and Mohsen Guizani. Compressed wideband spectrum sensing: Concept, challenges and enablers.

[9] Tanbir Haque, Rabia Tugce Yazicigil, Kyle Jung-Lin Pan, John Wright, and Peter R Kinget. Theory and design of a quadrature analog-to-information converter for energy-efficient wideband spectrum sensing. *IEEE Trans. on Circuits and Systems I: Regular Papers*, 62(2):527–535, 2015.

[10] Haitham Hassanieh, Lixin Shi, Omid Abari, Ezzeldin Hamed, and Dina Katabi. Ghz-wide sensing and decoding using the sparse fourier transform. In *Proc. of IEEE INFOCOM*, pages 2256–2264, 2014.

[11] Steven Siying Hong and Sachin Rajsekhar Katti. Dof: a local wireless information plane. In *ACM SIGCOMM Computer Communication Review*, volume 41, pages 230–241, 2011.

[12] Bassem Khalfi, Bechir Hamdaoui, and Mohsen Guizani. Extracting and exploiting inherent sparsity for efficient iot support in 5G: Challenges and potential solutions. *IEEE Wireless Communications Magazine*, Oct. 2017.

[13] Bassem Khalfi, Bechir Hamdaoui, Mohsen Guizani, and Nizar Zorba. Exploiting wideband spectrum occupancy heterogeneity for weighted compressive spectrum sensing. In *Computer Communications Workshops (INFOCOM WKSHPS), IEEE Conference on*, pages 1–6, 2017.

[14] Bassem Khalfi, Bechir Hamdaoui, Mohsen Guizani, and Nizar Zorba. Efficient spectrum availability information recovery for wideband DSA networks: A weighted compressive sampling approach. *IEEE Trans. on Wireless Communications*, 17(4), April 2018.

[15] Yehuda Koren, Robert Bell, and Chris Volinsky. Matrix factorization techniques for recommender systems. *Computer*, 42(8), 2009.

[16] Joonseok Lee, Seungyeon Kim, Guy Lebanon, Yoram Singer, and Samy Bengio. LLORMA: Local low-rank matrix approximation. *The Journal of Machine Learning Research*, 17(1):442–465, 2016.

[17] A Mancuso, S Probasco, and B Patil. Protocol to access white-space (paws) databases: Use cases and requirements. Technical report, 2013.

[18] Jia Jasmine Meng, Wotao Yin, Husheng Li, Ekram Hossain, and Zhu Han. Collaborative spectrum sensing from sparse observations in cognitive radio networks. *IEEE Journal on Selected Areas in Communications*, 29(2):327–337, 2011.

[19] Rohan Murty, Ranveer Chandra, Thomas Moscibroda, and Paramvir Bahl. Senseless: A database-driven white spaces network. *IEEE Trans. on Mobile Computing*, 11(2):189–203, 2012.

[20] Z Qin, Yang Gao, and Mark Plumbley. Malicious user detection based on low-rank matrix completion in wideband spectrum sensing. *IEEE Trans. on Signal Processing*, 2017.

[21] Zhijin Qin, Yue Gao, Mark D Plumbley, and Clive G Parini. Wideband spectrum sensing on real-time signals at sub-nyquist sampling rates in single and cooperative multiple nodes. *IEEE Trans. on Signal Processing*, 64(12):3106–3117, 2016.

[22] RadioSoft. White space database.

[23] Theodore S Rappaport, Yunchou Xing, George R MacCartney, Andreas F Molisch, Evangelos Mellios, and Jianhua Zhang. Overview of millimeter wave communications for fifth-generation (5g) wireless networks with a focus on propagation models. *IEEE Trans. on Antennas and Propagation*, 65(12):6213–6230, 2017.

[24] Lixin Shi, Paramvir Bahl, and Dina Katabi. Beyond sensing: Multi-ghz realtime spectrum analytics. In *Proc. of USENIX Symposium on Networked Systems Design and Implementation (NSDI)*, pages 159–172, 2015.

[25] Inc. Spectrum Bridge. White space database.

[26] Huan Zhao, Quanming Yao, James T Kwok, and Dik Lun Lee. Collaborative filtering with social local models. pages 1–10, Nov. 2017.

[27] Mariya Zheleva, Ranveer Chandra, Aakanksha Chowdhery, Ashish Kapoor, and Paul Garnett. Txminer: Identifying transmitters in real-world spectrum measure-

ments. In *Proc. of IEEE Int. Symposium on Dynamic Spectrum Access Networks (DySPAN)*, pages 94–105, 2015.

Optimizing Joint Data and Power Transfer in Energy Harvesting Multiuser Wireless Networks

Bassem Khalfi, Bechir Hamdaoui, Mahdi Ben Ghorbel, Mohsen Guizani, Xi Zhang, Nizar Zorba

Chapter 7: Manuscript 6: Optimizing Joint Data and Power Transfer in Energy Harvesting Multiuser Wireless Networks

Bassem Khalfi, Student Member, IEEE, Bechir Hamdaoui, Senior Member, IEEE, Mahdi Ben Ghorbel, Member, IEEE, Mohsen Guizani, Fellow, IEEE, Xi Zhang, Fellow, IEEE, and Nizar Zorba, Member, IEEE

Abstract

Energy harvesting emerges as a potential solution for prolonging the lifetime of the energy-constrained mobile wireless devices. In this paper, we focus on Radio Frequency (RF) energy harvesting for multiuser multicarrier mobile wireless networks. Specifically, we propose joint data and energy transfer optimization frameworks for powering mobile wireless devices through RF energy harvesting. We introduce a power utility that captures the power consumption cost at the base station (BS) and the used power from the users' batteries, and determine optimal power resource allocations that meet data rate requirements of downlink and uplink communications. Two types of harvesting capabilities are considered at each user: harvesting only from dedicated RF signals and hybrid harvesting from both dedicated and ambient RF signals. The developed frameworks increase the end users' battery lifetime at the cost of a slight increase in the BS power consumption. Several evaluation studies are conducted in order to validate our proposed frameworks.

Index terms— RF energy harvesting, power resource allocation, multicarrier multiuser mobile wireless networks.

7.1 Introduction

Minimizing energy consumption and prolonging network lifetime have become primal design goals of next-generation wireless networks, merely due to limited power resources of wireless devices. Wireless Energy Transfer (WET) technology emerges as a key solution for addressing such issues, and has recently attracted lots of research attention [29, 26, 32, 33, 31, 28, 23]. WET technology has even greater impact when considering battery-powered wireless devices whose batteries cannot (or are difficult to) be

replaced, as in the case of remote sensor nodes. In addition to carrying the energy, a new paradigm, called Simultaneous Wireless Information and Power Transfer (SWIPT), has recently emerged to allow for distant powering of devices during ongoing data communications [29, 14, 16, 22].

There are three proposed SWIPT design schemes: decoupled SWIPT, closed-loop SWIPT, and integrated SWIPT [14]. In decoupled SWIPT, the information and the power are sent from two separate sources that could be placed at different locations: a base station represents the information gateway and a power beacon represents the energy gateway. The closed-loop SWIPT scheme powers the device in the downlink and sends the data in the uplink. This scenario could be the case of data offloading in wireless sensor networks, where the main concern is how to offload the data from the sensors [16]. In the third design scheme, both the information and power are sent by the same source over the same signals [22]. However, the challenge lies on how to separate the data and power streams.

Broadly speaking, there are two energy harvesting techniques in single-input single-output systems: time switching and power splitting [21, 20, 12]. Time switching consists of splitting the time window into two portions, where during the first portion, the receiver converts the received RF signals into power while the second portion is dedicated to decoding the RF signals. Although simple, this technique requires a perfect synchronization; otherwise, it induces some information loss [18]. Power splitting, on the other hand, consists of splitting the received signal into two streams. The first serves for extracting power and the second for decoding the received information. The splitting ratio balances between the amounts of harvested power and the achieved data rate.

While lots of works focused either on optimizing the power allocation at the base station (BS) or on exploring the users' achieved data rates, the excessive use of power at the BS as well the available battery levels at the different users were not accounted for. In this work, we develop SWIPT techniques that account for power costs at the BS and battery energy available at the different users while harvesting RF energy from not only intended signals but also all nearby ambient RF signals (i.e., interference) intended for other users.

7.1.1 Related Works

Varshney et al. [29] are among the first researchers that highlighted the potential of transferring energy through RF signals. Since then, WET and SWIPT through RF signals have attracted numerous works [29, 26, 32, 33, 31, 21, 20, 12, 18, 7, 8, 21, 11, 36, 25, 13, 34, 5]. The authors in [26, 32, 33] proposed an interesting idea for transferring energy wirelessly to sensor network nodes. The idea is basically to have a designated wireless charging vehicle (WCV) that periodically travels inside the network to wirelessly charge sensors' batteries. They formulated an optimization problem whose objective is to maximize the ratio of the WCV's vacation time over the cycle time, and proved that the optimal traveling path for the WCV is the shortest Hamiltonian cycle. This idea has been further applied to networks with mobile base stations [31]. The authors in [31] studied the problem of whether and how the mobile BS can be co-located on the WCV to also serve as a charging vehicle. The authors formulated the co-location problem as an optimization problem while accounting for energy charging, WCV's stopping behavior, and data flow routing. Then, they proposed a formulation that depends only on location to serve as a simpler alternative for solving the same general problem. However, WCV can only charge a limited number of sensors at a given time, making the approach unscalable especially when considering large areas.

There have also been some research efforts studying the performance of RF energy harvesting [7, 34, 8, 17]. For instance, the authors in [7] investigated energy harvesting in cooperative networks, where a number of source-destination pairs are communicating with each other through an energy harvesting relay. This work proposed power splitting strategies that the relay can use to distribute the harvested energy among multiple users. In [34, 8, 17], performance tradeoffs between the power-splitting and the time-switching methods, when used for jointly transferring energy and data in various point-to-point systems, have been studied. For example, authors in [8] derived suboptimal power splitting ratios for point-to-point multi-channel systems. In [17], we investigated the minimization of the system total power while accounting for the received interference at each user.

Energy harvesting has also been studied in the context of multiuser access [11, 16, 38], MIMO systems [36, 25, 19], and cognitive radio networks [13, 37, 23]. In [16], the authors tackled closed-loop SWIPT in a multiuser system, where the optimal time allocation for

each user maximizing the sum rate is derived. OFDM access has been considered as well in [22] with the objective of maximizing the energy efficiency.

Unlike previous works, we consider optimizing the power consumption in the downlink and uplink of a multiuser multi-carrier system with simultaneous information and power transfers. The power utility includes the power cost at the BS required to communicate with the different users, as well as the amount of battery energy available at the users. Our approach integrates SWIPT with power splitting to increase spectrum efficiency, and allows each user to harvest not only from its dedicated signal, but also from ambient RF signals resulting from the communication between the BS and the other users.

7.1.2   Summary of the Contributions

The main contributions of this paper are:

- We develop joint data and energy transfer optimization frameworks for wirelessly powering mobile devices via RF energy harvesting. Unlike previous works, we propose a weighted power cost that captures the consumed power at the BS and the battery power available at the users.

- We analytically derive closed-form expressions of the optimal power allocations required for meeting the data rate requirements of the downlink and uplink communications between the BS and its mobile users.

- We study two system setups: (i) Users can only harvest energy from their intended/dedicated RF signals; and (ii) Users can harvest energy from any ambient RF signals intended for any user.

7.1.3   Roadmap

The rest of this paper is organized as follows. In Section 7.2, we present our system model. We formulate and solve the studied energy harvesting optimization problem in Section 7.3 for the case of dedicated RF signal-based energy harvesting, and in Section 7.4 for the case of hybrid dedicated and ambient RF signal-based energy harvesting. Our results are presented in Section 7.5, and our conclusions are provided in Section 7.6.
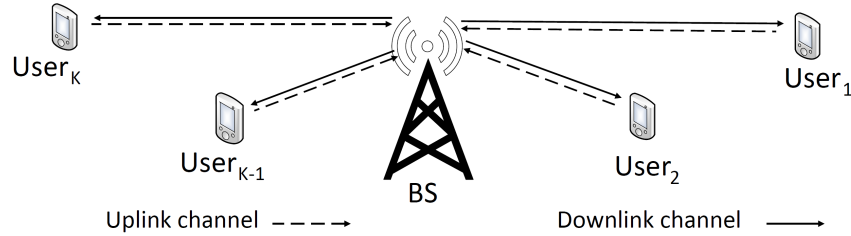
Figure 7.1: System model: a base station and K mobile users.

7.2 System Model

We consider a point-to-multipoint, half-duplex, OFDM network with a BS at the center of a cell and K mobile users, as illustrated in Fig. 7.1. The BS transmits over L orthogonal subcarriers with only N subcarriers are used to communicate with each user. We assume that the number N is the same for all users, i.e., $L = K \times N$. Without loss of generality, we assume that the first N subcarriers are used to communicate with the first user, the second N subcarriers are used to communicate with the second user and so on. In the uplink, each user adopts SC-FDMA and communicates with the BS over N subcarriers. The downlink and uplink channels between the BS and the kth user over the ith subcarrier are $h_{BS,k}^i$ and $h_{k,BS}^i$, respectively. Note that we defined the uplink and the downlink channels to be different so that our frameworks can fit both TDD and FDD modes. It is also assumed that the BS has perfect knowledge of the different channel gains. We consider that the BS uses the integrated SWIPT to power and communicate with users, and each user relies on the power splitting technique to separate the power and the information streams. We illustrate the high-level receiver's architecture of each device in Fig. 7.2. The received RF signal affected by the receiver's noise is split into two portions: a first portion is directed to the energy harvesting unit while the second portion is fed to the data processing unit. This paper's focus is on power allocation in multicarrier energy harvesting wireless systems. Subcarrier scheduling is beyond the scope of this work (see [2, 35] if interested).

The communication process adopts the model of [8]. During the first half of time slot t, the BS communicates with all the users over the non-interfering subcarriers using a total power $\sum_{k=1}^{K} \sum_{i=1}^{N} P_{BS,k}^i$, where $P_{BS,k}^i$ is the power used in the downlink to communicate with user k over the ith subcarrier. In the second half of time slot t, each user relies

on the power splitting technique [20] to harvest part of the received RF signal power and uses it, in addition to its remaining battery power $P_k^{bat}(t)$, to communicate back with the BS. The battery power's level changes over time as $P_k^{bat}(t+1) = P_k^{bat}(t) + Q_k(t) - P_k^{proc}(t)$, where $P^{bat}(t)$ is the available power at the beginning of time slot t, $Q_k(t)$ is the harvested power, and $P_k^{proc}(t)$ is the power used for information processing. This model covers the case where the users are battery-free, which corresponds to $P_k^{bat}(t) = 0$. In the rest of the paper, we drop the time index of the time slot as we are concerned with the optimal power at each time slot. The signals received by user k, $y_{BS,k}^i$ and by the BS, $y_{k,BS}^i$ can be expressed as

$$y_{BS,k}^i = x_k^i \sqrt{P_{BS,k}^i} h_{BS,k}^i + n_{BS,k}^i, \tag{7.1a}$$

$$y_{k,BS}^i = z_k^i \sqrt{P_{k,BS}^i} h_{k,BS}^i + n_{k,BS}^i, \tag{7.1b}$$

for $i \in [1, ..., N]$ where x_k^i and z_k^i are the unit-power symbols transmitted by the BS and the kth user, respectively. $P_{BS,k}^i$ and $P_{k,BS}^i$ are the transmission powers at the ith subcarrier in the downlink and the uplink, respectively. $n_{BS,k}^i$ and $n_{k,BS}^i$ are Additive White Gaussian Noises (AWGN) with zero mean and variance $\sigma_{BS,k}^i$ and $\sigma_{k,BS}^i$. We consider $\sigma_{k,BS}^i = \sigma_{BS,k}^i = N_0 B$ where N_0 is the noise power density.

When using the power splitting approach, the amount of harvested energy at the mobile user k is then expressed as $Q_k = \eta \rho_k (\sum_{i=1}^N P_{BS,k}^i |h_{BS,k}^i|^2 + \sigma_{BS,k}^i)$, where η, $0 < \eta < 1$, is the energy harvesting efficiency that is characteristic of the RF circuitry. ρ_k is the power splitting ratio that balances between the amount of the RF signal used for harvesting energy and the RF signal used to decode the sent signal. The user considers the second stream for information decoding. A noise term is added at the decoding unit which leads to an achieved rate by the BS of $R_{BS,k} = \sum_{i=1}^N B \log_2(1 + \frac{(1-\rho_k)P_{BS,k}^i |h_{BS,k}^i|^2}{\sigma_{BS,k}^i})$, where B is the bandwidth of each sub-band. We assume that all the sub-bands are equal. To simplify the analysis, we assumed that $\sigma_{BS,k}^i \approx (1 - \rho_k)\sigma_{BS,k}^i + \sigma_2^2$ where σ_2^2 is the power of the noise term introduced at the decoding unit. In the uplink, the mobile user k uses the amount of the harvested power Q_k, along with its remaining battery power $P_k^{bat}(t)$, to communicate with the BS. Using Equation (7.1b), the achieved rate in the uplink can be expressed as $R_{k,BS} = \sum_{i=1}^N B \log_2(1 + \frac{P_{k,BS}^i |h_{k,BS}^i|^2}{\sigma_{k,BS}^i})$.

Optimizing the transmit power at the BS and at the users while satisfying some
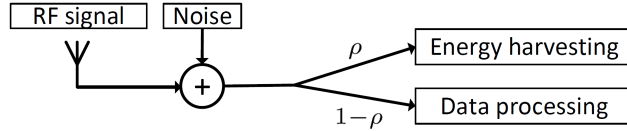
Figure 7.2: Power splitting based receiver structure.

data rate constraints over a long-term interval has its advantages and disadvantages. While power saving can be achieved by taking advantage of the batteries' dynamic, acquiring the channel CSI ahead of time can be very challenging. This is due to the inherent time-varying nature of the wireless channel. On the other hand, optimizing the power instantaneously allows to achieve optimal power allocation by exploiting all the available information (channels' gains, power cost, battery levels, etc). Therefore, we focus on determining the optimal power levels that should be allocated by the BS and each device so that both the BS's and users' data rate requirements are met. We consider two system setups: i) each user can only harvest energy from its dedicated RF subcarrier signals over which it is receiving its data from the BS, and ii) we extend the harvesting capability to the case where each user can also take advantage of the downlink channels of the other users and harvest energy from any ambient RF signals communicated between the BS and other users. In the next section, we consider the first system setup and in the following section, we elaborate the second setup.

7.3   Dedicated RF Signal Based Energy Harvesting

The focus of this section is to optimize a power utility for the whole system. The utility function balances between two entities: the cost of the power that the BS will use to communicate with all the users, and the amount of power used by each user from its battery. We consider the BS to be equipped with multiple antennas. To serve the different users, the BS uses a total transmission power P_{BS} that follows the following model [24],

$$P_{BS} = \theta . \sum_{k=1}^{K} \sum_{i=1}^{N} P_{BS,k}^{i} + \varepsilon \tag{7.2}$$

The coefficient θ captures the power consumption which scales with the radiated power due to amplifier and feeder losses. The term ε models the offset of power consumed by the BS regardless of the radiated power due to information processing, battery backup, and cooling. The BS is powered from a retailer. Assume π is the cost of one unit of energy (e.g. the price of $1KWh$) provided by a retailer. We consider just one time slot Δ_t. Hence, the total cost of the procured energy is [10]

$$\mathcal{C}_{BS} = \pi.\Delta_t.P_{BS}. \tag{7.3}$$

At the BS side, substituting the expression of the power given by Equation (7.2) in Equation (7.3), we get

$$\begin{aligned}
\mathcal{C}_{BS} &= \pi.\Delta_t.(\theta.\sum_{k=1}^{K}\sum_{i=1}^{N} P_{BS,k}^i + \varepsilon) \\
&= \pi.\Delta_t.\theta.\sum_{k=1}^{K}\sum_{i=1}^{N} P_{BS,k}^i + \pi.\Delta_t.\varepsilon \\
&= \alpha \sum_{k=1}^{K}\sum_{i=1}^{N} P_{BS,k}^i + \varsigma \tag{7.4}
\end{aligned}$$

where $\alpha = \pi.\Delta_t.\theta$ and $\varsigma = \pi.\Delta_t.\varepsilon$ are parameters to characterize the BSs' power consumption cost. At each user's side, the amount of energy required to receive packets from the BS is (ignoring the acknowledgement) [30] $E_k^r = P_0\Delta_t$ where P_0 is an amount of power used for receiving packets. This power may include the required power for performing the channel estimation. On the other hand, to offload its data to the BS during time slot t, the user consumes [30] $E_k^s = \left(P_0' + \sum_{i=1}^{N} P_{k,BS}^i\right)\Delta_t$ Joules where P_0' is the processing power required prior to sending at each user. Thus, the total transmit and receive power required at each user is $P_k^{\text{tot}} = P_0 + P_0' + \sum_{i=1}^{N} P_{k,BS}^i$.

On the other hand, the cost of the power consumed by each user from its battery is $\mathcal{C}_k = \beta_k(P_k^{\text{tot}} - Q_k)$, where β_k is a weighting coefficient that captures the attitude of each user whether to rely on its battery or harvesting from the received RF signals. Note that typical numbers for the different parameters used to define the cost functions can be found in [24, 10, 30]. Since some of these variables are changing over time (e.g., π) and may change from one device to another, we instead introduce the variable $\kappa_k = \frac{\beta_k}{\alpha}$ and

study its effect. When κ_k is very small, the behavior of the system encourages the users to consume power from their batteries first. In the other case, it encourages harvesting from the BS's RF signal.

We start by the case where the BS powers the devices using dedicated subcarriers signals. Note that this scenario is appropriate for devices with limited hardware capabilities [15, 4, 1] typically used for health and fitness (body sensor devices) or industrial IoTs applications. Hardware restrictions limit devices to only tune and communicate over a small number of channels (e.g., the N subcarriers/channels assigned to each user), but not over a large number of channels to cover all the $K \times N$ channels used by the BS (as in the second system setup presented in Section 7.4).

When each user can only harvest energy from its dedicated RF subcarrier signals, the global problem of jointly minimizing the power utility is formulated as

$$\min_{\{\rho_k, \{P_{BS,k}^i\}_{i=1}^N, \{P_{k,BS}^i\}_{i=1}^N\}_{k=1}^K} \quad \mathcal{C}_{BS} + \sum_{k=1}^K \mathcal{C}_k \tag{7.5a}$$

$$\text{s.t. } P_k^{\text{tot}} - P_k^{bat} \leq Q_k, \tag{7.5b}$$

$$R_{BS,k} \geq r_{BS,k}^{th}, \tag{7.5c}$$

$$R_{k,BS} \geq r_{k,BS}^{th}, \tag{7.5d}$$

$$P_{BS,k}^i \geq 0, \ P_{k,BS}^i \geq 0, \tag{7.5e}$$

$$0 \preceq \boldsymbol{\rho} \preceq 1 \tag{7.5f}$$

where $\boldsymbol{\rho} = [\rho_1, ..., \rho_K]^T$. Equation (7.5a) expresses the global objective. Constraint (7.5b) controls the total power budget at the kth user, so that it does not exceed the harvested power plus the remaining battery's power. Constraints (7.5c) and (7.5d) are used to meet the data rates for the downlink and uplink streams, respectively. $r_{BS,k}^{th}$ is the minimum downlink rate threshold that should be achieved by the BS when communicating with user k [39], while $r_{k,BS}^{th}$ is the data rate threshold that should be achieved in the uplink by user k. Constraints (7.5e) and (7.5f) ensure the positivity of the allocated power levels and the splitting ratios.

Proposition 7. *Under fixed splitting ratio $\boldsymbol{\rho}$, the optimization problem (7.5) is a convex optimization problem.*

Proof. See Appendix A. ∎

The original optimization problem (7.5) is not convex which makes it hard to find optimal solution via standard optimization tools. Using Proposition 7, if we fix $\boldsymbol{\rho}$ to the optimal splitting ratio $\boldsymbol{\rho}^{opt}$, this optimization problem can be formulated as two successive convex optimization problems that can be solved efficiently by feeding the optimal solution of the first optimization to the second optimization. Therefore, we propose to proceed as follows. We compute the amount of power to be needed in the uplink as a first step to quantify how much power should be harvested by each user. In a second step, we determine the downlink power levels that are to be used at the BS to meet the downlink data rate threshold, as well as the amount of power needed by the users for the uplink communications, as determined in the previous step. Then, we perform an exhaustive search for the optimal splitting ratio ρ_k^{opt} that minimizes the total consumed power.

Next, we determine the amount of energy needed by user k to meet its required uplink data rate, $r_{k,BS}^{th}$.

7.3.1   Optimal Uplink Power Allocation

In the uplink, each user minimizes its transmit power subject to meeting its required data rate. This can be formulated as:

$$\min_{\{P_{k,BS}^i\}_{i=1}^N} \quad \mathcal{C}_k, \tag{7.6a}$$

$$\text{s.t.} \quad R_{k,BS} \geq r_{k,BS}^{th} \tag{7.6b}$$

The solution to (7.6) is given by the following lemma

Lemma 4. *(The power allocation in the uplink)*
The optimal power allocation in the uplink for user k is

$$P_{k,BS}^{i*} = \left[\nu_k - \frac{\sigma_{k,BS}^i}{|h_{k,BS}^i|^2} \right]_0^+ \tag{7.7}$$

where

$$\nu_k = \left(2^{\frac{r_{k,BS}^{th}}{B}} / (\prod_{j \in \mathcal{U}_k} |h_{k,BS}^j|^2 / \sigma_{k,BS}^j) \right)^{1/|\mathcal{U}_k|} \tag{7.8}$$

and $\mathcal{U}_k = \{i|\nu_k - \sigma_{k,BS}^i/|h_{k,BS}^i|^2 \geq 0\}$. $|\mathcal{X}|$ *is the cardinality of* $\mathcal{X}$ *and* $[x]_0^+ = \max\{0, x\}$.

Proof. See Appendix B. ∎

Having determined the power level, $P_{k,BS}^{i*}$, user k needs to be able to communicate its data over subcarrier i, which allows us to set the variable, $P_{BS,k}^i$, in the optimization problem (7.5) to $P_{k,BS}^{i*}$, and solve for the downlink power variables, $P_{BS,k}^i$.

7.3.2 Optimal Downlink Power Allocation

In the downlink, the BS aims to find the optimal power level that it has to transmit in order to meet each user k's downlink data rate, $r_{BS,k}^{th}$, and to be able to power each user k with enough power to allow it to meet its required uplink rate, $r_{k,BS}^{th}$. This is derived with respect to the power utility defined earlier. In this first system setup, each user can only harvest from its RF signal subcarriers. Given the uplink power needed at each user, which is determined by Equation (7.7), the optimization problem at the BS is then formulated as

$$\min_{\left\{\{P_{BS,k}^i\}_{i=1}^N\right\}_{k=1}^K} \tilde{\varsigma} + \sum_{k=1}^K \sum_{i=1}^N \tilde{\alpha}_k^i P_{BS,k}^i, \tag{7.9a}$$

$$\text{s.t. } R_{BS,k} \geq r_{BS,k}^{th}, \ k \in [1..K], \tag{7.9b}$$

$$\sum_{i=1}^N P_{BS,k}^i |h_{BS,k}^i|^2 \geq P_k^{th}, \ k \in [1..K], \tag{7.9c}$$

where $\tilde{\varsigma} = \varsigma + \sum_{k=1}^K \beta_k (\sum_{i=1}^N (P_{k,BS}^{i*} - \eta\rho_k\sigma_{BS,k}^i) + P_0 + P_0')$ and $\tilde{\alpha}_k^i = \alpha - \beta\eta\rho_k|h_{BS,k}^i|^2$. The quantity P_k^{th} represents a power threshold that we deduce from the constraint (7.5b). It depends on the amount of power needed for achieving the required uplink data rate, the amount of power available in the battery, the splitting ratio, the conversion efficiency, and the noise power, and is expressed as

$$P_k^{th} = \frac{\sum_{i=1}^N P_{k,BS}^{i*} + P_0 + P_0' - P_k^{bat}}{\eta\rho_k} - \sum_{i=1}^N \sigma_{k,BS}^i \tag{7.10}$$

Minimizing the affine objective function given by Equation (7.9a) is equivalent to minimizing the linear quantity $\sum_{k=1}^{K} \sum_{i=1}^{N} \tilde{\alpha}_k^i P_{BS,k}^i$. Hence, we could re-write the problem for each $k \in [1..K]$ as follows

$$\min_{\{P_{BS,k}^i\}_{i=1}^N} \quad \sum_{i=1}^N \tilde{\alpha}_k^i P_{BS,k}^i, \tag{7.11a}$$

$$\text{s.t.} \quad R_{BS,k} \geq r_{BS,k}^{th}, \tag{7.11b}$$

$$\sum_{i=1}^N P_{BS,k}^i |h_{BS,k}^i|^2 \geq P_k^{th} \tag{7.11c}$$

The optimal per-user per-subcarrier downlink power allocation is given by the following theorem.

Theorem 8. *The solution to* (7.11) *above is*

$$P_{BS,k}^{i*} = \left[\frac{\lambda_k}{\tilde{\alpha}_k^i - \psi_k |h_{BS,k}^i|^2} - \frac{\sigma_{BS,k}^i}{(1 - \rho_k)|h_{BS,k}^i|^2} \right]_0^+, \tag{7.12}$$

for $i \in [1..N]$ and $k \in [1..K]$, where

$$\bullet \ \lambda_k = 2^{\frac{r_{BS,k}^{th}}{B|\mathcal{S}_k|} - \frac{1}{|\mathcal{S}_k|} \log_2 \left(\prod_{i \in \mathcal{S}_k} \frac{(1 - \rho_k)|h_{BS,k}^i|^2}{(\tilde{\alpha}_k^i - \psi_k|h_{BS,k}^i|^2)\sigma_{BS,k}^i} \right)}$$

$\bullet \ \mathcal{S}_k = \{i \,|\, \lambda_k / (\tilde{\alpha}_k^i - \psi_k|h_{BS,k}^i|^2) > \sigma_{BS,k}^i / (1 - \rho_k)|h_{BS,k}^i|^2 \}$,

$\bullet \ \psi_k$ *is the zero of the function*

$$f(x) = \frac{2^{r_{BS,k}^{th}/B|\mathcal{S}_k|} \sum_{i \in \mathcal{S}_k} \frac{|h_{BS,k}^i|^2}{\tilde{\alpha}_k^i - x|h_{BS,k}^i|^2}}{\left(\prod_{i \in \mathcal{S}_k} \frac{(1 - \rho_k)|h_{BS,k}^i|^2}{(\tilde{\alpha}_k^i - x|h_{BS,k}^i|^2)\sigma_{BS,k}^i} \right)^{\frac{1}{|\mathcal{S}_k|}}}$$

$$- \quad P_k^{th} - \sum_{i \in \mathcal{S}_k} \frac{\sigma_{BS,k}^i}{1 - \rho_k} \tag{7.13}$$

Proof. See Appendix C. ∎

The theorem provides the optimal power levels in the downlink, but requires to find the zero of the function f. In what follows, we first prove the existence of a zero, and then present a technique for finding it.

To examine the monotony of f, we take the derivative over x. It follows that the sign of f' is the sign of

$$\sum_{i \in \mathcal{S}_k} \frac{|h_{BS,k}^i|^4}{(\tilde{\alpha}_k^i - x|h_{BS,k}^i|^2)^2} - \frac{1}{|\mathcal{S}_k|} \Big(\sum_{i \in \mathcal{S}_k} \frac{|h_{BS,k}^i|^2}{\tilde{\alpha}_k^i - x|h_{BS,k}^i|^2} \Big)^2 \tag{7.14}$$

Recalling Cauchy-Schwartz inequality, $\left(\sum_{i=1}^{N} |x_i| \right)^2 \leq N \sum_{i=1}^{N} |x_i|^2$, we conclude that f is a non-decreasing function. Since f presents some points of singularity, it is sufficient to prove the existence of an interval where f is continuous and the signs of f at the interval boundaries are opposite. Let $\phi_0 = 0$ and $\phi_i = \tilde{\alpha}_k^i / |h_{BS,k}^i|^2$. Without loss of generality, we assume that $\phi_0 < \phi_1 < \phi_2 < ...$ Now, the $\lim_{x \to \phi_0^+} f(x)$ is finite, but could be positive or negative, depending on the numerical values of the different systems parameters. On the other hand, $\lim_{x \to \phi_1^-} f(x)$ goes to $+\infty$. Hence, if $\lim_{x \to \phi_0^+} f(x)$ is negative, then there is a zero of f in this interval. Otherwise, we check the next interval. Note that the search is restricted to the intervals $\mathcal{I}_l =]\phi_l, \phi_{l+1}[$ with $l \in \{0, 2, 4, 6, ..\}$ to ensure the non negativity of $\Big(\prod_{i \in \mathcal{S}_k} \frac{(1 - \rho_k)|h_{BS,k}^i|^2}{(\tilde{\alpha}_k^i - \psi_k |h_{BS,k}^i|^2)\sigma_{BS,k}^i} \Big)$ in order to satisfy Equation (7.13). Since $\lim_{x \to \phi_2^+} f(x) = -\infty$ and $\lim_{x \to \phi_3^-} f(x) = +\infty$, then there is a zero in this interval. Given the presence of the intervals of singularities, we propose to use the bisection method to find the zero of f, which essentially searches for the zero of f incrementally in each interval. A check of the sign of their product $\Big(\lim_{x \to \phi_l^+} f(x) . \lim_{x \to \phi_{l+1}^-} f(x) \Big)$, $l = 0, 2, ..$ will be sufficient to decide the search.

So far, we have analytically derived the optimal power levels that need to be allocated by the BS to achieve its required downlink data rates (i.e., from the BS to each user), as well as to allow each user to achieve its uplink data rates (i.e., from the users to the BS) by giving it enough power to harvest and use for uplink communication. We now propose an efficient and practical algorithm that finds these optimal power levels. This

algorithm is based on the theory developed in this section.

7.3.3 An Efficient Algorithm for Solving the Joint Uplink and Downlink Optimization Formulation

After deriving the optimal power for the uplink and downlink communications in the two previous subsections, we now use these results to propose our Algorithm 3. Remember that we kept the splitting ratio ρ_k as a design parameter in a first step to make the problem convex. This parameter could be optimized at this level using an exhaustive search method to derive the optimal splitting ratio ρ_k^{opt} that minimizes the total power consumption. Also, note that this parameter could be optimized for every time slot as it depends on the channels' quality. The numerical evaluations of our optimization are

---

Algorithm 3 Joint Power Allocation

Require: $\{r_{BS,k}^{th}\}_{k=1}^{K}$, $\{r_{k,BS}^{th}\}_{k=1}^{K}$, $|h_{BS,k}^{i}|^{2}$, $|h_{k,BS}^{i}|^{2}$, N, and $\{\bar{P}_k\}_{k=1}^{K}$
1: **for** $k = 1 : K$ **do**
2:     Compute $\{P_{k,BS}^{j}\}_{j=1}^{N}$ using (7.7)
3:     **for** $\rho_k = 0 : 1$ **do**
4:         Find ψ_k using bisection method applied to (7.13)
5:         Compute λ_k using (7.13)
6:         Compute $\{P_{BS,k}^{i}\}_{i=1}^{N}$ using (7.12)
7:     **end for**
8:     Find ρ_k^{opt}
9: **end for**
10: **return** $\{P_{BS,k}^{i}\}_{i=1}^{N}$, $\{P_{k,BS}^{i}\}_{i=1}^{N}$, ρ_k^{opt} $\forall k \in [1..K]$

---

provided in Section 7.5. It is worth mentioning that our framework considers that the BS has enough processing capabilities to handle the computation complexity of Algorithm 3.

While our approach allows users to communicate with the BS using harvested energy, additional power savings can further be achieved when users have sufficient hardware capabilities. For instance, when equipped with appropriate hardware, having each user also harvest from the subcarriers used by any other user will result in harvesting more energy. Moreover, a user can also harvest from any other RF signals sent by any neighboring BSs, though in this case there is no guarantee that the BS is transmitting with the least amount of power. The essence of our proposed optimization framework is to guarantee

that the harvested amount of energy is enough for the users to meet their required rates in the uplink, and to do so with the least possible amount of power the BS will have to consume. Now that we considered the case of harvesting from dedicated RF signals only, in the next section, we consider the case of minimizing the BS's power consumption while assuming that users are equipped with sufficient hardware capability that allows them to harvest energy from their dedicated RF signals as well as the other users' signals. That is, each user can harvest energy from any ambient RF signal sent by its BS, whether destined to it or to other users serviced by the same BS.

7.4 Hybrid Dedicated and Ambient RF Signal Based Energy Harvesting

In the previous section, we considered the case where a user can harvest energy only from the RF signals that are intended for it by the BS. However, a user can still receive RF signals, though as interference, even when the signals are not meant to be sent to it. Therefore, a more general setup we consider here is to assume that a user can harvest energy not only from its intended RF signals, but also from all other ambient RF signals sent by the BS to any user. We anticipate that by doing so, the overall amount of energy to be consumed by the system will be reduced. In this section, we solve the power allocation optimization problem for this general setup.

The problem formulation remains the same as in (7.5) except that Q_k in the Constraint (7.5b) needs to be replaced by

$$Q_k = \eta \rho_k \sum_{l=1}^{K} \sum_{i=1}^{N} P_{BS,l}^i |h_{BS,l}^{i,k}|^2 + \sigma_{BS,l}^i, \qquad (7.15)$$

where $h_{BS,l}^{i,k}$ is the downlink channel impulse between the BS and the kth user that corresponds to the $(l-1) \times N + i$ subcarrier that is normally allocated for the communication between the BS and user l.

We use the same steps as in the previous section for solving this problem. We start by computing the amount of power needed by each user in the uplink. Here, the optimal power over each subcarrier is the same as the one derived in the previous section, given by Equation (7.7). In the downlink, the BS accounts for power needed by each user k

so that the harvested amount of power satisfies $Q_k + P_k^{bat} \geq \sum_i^N P_{k,BS}^{i*}$. In addition, the BS should meet the downlink rate $r_{BS,k}^{th}$.

Let $\boldsymbol{P}_{BS,k} = \left[P_{BS,k}^1, ..., P_{BS,k}^N \right]$ be the vector containing the power levels that the BS allocates for communication with user k, and $\boldsymbol{P} = [\boldsymbol{P}_{BS,1}, ..., \boldsymbol{P}_{BS,K}]^T$ be the vector containing the power levels used for the communication with all the users. Also, let $\boldsymbol{h}_{BS,k}^l = \left[|h_{BS,k}^{1,l}|^2, ..., |h_{BS,k}^{N,l}|^2 \right]$ and $\boldsymbol{h}_l = [\boldsymbol{h}_{BS,1}^l, ..., \boldsymbol{h}_{BS,K}^l]^T$. Hence, the optimal downlink power allocation for each user is the solution to

$$\min_{\{\{P_{BS,k}^i\}_{i=1}^N\}_{k=1}^K} \varsigma' + \tilde{\boldsymbol{\alpha}}^T \boldsymbol{P}, \tag{7.16a}$$

$$\text{s.t.} R_{BS,k} \geq r_{BS,k}^{th}, \tag{7.16b}$$

$$\boldsymbol{P}^T \boldsymbol{h}_k \geq P_k^{th} \tag{7.16c}$$

$$\boldsymbol{P} \succeq 0, \tag{7.16d}$$

where $\varsigma' = \varsigma + \sum_{k=1}^K \beta_k \left[\sum_{i=1}^N P_{k,BS}^{i*} + P_0 + P_0' - \eta \rho_k \sum_{l=1}^K \sum_{j=1}^N \sigma_{BS,l}^j \right]$, $\tilde{\boldsymbol{\alpha}} = \alpha \boldsymbol{1} + \sum_{k=1}^K \beta_k \eta \rho_k \boldsymbol{h}_k$ and $P_k^{th} = \frac{\sum_{i=1}^N P_{k,BS}^{i*} + P_0 + P_0' - \bar{P}_k}{\eta \rho_k} - \sum_{l=1}^K \sum_{i=1}^N \sigma_{l,BS}^i$.

Our objective is to derive the optimal downlink power for each user such that the total cost is minimized. The following theorem gives the optimal power allocation in this scenario.

Theorem 9. *The solution to the optimization problem* (7.16) *is*

$$P_{BS,k}^{i*} = \left[\frac{\lambda_k'}{\tilde{\alpha}_k^i - \sum_{l=1}^K \psi_l |h_{BS,k}^{i,l}|^2} - \frac{\sigma_{BS,k}^i}{(1 - \rho_k)|h_{BS,k}^i|^2} \right]_0^+ \tag{7.17}$$

where λ_k' and ψ_k are the K.K.T. multipliers to be specified later.

Proof. See Appendix D. ∎

Note that with comparison to the power level that we have derived in the other section (given by Equation (7.12)), the expression accounts for the interference channels between users. In total, we have $2K$ K.K.T. multipliers, $\{\lambda_k', \psi_k\}_{k=1}^K$, that we compute by replacing $P_{BS,k}^{i*}$ in the K.K.T. conditions. The following lemma provides a characterization of $\{\lambda_k', \psi_k\}_{k=1}^K$.

Lemma 5. *The expression of λ'_k is given by*

$$\lambda'_k = 2^{\frac{r^{th}_{BS,k}}{B|\mathcal{C}_k|}} \left(\prod_{i \in \mathcal{C}_k} \frac{\gamma^i_k}{\tilde{\alpha}^i_k - \sum_{l=1}^{K} \psi_l |h^{i,l}_{BS,k}|^2} \right)^{-\frac{1}{|\mathcal{C}_k|}}, \tag{7.18}$$

where $\mathcal{C}_k = \{i | \lambda'_k / (\tilde{\alpha}^i_k - \sum_{l=1}^{K} \psi_l |h^{i,l}_{BS,k}|^2) \geq 1/\gamma^i_k\}$ and $\boldsymbol{\psi} = [\psi_1 ... \psi_K]^T$ is the zero of the functions

$$f_k(\boldsymbol{x}) = \frac{2^{\frac{r^{th}_{BS,k}}{B|\mathcal{C}_k|}} \sum_{l=1}^{K} \sum_{i \in \mathcal{C}_l} \frac{|h^{i,k}_{BS,l}|^2}{\tilde{\alpha}^i_l - \sum_{m=1}^{K} x_m |h^{i,m}_{BS,l}|^2}}{\left(\prod_{i \in \mathcal{C}_k} \frac{\gamma^i_k}{\tilde{\alpha}^i_k - \sum_{l=1}^{K} x_l |h^{i,l}_{BS,k}|^2} \right)^{\frac{1}{|\mathcal{C}_k|}}}$$

$$- \sum_{l=1}^{K} \sum_{i \in \mathcal{C}_l} \frac{|h^{i,k}_{BS,l}|^2}{\gamma^i_l} - P^{th}_k \tag{7.19}$$

Proof. See Appendix E. ■

Note that in Equation (7.19), we have K unknowns $\{x_l\}_{l=1}^K$. But since we have K equations, theoretically, we could solve for $\{\psi_l\}_{l=1}^K$. To prove the existence of a zero of the function $\boldsymbol{f}$ defined as $\boldsymbol{f}(\boldsymbol{\psi}) = [f_1(\boldsymbol{\psi}) ... f_K(\boldsymbol{\psi})]^T$ where $f_k(\boldsymbol{\psi})$ is given by Equation (7.19), we proceed similarly to the proof in the case of the single variable by considering ψ_j to be variable and fixing the other $K - 1$ variables. We end up with the previous scenario where the bounds of the search intervals are $\phi_0 = 0$ and $\phi_n = \tilde{\alpha}^i_k / |h^{i,j}_{BS,k}|^2 - \sum_{l \in \mathcal{C}_k, l \neq j} \psi_l |h^{i,l}_{BS,k}|^2 / |h^{i,j}_{BS,k}|$ for $n \in \mathcal{C}_k$ and we restrict ψ_k to be positive. Then a sign check of the limit of the continuous function f_k in the bounds of the intervals is sufficient to prove that a zero exists.

Deriving a closed-form expression of $\boldsymbol{\psi}$ is not possible due to function nonlinearity. However, it could be derived iteratively using the Newton method where, at each iteration,

$$\boldsymbol{\psi}^{n+1} = \boldsymbol{\psi}^n - \left(\nabla \boldsymbol{f}(\boldsymbol{\psi}^n) \right)^{-1} \boldsymbol{f}(\boldsymbol{\psi}^n) \tag{7.20}$$

where $\left(\nabla \boldsymbol{f}(\boldsymbol{\psi})\right)_{kj} = \frac{\partial f_k(\boldsymbol{\psi})}{\partial \psi_j} = \xi'(\boldsymbol{\psi})\zeta(\boldsymbol{\psi}) + \xi(\boldsymbol{\psi})\zeta'(\boldsymbol{\psi})$, with

$$\xi(\boldsymbol{\psi}) = \frac{2^{\frac{r_{BS,k}^{th}}{B|\mathcal{C}_k|}}}{\left(\prod_{i\in\mathcal{C}_k} \frac{\gamma_{i,k}}{\tilde{\alpha}_k^i - \sum_{l=1}^{K}\psi_l|h_{BS,k}^{i,l}|^2}\right)^{\frac{1}{|\mathcal{C}_k|}}} \tag{7.21a}$$

$$\zeta(\boldsymbol{\psi}) = \sum_{l=1}^{K}\sum_{i\in\mathcal{C}_l} \frac{|h_{BS,l}^{i,k}|^2}{\tilde{\alpha}_l^i - \sum_{m=1}^{K}\psi_m|h_{BS,l}^{i,m}|^2} \tag{7.21b}$$

$$\xi'(\boldsymbol{\psi}) = -\frac{1}{|\mathcal{C}_k|} \frac{2^{\frac{r_{BS,k}^{th}}{B|\mathcal{C}_k|}} \sum_{i\in\mathcal{C}_k} \frac{|h_{BS,k}^{i,j}|^2}{\tilde{\alpha}_k^i - \sum_{m=1}^{K}\psi_m|h_{BS,k}^{i,m}|^2}}{\left(\prod_{i\in\mathcal{C}_k} \frac{\gamma_k^i}{\tilde{\alpha}_k^i - \sum_{l=1}^{K}\psi_l|h_{BS,k}^{i,l}|^2}\right)^{\frac{1}{|\mathcal{C}_k|}}} \tag{7.21c}$$

$$\zeta'(\boldsymbol{\psi}) = \sum_{l=1}^{K}\sum_{i\in\mathcal{C}_l} \frac{|h_{BS,l}^{i,k}|^2|h_{BS,l}^{i,j}|^2}{\left(\tilde{\alpha}_l^i - \sum_{m=1}^{K}\psi_m|h_{BS,l}^{i,m}|^2\right)^2} \tag{7.21d}$$

With the use of the Newton method for deriving $\boldsymbol{\psi}$, there is a tradeoff between precision and computational complexity. An accuracy ϵ of 10^{-5} is sufficient to get the Newton method converge in a relatively small computational time.

7.5 Numerical Evaluation

We consider that the BS is placed at the center of a cell with radius $d_0 = 1$ and that the users are uniformly distributed within the cell. The fading of the channels is modeled as Rayleigh with mean $\sqrt{[d_0/d_k]^\alpha}$ where α is the pathloss exponent set to 3, and d_k is the normalized distance between the mobile user k and the BS and is generated randomly between 0 and 1. At each user, the energy harvesting conversion efficiency η is chosen to be equal to 0.8 while the noise power density is taken equal to $N_0 = -174\ dBm$ as in [9]. The bandwidth of each sub-band is $15kHz$. The number of subcarriers used to communicate with each user, N, is taken equal to 10 unless otherwise specified. Since, the processing time for sending and receiving packets is negligible compared to the transmission power, then we set $P_0 = P_0' \approx 0$.
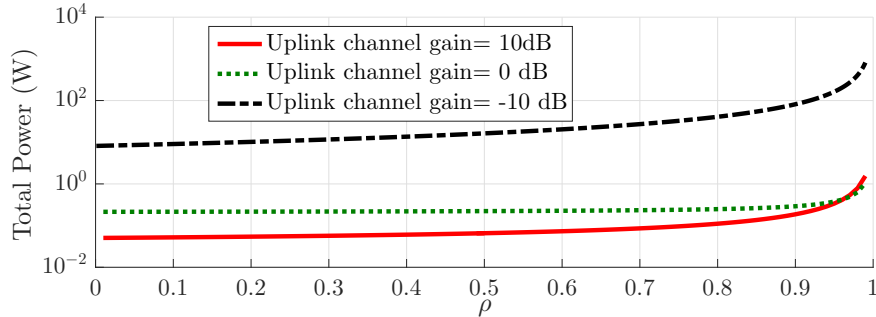
Figure 7.3: The sum power function of the splitting ratio ρ. The system parameters are as follows: the number of subcarriers $N = 5$, the downlink channel SNR= 10dB, and $r_{BS,k}^{th} = 15Kbit/s$ and $r_{k,BS}^{th} = 30Kbit/s$.

A key parameter in RF energy harvesting systems based on power splitter is the splitting ratio ρ_k. We first study its impact on the total power in the system when setting the battery power to zero. Consider the case where the BS communicates with one user, i.e., $K = 1$, and we take $\alpha = \beta = 1$ and plot the total power in the system as a function of the splitting ratio ρ_k in Fig. 7.3. First, observe that the required power varies as a function of the splitting ratio, as well as the SNR of the uplink and downlink channels. It decreases with the increase of ρ_k up to ρ_k^{opt}, and it starts to increase as ρ_k goes beyond ρ_k^{opt}. When $\rho_k < \rho_k^{opt}$, more power is needed to be harvested to meet the user's rate threshold, $r_{k,BS}^{th}$. On the other hand, if $\rho_k > \rho_k^{opt}$, then the user's needed power is met while the BS needs to increase its transmission power in order to meet $r_{BS,k}^{th}$. Hence, the splitting ratio strikes a balance between the amount of harvested power and the needed power to meet the data rate. Second, we investigate the effect of the uplink channels' SNR on the total power. As the uplink channels' SNR becomes stronger, less power consumption is needed. Third, for a strong downlink channels' SNR (chosen to be 10 dB), the optimal splitting ratio ρ_k^{opt} becomes closer to 0 as the uplink channels' SNR increases. This is because as the channels' SNR becomes stronger, less power is needed to be harvested (proportional to the splitting ratio).

In Fig. 7.4, we plot the optimal splitting ratio ρ_k^{opt}, found using Algorithm 3, as a function of the uplink channels' SNR. Observe that the optimal splitting ratio decreases as the uplink channels' SNR increases. This confirms the result shown in Fig. 7.3 since
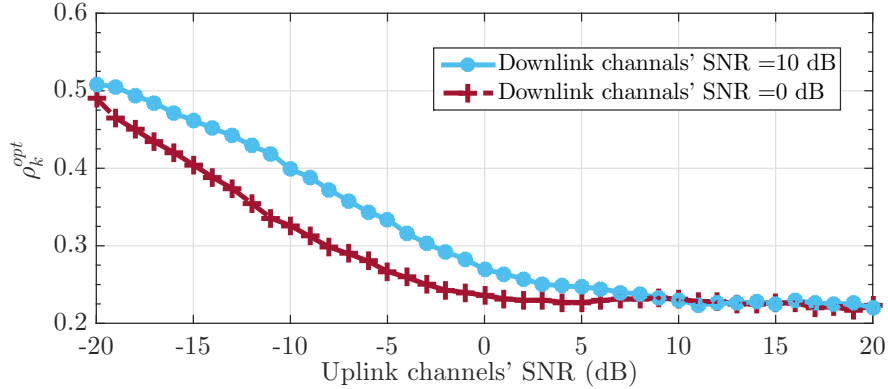
Figure 7.4: The optimal splitting ratio ρ_k as a function of the uplink channels' SNR. The system parameters are as follows: the number of subcarriers $N = 5$, the downlink channel SNR= 10dB, $r_{BS,k}^{th} = 300 Kbit/s$ and $r_{k,BS}^{th} = 150 Kbit/s$.

if the uplink channel quality increases, less power is needed to meet the user's rate requirement and therefore less amount of harvested energy is required. If the downlink channels' quality becomes worse, the optimal splitting ratio decreases in the low SNR regime. In fact, more power should be dedicated to meet the downlink rate requirement $r_{BS,k}^{th}$. This is equivalent to the increase of the portion dedicated for decoding (i.e., $1 - \rho_k$).

In Fig. 7.5, we investigate the effect of the downlink channels' SNR for a fixed ρ_k and for the optimal ρ_k^{opt} under different channels' SNR values. We plot the total power consumption while varying the downlink channels' SNR for a fixed splitting ratio, $\rho = 0.5$. Note that the total power consumption decreases as the downlink channels' SNR increases. As the downlink channel gains become stronger, less power is required to achieve the required data rate, $r_{BS,k}^{th}$. Also, as the uplink channels' SNR increases, the total power consumption decreases. This is because the user needs less power to achieve its required data rate, $r_{k,BS}^{th}$. Furthermore, we plot in the same figure the sum power using the optimal splitting ratio ρ_k^{opt}. Note that an additional gain in the power consumption is obtained with the optimal splitting ratio. However, from a practical perspective, this comes at the expense of a more sophisticated circuitry design, as the optimal ratio needs to be found at each time slot, depending on the channels' gains.

Having studied the impact of the splitting ratio in the case of one single user, we
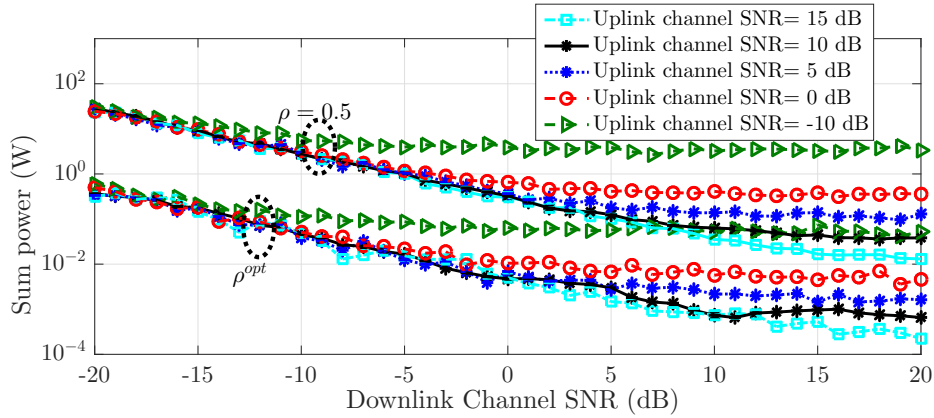
Figure 7.5: The sum power as a function of the downlink channel SNR between the BS and one user. The system parameters are as follows: the number of subcarriers $N = 5$, $r_{BS,k}^{th} = 15 Kbit/s$, and $r_{k,BS}^{th} = 30 Kbit/s$.

now assess the performance of our framework by considering the following metrics: the total power cost (utility cost) and the system lifetime. Note that in the case of not harvesting from the received RF signals and if the power at the users' batteries is not sufficient to meet their data rates, an outage performance occurs. That is, the users can not offload their data. On the other hand, the system lifetime is usually maximal when the harvesting capability enabled.

We assume that $\kappa_k = \kappa = \beta/\alpha$ and to ensure the non negativity of $\tilde{\alpha}_k^i$ as well as κ, the values of κ should be picked in the interval $[0.. \min_{k,i \in \mathcal{C}_k} (1/(\eta\rho|h_{BS,k}^i|^2))]$. In Fig. 7.6, we plot the power utility as a function of κ. Observe that relaying on harvesting results on a higher cost compared to the case when relaying solely on the batteries at the different users. Furthermore, we observe that the utility cost for both systems enhances as κ increases. In fact, as κ increases, β increases as well, and hence, the cost relative to the power used from the battery augments and affects the total cost.

The second performance metric that we consider is the lifetime. While in wireless sensors networks problems, the lifetime is often defined as the number of transmission time slots from the deployment up to when the first sensor's battery dies [6], we define it here as the overage time until the users' battery dies. We consider that the users have an equal initial amount of power P_k^{bat}. In Fig. 7.7, we plot the lifetime as a function of the users' number. We define ϵ as the portion of power used from the battery, while
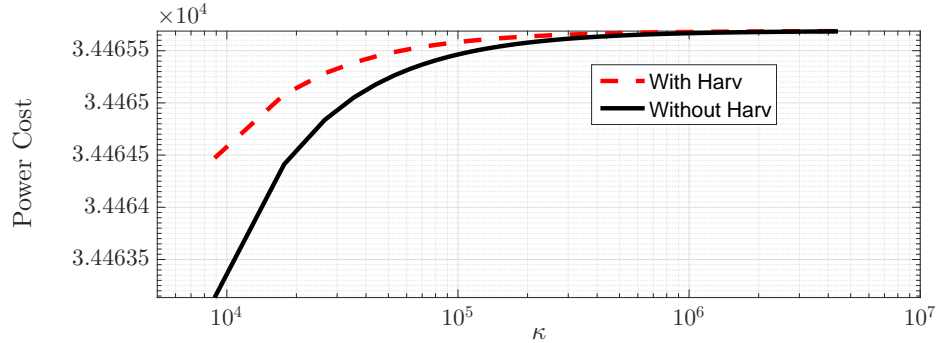
Figure 7.6: The power utility as a function of κ. The system parameters are as follows: $K = 50$ with $N = 5$ subcarriers in the uplink and N in the downlink, the uplink and downlink channels SNR= 10dB, $r_{BS,k}^{th} = 15Kbit/s$ and $r_{k,BS}^{th} = 30Kbit/s$.

(1-ϵ) is the portion of power harvested from the BS's signal. Hence, $\epsilon = 1$ corresponds to the use of the total power needs from the battery. First, we notice that regardless of the number of users in the system, as long as we harvest a portion of the power, we achieve a higher lifetime compared to the case when we solely rely on the user's battery. Second, as the portion of the power taken from the battery decreases, a higher system lifetime is achieved. When ϵ tends to zero, the lifetime goes to infinity. This is because almost all the power is harvested from the RF signals. Third, normally the placement of the users themselves in the cell affects the performance. However, the figure shows that the curves are almost flat as a function of the number of users. This is because, we average over a large number of users' placement. Last, recalling Figure 7.6, a tradeoff between the cost and the lifetime should be struck.

Now, we look at the BS power allocation as a function of the channels' variations. When accounting for harvesting from the signals intended to the other users, we anticipate to achieve further power savings at the BS. Hence, we compare the total power allocated for powering and communicating with the different users in the two system setups: when each user harvests power only from its intended signals and when, in addition to that, each user harvests energy from the signals dedicated to the other users. In Fig. 7.8, we plot the total power used by the BS for the two setups and for different number of users as a function of the downlink channels' SNR. Note that the users are assumed to have equal average downlink channels' SNR; however, the results are still
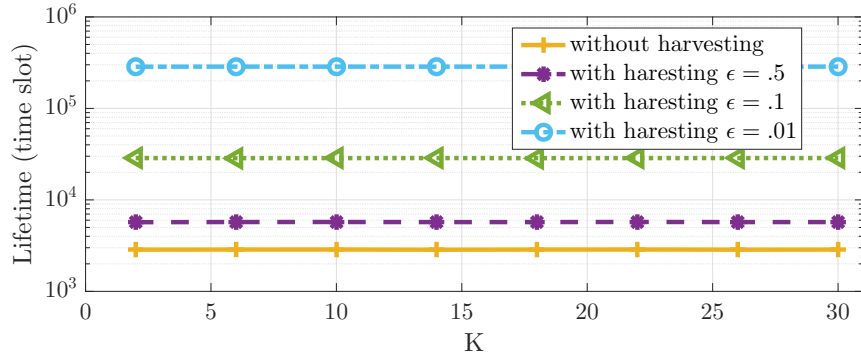
Figure 7.7: The system lifetime as a function of the uniformly deployed sensors. The system parameters are as follows: One user with $N = 5$ subcarriers in the uplink and N in the downlink, the uplink and downlink channels SNR= 10dB, and $r_{BS,k}^{th} = 100Kbit/s$ and $r_{k,BS}^{th} = 1Mbit/s$.

valid for a more general system. First, remark that an increase in the number of users results in an augmentation in the needed transmission power at the BS. On the other hand, the second system setup allows to achieve less power consumption when compared with the first one. This is because accounting for the received interference at each user, which leads to increasing the amount of the harvested power, decreases the total required power at the BS to serve the users. However, this substantial gain comes at the expense of the prior knowledge of all the channel gains between the BS and the users. Fortunately, this is required in spectrum assignment process.

7.6 Conclusion

This paper investigates the optimal power allocation for a multiuser multicarrier communication system composed of a base station and mobile users. We solved the optimal power allocation at the base station to enable data communication as well as powering the users using RF energy harvesting. We studied the tradeoff between the power cost and system lifetime. Our performance analysis shows that the power consumption gain takes advantage of the variability of channels' gains, the splitting ratio, and the number of subcarriers. Energy harvesting capability increases the network lifetime, however, this comes with the expense of a higher power cost.
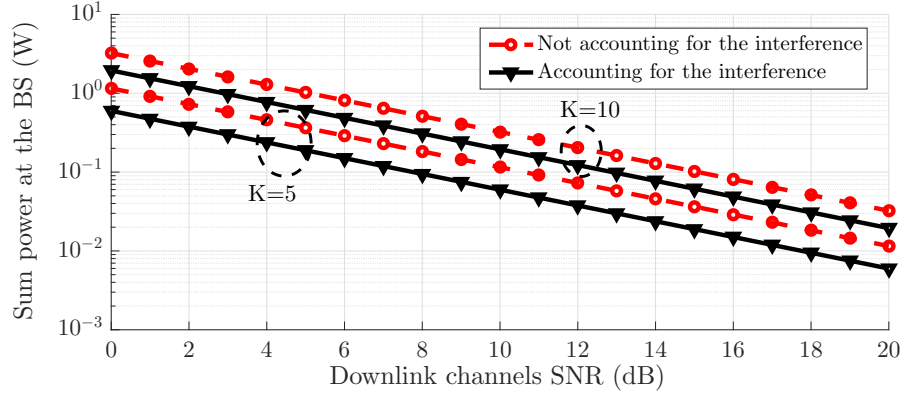
Figure 7.8: Comparison of the BS's sum power allocated to power the users and achieve their downlink rate for the two scenarios: each user harvests only from the subcarriers used for its communication and when each user harvests also from the interference. The system parameters: the uplink channels' SNR 10 dB and $r_{BS,k}^{th}15kHz$ and $r_{k,BS}^{th} = 30Kbit/s$.

7.7 Appendix

7.7.1 Proof of Proposition 7

Proof. In general, the optimization problem (7.5) is not convex. While the objective and the first constraint are affine functions, the two constraints (7.5c) and (7.5d), as function of $\boldsymbol{\rho}$, are not convex. By fixing its value, $\boldsymbol{\rho}$ is no longer an optimization parameter, and hence, the problem becomes convex. ∎

7.7.2 Proof of lemma 7

Proof. The solution to (7.6) is straightforwardly derived by minimizing the Lagrangian dual function. It is the classical water filling [3]. ∎

7.7.3   Proof of Theorem 8

Proof. Since the optimization problem (7.11) is convex, we consider the dual problem using the Karush-Kuhn-Tucker (K.K.T) conditions. The Lagrangian can be written as

$$
\mathcal{L}_k\big(\{P^i_{BS,k}\}^N_{i=1}\big) \;=\; \sum_{i=1}^{N} \tilde{\alpha}^i_k P^i_{BS,k} - \lambda_k(R_{BS,k} - r^{th}_{BS,k})
$$
$$
-\; \psi_k\Big(\sum_{i=1}^{N} P^i_{BS,k}|h^i_{BS,k}|^2 - P^{th}_k\Big), \tag{7.22}
$$

where λ_k and ψ_k are the K.K.T. multipliers [27]. By taking the derivative of the Lagrangian $\mathcal{L}_k$ over $P^i_{BS,k}$ and set it to zero, we get

$$
\tilde{\alpha}^i_k \;-\; \frac{\lambda_k(1-\rho_k)|h^i_{BS,k}|^2/\sigma^i_{BS,k}}{(1+P^i_{BS,k}(1-\rho_k)|h^i_{BS,k}|^2/\sigma^i_{BS,k})\log(2)}
$$
$$
-\; \psi_k|h^i_{BS,k}|^2 = 0 \tag{7.23}
$$

From Equation (7.23) and by letting $\lambda'_k = \lambda_k/\log(2)$, the power level $P^i_{BS,k}$ is, therefore, expressed as

$$
P^i_{BS,k} = \frac{\lambda'_k}{\tilde{\alpha}^i_k - \psi_k|h^i_{BS,k}|^2} - \frac{\sigma^i_{BS,k}}{(1-\rho_k)|h^i_{BS,k}|^2}. \tag{7.24}
$$

Then, we restrict the power to be positive or null to ensure the positivity of the power levels. To find the Lagrange multipliers λ'_k and ψ_k, we rely on the K.K.T. conditions. Given

$$
\lambda'_k\left(\frac{r^{th}_{BS,k}}{B} - \sum_{i=1}^{N}\log_2\left(1 + \frac{(1-\rho_k)P^{i^*}_{BS,K}|h^i_{BS,K}|^2}{\sigma^i_{BS,K}}\right)\right) = 0, \tag{7.25}
$$

it follows that either $\lambda'_k = 0$ or

$$
\frac{r^{th}_{BS,k}}{B} = \sum_{i=1}^{N}\log_2\left(1 + \frac{(1-\rho_k)P^{i^*}_{BS,K}|h^i_{BS,K}|^2}{\sigma^i_{BS,K}}\right) \tag{7.26}
$$

λ'_k cannot be 0, since otherwise $P^{i^*}_{BS,k} = 0$ for all $i \in [1..N]$, which does not meet the rate constraint. Now substituting the expression of the optimal power $P^{i^*}_{BS,k}$, given in

Equation (7.12), into Equation (7.26) yields

$$
|\mathcal{S}_k| \log_2(\lambda_k') = \frac{r_{BS,k}^{th}}{B}
$$
$$
- \log_2 \left(\prod_{i \in \mathcal{S}_k} \frac{(1-\rho_k)|h_{BS,k}^i|^2}{(\tilde{\alpha}_k^i - \psi_k |h_{BS,k}^i|^2)\sigma_{BS,k}^i} \right) \tag{7.27}
$$

The second K.K.T. condition gives

$$
\psi_k \left(P_k^{th} - \sum_{i=1}^{N} P_{BS,k}^{i*} |h_{BS,k}^i|^2 \right) = 0 \tag{7.28}
$$

If $\psi_k \neq 0$, then $P_k^{th} = \sum_{i=1}^{N} P_{BS,k}^{i*} |h_{BS,k}^i|^2$ must hold. In this case, substituting $P_{BS,k}^{i*}$ with its expression given in Equation (7.12), results in

$$
\begin{aligned}
P_k^{th} &= \sum_{i \in \mathcal{S}_k} P_{BS,k}^{i*} |h_{BS,k}^i|^2 \\
&= \lambda_k' \sum_{i \in \mathcal{S}_k} \frac{|h_{BS,k}^i|^2}{\tilde{\alpha}_k^i - \psi_k |h_{BS,k}^i|^2} - \sum_{i \in \mathcal{S}_k} \frac{\sigma_{BS,k}^i}{1 - \rho_k}
\end{aligned} \tag{7.29}
$$

Now combining Equations (7.27) and (7.29) yields

$$
P_k^{th} = \frac{2^{r_{BS,k}^{th}/B|\mathcal{S}_k|} \sum_{i \in \mathcal{S}_k} \frac{|h_{BS,k}^i|^2}{\tilde{\alpha}_k^i - \psi_k |h_{BS,k}^i|^2}}{\left(\prod_{i \in \mathcal{S}_k} \frac{(1-\rho_k)|h_{BS,k}^i|^2}{(\tilde{\alpha}_k^i - \psi_k |h_{BS,k}^i|^2)\sigma_{BS,k}^i} \right)^{\frac{1}{|\mathcal{S}_k|}}} - \sum_{i \in \mathcal{S}_k} \frac{\sigma_{BS,k}^i}{1 - \rho_k} \tag{7.30}
$$

The value of ψ_k that satisfies Equation (7.30) is the zero of the function f. This ends the proof of the theorem. Note that for consistency, recalling the second K.K.T. condition, $\psi_k = 0$ remains a special case of the solution. ∎

7.7.4   Proof of Theorem 9

Proof. Since the optimization problem (7.16) is convex, we rely on the Lagrangian multiplier, which can be written as

$$\mathcal{L}\big(\boldsymbol{P}, \{\lambda_k, \psi_k\}_{k=1}^{K}\big) = \varsigma' - \sum_{k=1}^{K} \lambda_k (R_{BS,k} - r_{BS,k}^{th})$$
$$- \sum_{k=1}^{K} \psi_k \big(\boldsymbol{P}^T \boldsymbol{h}_k - P_k^{th}\big) + \tilde{\boldsymbol{\alpha}}^T \boldsymbol{P} \tag{7.31}$$

For simplicity, let $\gamma_k^i = (1 - \rho_k)|h_{BS,k}^i|^2 / \sigma_{BS,k}^i$. By taking the derivative of $\mathcal{L}$ over $P_{BS,k}^i$, it follows that

$$\tilde{\alpha}_k^i - \frac{\lambda_k \gamma_k^i}{(1 + P_{BS,k}^i \gamma_k^i) \log(2)} - \sum_{l=1}^{K} \psi_l |h_{BS,k}^{i,l}|^2 = 0 \tag{7.32}$$

where $\alpha_k^i = \alpha + \sum_{l}^{K} \beta_l \eta \rho_l |h_{BS,k}^{i,l}|^2$. By letting $\lambda_k' = \lambda_k / \log(2)$, the optimal power level allocated at the BS to user k over the subcarrier i can be derived as

$$P_{BS,k}^i = \frac{\lambda_k'}{\tilde{\alpha}_k^i - \sum_{l=1}^{K} \psi_l |h_{BS,k}^{i,l}|^2} - \frac{1}{\gamma_k^i} \tag{7.33}$$

Then, we restrict the power to be positive. ∎

7.7.5   Proof of Lemma 5

Proof. Using the K.K.T. condition,

$$\lambda_k' \big(R_{BS,k} - r_{BS,k}^{th}\big) = 0, \tag{7.34}$$

and replacing the expression of the optimal power level given by Equation (7.33), the expression of the K.K.T. multiplier λ_k' can be written as

$$\log_2(\lambda_k') = \frac{r_{BS,k}^{th}}{B|\mathcal{C}_k|} - \frac{\log_2 \left(\prod_{i \in \mathcal{C}_k} \frac{\gamma_k^i}{\tilde{\alpha}_k^i - \sum_{l=1}^{K} \psi_l |h_{BS,k}^{i,l}|^2} \right)}{|\mathcal{C}_k|} \tag{7.35}$$

Hence, we get the expression of λ'_k as in Equation (7.18). Hence, getting λ'_k requires the knowledge of $\boldsymbol{\psi}$. Now, to characterize $\boldsymbol{\psi}$, we consider the second K.K.T condition $\psi_k\left(\sum_{l=1}^{K}\sum_{i=1}^{N}P_{BS,l}^{i*}\left|h_{BS,l}^{i,k}\right|^2 - P_k^{th}\right) = 0$, if $\psi_k \neq 0$, then we can write

$$
\begin{aligned}
P_k^{th} &= \sum_{l=1}^{K}\sum_{i\in\mathcal{C}_l}P_{BS,l}^{i*}\left|h_{BS,l}^{i,k}\right|^2 \\
&= \lambda'_k\sum_{l=1}^{K}\sum_{i\in\mathcal{C}_l}\frac{\left|h_{BS,l}^{i,k}\right|^2}{\tilde{\alpha}_l^i - \sum_{m=1}^{K}\psi_m\left|h_{BS,l}^{i,m}\right|^2} - \sum_{l=1}^{K}\sum_{i\in\mathcal{C}_l}\frac{\left|h_{BS,l}^{i,k}\right|^2}{\gamma_l^i}
\end{aligned}
\tag{7.36}
$$

Now, substituting Equation (7.18) into Equation (7.36) gives

$$
\begin{aligned}
P_k^{th} &= \frac{2^{\frac{r_{BS,k}^{th}}{B|\mathcal{C}_k|}}}{\left(\prod_{i\in\mathcal{C}_k}\frac{\gamma_k^i}{\tilde{\alpha}_k^i - \sum_{l=1}^{K}\psi_l\left|h_{BS,k}^{i,l}\right|^2}\right)^{\frac{1}{|\mathcal{C}_k|}}} \\
&\times \sum_{l=1}^{K}\sum_{i\in\mathcal{C}_l}\frac{\left|h_{BS,l}^{i,k}\right|^2}{\tilde{\alpha}_l^i - \sum_{m=1}^{K}\psi_m\left|h_{BS,l}^{i,m}\right|^2} - \sum_{l=1}^{K}\sum_{i\in\mathcal{C}_l}\frac{\left|h_{BS,l}^{i,k}\right|^2}{\gamma_l^i}.
\end{aligned}
$$

Hence, it is clear that $\boldsymbol{\psi}$ is the zero of the functions f_k ■

Acknowledgement

Bibliography

[1] https://www.advanticsys.com/shop/mtmcm5000msp-p-14.html.

[2] R. Aggarwal, M. Assaad, C.E. Koksal, and P. Schniter. Joint scheduling and resource allocation in the ofdma downlink: Utility maximization under imperfect

channel-state information. *IEEE Trans. on Signal Processing*, 59(11):5589–5604, 2011.

[3] Stephen Boyd and Lieven Vandenberghe. *Convex Optimization*. Cambridge University Press, New York, NY, USA, 2004.

[4] John Buckley, Brendan O'Flynn, Loizos Loizou, Peter Haigh, David Boyle, Philip Angove, John Barton, CO'Mathuna E Popovici, and S O'Connell. A novel and miniaturized 433/868mhz multi-band wireless sensor platform for body sensor network applications. In *Proc. of Int'l Conference on Wearable and Implantable Body Sensor Networks (BSN)*, pages 63–66. IEEE, 2012.

[5] H. Chen, Y. Ma, Z. Lin, Y. Li, and B. Vucetic. Distributed power control in interference channels with qos constraints and rf energy harvesting: A game-theoretic approach. *IEEE Trans. on Vehicular Technology*, PP(99):1–1, 2016.

[6] Yunxia Chen and Qing Zhao. On the lifetime of wireless sensor networks. *IEEE Communications Letters*, 9(11):976–978, Nov 2005.

[7] Zhiguo Ding, S.M. Perlaza, I. Esnaola, and H.V. Poor. Power allocation strategies in energy harvesting wireless cooperative networks. *IEEE Trans. on Wireless Communications*, 13(2):846–860, February 2014.

[8] Zhaoxi Fang, Tianlong Song, and Tongtong Li. Energy harvesting for two-way OFDM communications under hostile jamming. *IEEE Signal Processing Letters*, 22(4):413–416, April 2015.

[9] Shu Fu, Hong Wen, and Bin Wu. Power-fractionizing mechanism: Achieving joint user scheduling and power allocation via geometric programming. *IEEE Trans. on Vehicular Technology*, 2017.

[10] Hakim Ghazzai, Elias Yaacoub, Mohamed-Slim Alouini, and Adnan Abu-Dayya. Performance of green lte networks powered by the smart grid with time varying user density. In *Proc. of IEEE VTC-Fall*, pages 1–6, 2013.

[11] M. Gregori and M. Payaro. Multiuser communications with energy harvesting transmitters. In *Proc. of IEEE Int'l Conference on Communications (ICC)*, pages 5360–5365, June 2014.

[12] Yanju Gu and Sonia Aïssa. Rf-based energy harvesting in decode-and-forward relaying systems: Ergodic and outage capacities. *IEEE Trans. on Wireless Communications*, 14(11):6425–6434, 2015.

[13] D.T. Hoang, D. Niyato, P. Wang, and D.I. Kim. Performance optimization for cooperative multiuser cognitive radio networks with RF energy harvesting capability. *IEEE Trans. on Wireless Communications*, 14(7):3614–3629, July 2015.

[14] Kaibin Huang and Xiangyun Zhou. Cutting the last wires for mobile communications by microwave power transfer. *IEEE Communications Magazine*, 53(6):86–93, 2015.

[15] Ozlem Durmaz Incel. A survey on multi-channel communication in wireless sensor networks. *Comp. Net.*, 55(13):3081–3099, 2011.

[16] Hyungsik Ju and Rui Zhang. Throughput maximization in wireless powered communication networks. *IEEE Trans. on Wireless Communications*, 13(1):418–428, 2014.

[17] Bassem Khalfi, Bechir Hamdaoui, Mahdi Ben Ghorbel, Mohsen Guizani, and Xi Zhang. Joint data and power transfer optimization for energy harvesting wireless networks. In *Proc. of IEEE INFOCOM WKSHPS,*, pages 742–747, 2016.

[18] I. Krikidis, S. Timotheou, S. Nikolaou, Gan Zheng, D.W.K. Ng, and R. Schober. Simultaneous wireless information and power transfer in modern communication systems. *IEEE Communications Magazine*, 52(11):104–110, Nov 2014.

[19] Thanh Tu Lam, Marco Di Renzo, and Justin P Coon. System-level analysis of swipt mimo cellular networks. *IEEE Comm. Letters*, 20(10):2011–2014, 2016.

[20] Liang Liu, Rui Zhang, and Kee-Chaing Chua. Wireless information transfer with opportunistic energy harvesting. In *Proc. of IEEE Int. Symp. on Information Theory (ISIT)*, pages 950–954, July 2012.

[21] Xiao Lu, Ping Wang, D. Niyato, Dong In Kim, and Zhu Han. Wireless networks with RF energy harvesting: A contemporary survey. *IEEE Communications Surveys Tutorials*, 17(2):757–789, 2nd Q 2015.

[22] Derrick Wing Kwan Ng, Ernest S Lo, and Robert Schober. Wireless information and power transfer: Energy efficiency optimization in ofdma systems. *IEEE Trans. on Wireless Communications*, 12(12):6352–6370, 2013.

[23] S. Khoshabi Nobar, K. Adli Mehr, and J. Musevi Niya. Rf-powered green cognitive radio networks: Architecture and performance analysis. *IEEE Communications Letters*, 20(2):296–299, Feb 2016.

[24] Fred Richter, Albrecht J Fehske, and Gerhard P Fettweis. Energy efficiency aspects of base station deployment strategies for cellular networks. In *Proc. of IEEE VTC-Fall,*, pages 1–5, 2009.

[25] Javier Rubio and Antonio Pascual-Iserte. Harvesting management in multiuser mimo systems with simultaneous wireless information and power transfer. In *Proc. of IEEE VTC-Spring*, pages 1–5, May 2015.

[26] Yi Shi, Liguang Xie, Y Thomas Hou, and Hanif D Sherali. On renewable sensor networks with wireless energy transfer. In *Proc. of IEEE INFOCOM*, pages 1350–1358, 2011.

[27] Boyd Stephen and Vandenberghe Lieven. *Convex Optimization*. Cambridge University Press, 2004.

[28] Bin Tong, Zi Li, Guiling Wang, and Wensheng Zhang. How wireless power charging technology affects sensor network deployment and routing. In *Proc. of IEEE ICDCS*, pages 438–447, June 2010.

[29] Lav R Varshney. Transporting information and energy simultaneously. In *Proc. of IEEE Int'l Symp. on Infor. Theory*, pages 1612–1616, 2008.

[30] Javad Vazifehdan, R Venkatesha Prasad, Martin Jacobsson, and Ignas Niemegeers. An analytical energy consumption model for packet transfer over wireless links. *IEEE Communications Letters*, 16(1):30–33, 2012.

[31] Liguang Xie, Yi Shi, Y Thomas Hou, Wenjing Lou, Hanif Sherali, and Scott F Midkiff. Bundling mobile base station and wireless energy transfer: Modeling and optimization. In *Proc. of IEEE INFOCOM*, pages 1636–1644, 2013.

[32] Liguang Xie, Yi Shi, Y Thomas Hou, Wenjing Lou, Hanif D Sherali, and Scott F Midkiff. On renewable sensor networks with wireless energy transfer: the multi-node case. In *Proc. of IEEE SECON*, pages 10–18, 2012.

[33] Liguang Xie, Yi Shi, Y Thomas Hou, and Hanif D Sherali. Making sensor networks immortal: An energy-renewal approach with wireless power transfer. *IEEE/ACM Trans. on Netw.*, 20(6):1748–1761, 2012.

[34] Zhou Xun, Zhang Rui, and Ho Chin Keong. Wireless information and power transfer: Architecture design and rate-energy tradeoff. *IEEE Trans. on Communications*, 61(11):4754–4767, November 2013.

[35] E. Yaacoub and Z. Dawy. A survey on uplink resource allocation in ofdma wireless networks. *IEEE Communications Surveys Tutorials*, 14(2):322–337, 2012.

[36] Weiliang Zeng, Yahong Rosa Zheng, and Robert Schober. Online resource allocation for energy harvesting downlink multiuser systems: Precoding with modulation, coding rate, and subchannel selection. *IEEE Trans. on Wireless Communications*, 14(10):5780–5794, 2015.

[37] Chao Zhai, Ju Liu, and Lina Zheng. Relay-based spectrum sharing with secondary users powered by wireless energy harvesting. *IEEE Trans. on Communications*, 64(5):1875–1887, 2016.

[38] Xun Zhou, Chin Keong Ho, and Rui Zhang. Wireless power meets energy harvesting: a joint energy allocation approach in ofdm-based system. *IEEE Trans. on Wireless Comm.*, 15(5):3481–3491, 2016.

[39] Nizar Zorba and Christos Verikoukis. Energy optimization for bidirectional multimedia communication in unsynchronized tdd systems. *IEEE Systems Journal*, 10(2):797–804, 2016.

Chapter 8: Conclusions

This dissertation presents algorithms and frameworks that we proposed to enable efficient resource sensing and sharing. In particular, based on compressive sampling theory, we proposed a weighted ℓ_1-minimization recovery approach that accounts for the block-like structure inherent to the heterogeneous nature of wideband spectrum allocation. We showed that the proposed approach outperforms existing approaches by achieving lower mean square errors, enabling higher detection probability, and requiring lesser numbers of measurements when compared to the-state-of-the-art approaches. Moreover, we applied supervised learning to provide accurate estimates of the wideband spectrum occupancy and exploit it to help improve the spectrum recovery scheme. We showed that our scheme makes great performance enhancements in terms of sensing overhead, sensing energy, and spectrum decision accuracy. Furthermore, we leveraged user cooperation to overcome receiver hardware limitations as well as time variability of band occupancy during wideband spectrum sensing. We showed that cooperation overcomes these issues by enabling distributed compressive sampling-based spectrum sensing, and does so by requiring smaller numbers of measurements by each user only. Also, we designed efficient non-uniform sensing matrices suitable for such an environment. The results show that when the impact of fading is not so significant (for instance by considering close-by SUs), comparable performance can still be achieved from a smaller number of SUs. In addition to that, we presented a framework that builds an accurate spectrum occupancy map for wideband spectrum sharing. The framework exploits the under-utilization of the wideband spectrum, the heterogeneity in the spectrum occupancy, and the spatial correlation between sensing nodes to achieve scalable decisions for the spectrum occupancy while incurring small network communication overhead. Finally, we investigated the optimal power allocation for a multiuser multicarrier communication system composed of a base station and mobile users. We solved the optimal power allocation at the base station to enable data communication as well as powering the users using RF energy harvesting. We studied the tradeoff between the power cost and system lifetime. Our performance analysis shows that the power consumption gain takes advantage of

the variability of channels' gains, the splitting ratio, and the number of subcarriers. Energy harvesting capability increases the network lifetime, however, this comes with the expense of a higher power cost.

Bibliography

[1] https://www.advanticsys.com/shop/mtmcm5000msp-p-14.html.

[2] Ieee standard for information technology–telecommunications and information exchange between systems–local and metropolitan area networks–specific requirements part 22.1: Standard to enhance harmful interference protection for low-power licensed devices operating in tv broadcast bands. *IEEE Std 802.22.1-2010*, pages 1–145, Nov 2010.

[3] FCC: GN docket no: 14-177, report and order and further notice of proposed rulemaking, July 2016.

[4] 3GPP TR 23.799 V1.0.0. 3rd generation partnership project; technical specification group services and system aspects; study on architecture for next generation system (release 14). Technical report, 3GPP, Sept. 2016.

[5] Omid Abari, Fabian Lim, Fred Chen, and Vladimir Stojanović. Why analog-to-information converters suffer in high-bandwidth sparse signal applications. *IEEE Trans. on Circuits and Systems I: Regular Papers*, 60(9):2273–2284, 2013.

[6] Sherif Abdelwahab, Bechir Hamdaoui, Mohsen Guizani, and Taieb Znati. Replisom: Disciplined tiny memory replication for massive iot devices in LTE edge cloud. *IEEE Internet of Things Journal*, 3(3):327–338, 2016.

[7] R. Aggarwal, M. Assaad, C.E. Koksal, and P. Schniter. Joint scheduling and resource allocation in the ofdma downlink: Utility maximization under imperfect channel-state information. *IEEE Trans. on Signal Processing*, 59(11):5589–5604, 2011.

[8] M Eren Ahsen and M Vidyasagar. Error bounds for compressed sensing algorithms with group sparsity: A unified approach. *Applied and Computational Harmonic Analysis*, 2015.

[9] Ian F. Akyildiz, Brandon F. Lo, and Ravikumar Balakrishnan. Cooperative spectrum sensing in cognitive radio networks: A survey. *Physical Communication*, 4:40–62, 2011.

[10] Fadi M Al-Turjman. Information-centric sensor networks for cognitive iot: an overview. *Annals of Telecommunications*, pages 1–16, 2016.

[11] Olusegun Peter Awe and Sangarapillai Lambotharan. Cooperative spectrum sensing in cognitive radio networks using multi-class support vector machine algorithms. In *Proc. of International Conference on Signal Processing and Communication Systems (ICSPCS),*, pages 1–7. IEEE, 2015.

[12] F. Azmat, Y. Chen, and N. Stocks. Analysis of spectrum occupancy using machine learning algorithms. *IEEE Trans. on Vehicular Technology*, 65(9):6853–6860, Sept 2016.

[13] Dror Baron, Marco F Duarte, Michael B Wakin, Shriram Sarvotham, and Richard G Baraniuk. Distributed compressive sensing. *arXiv preprint arXiv:0901.3403*, 2009.

[14] S Becker, EJ Candes, and M Grant. TFOCS: Templates for first-order conic solvers, version 1.3. 1, 2014.

[15] Andrea Biral, Marco Centenaro, Andrea Zanella, Lorenzo Vangelista, and Michele Zorzi. The challenges of M2M massive access in wireless cellular networks. *Digital Communications and Networks*, 1(1):1–19, 2015.

[16] Mario Bkassiny, Yang Li, and Sudharman K Jayaweera. A survey on machine-learning techniques in cognitive radios. *IEEE Communications Surveys & Tutorials*, 15(3):1136–1159, 2013.

[17] Flavio Bonomi, Rodolfo Milito, Jiang Zhu, and Sateesh Addepalli. Fog computing and its role in the internet of things. In *Proceedings of the first edition of the MCC workshop on Mobile cloud computing*, pages 13–16. ACM, 2012.

[18] Stephen Boyd and Lieven Vandenberghe. *Convex Optimization*. Cambridge University Press, New York, NY, USA, 2004.

[19] John Buckley, Brendan O'Flynn, Loizos Loizou, Peter Haigh, David Boyle, Philip Angove, John Barton, CO'Mathuna E Popovici, and S O'Connell. A novel and

miniaturized 433/868mhz multi-band wireless sensor platform for body sensor network applications. In *Proc. of Int'l Conference on Wearable and Implantable Body Sensor Networks (BSN)*, pages 63–66. IEEE, 2012.

[20] Emmanuel J Candès and Benjamin Recht. Exact matrix completion via convex optimization. *Foundations of Computational mathematics*, 9(6):717, 2009.

[21] Emmanuel J Candès, Justin Romberg, and Terence Tao. Robust uncertainty principles: Exact signal reconstruction from highly incomplete frequency information. *IEEE Trans. on inf. theory*, 52(2):489–509, 2006.

[22] Emmanuel J Candes, Justin K Romberg, and Terence Tao. Stable signal recovery from incomplete and inaccurate measurements. *Communications on pure and applied mathematics*, 59(8):1207–1223, 2006.

[23] Emmanuel J Candes and Terence Tao. Decoding by linear programming. *IEEE Trans. on information theory*, 51(12):4203–4215, 2005.

[24] Emmanuel J Candes, Michael B Wakin, and Stephen P Boyd. Enhancing sparsity by reweighted ℓ_1-minimization. *Journal of Fourier analysis and applications*, 14(5-6):877–905, 2008.

[25] Ayon Chakraborty, Md Shaifur Rahman, Himanshu Gupta, and Samir R Das. Specsense: Crowdsensing for efficient querying of spectrum occupancy. In *Proc. of IEEE INFOCOM*, pages 1–9, May 2017.

[26] Bolin Chen, Jiming Chen, Yuan Gao, and Jie Zhang. Coexistence of LTE-LAA and Wi-Fi on 5 GHz with corresponding deployment scenarios: A survey. *IEEE Comm. Surveys & Tutorials*, 19(1):7–32, 2017.

[27] H. Chen, Y. Ma, Z. Lin, Y. Li, and B. Vucetic. Distributed power control in interference channels with qos constraints and rf energy harvesting: A game-theoretic approach. *IEEE Trans. on Vehicular Technology*, PP(99):1–1, 2016.

[28] Yunfei Chen and Hee-Seok Oh. A survey of measurement-based spectrum occupancy modeling for cognitive radios. *IEEE Communications Surveys & Tutorials*, 18(1):848–859, 2014.

[29] Yunxia Chen and Qing Zhao. On the lifetime of wireless sensor networks. *IEEE Communications Letters*, 9(11):976–978, Nov 2005.

[30] Visual Networking Index Cisco. Global mobile data traffic forecast update, 2016–2021. *White Paper*, 2017.

[31] Deborah Cohen, Shahar Tsiper, and Yonina C Eldar. Analog-to-digital cognitive radio: Sampling, detection, and hardware. *IEEE Signal Processing Magazine*, 35(1):137–166, Jan 2018.

[32] Federal Communications Commission. Tv white space.

[33] Federal Communications Commission et al. Fcc online table of frequency allocations. *Online:[https://transition.fcc.gov/oet/spectrum/table/fcctable.pdf]*, 2017.

[34] Carlos Cordeiro, Kiran Challapali, Dagnachew Birru, and Sai Shankar. Ieee 802.22: the first worldwide wireless standard based on cognitive radios. In *New Frontiers in Dynamic Spectrum Access Networks, 2005. DySPAN 2005. 2005 First IEEE International Symposium on*, pages 328–337. Ieee, 2005.

[35] Mark A Davenport, Petros T Boufounos, Michael B Wakin, and Richard G Baraniuk. Signal processing with compressive measurements. *IEEE Journal of Selected Topics in Signal Processing*, 4(2):445–460, 2010.

[36] Mark A Davenport, Marco F Duarte, Yonina C Eldar, and Gitta Kutyniok. Introduction to compressed sensing. *Preprint*, 93(1):2, 2011.

[37] Fadel F Digham, Mohamed-Slim Alouini, and Marvin K Simon. On the energy detection of unknown signals over fading channels. *IEEE Trans. on communications*, 55(1):21–24, 2007.

[38] Zhiguo Ding, S.M. Perlaza, I. Esnaola, and H.V. Poor. Power allocation strategies in energy harvesting wireless cooperative networks. *IEEE Trans. on Wireless Communications*, 13(2):846–860, February 2014.

[39] David L Donoho. Compressed sensing. *IEEE Trans. on information theory*, 52(4):1289–1306, 2006.

[40] Samina Ehsan, Bechir Hamdaoui, and Mohsen Guizani. Radio and medium access contention aware routing for lifetime maximization in multichannel sensor networks. *IEEE Trans. on Wireless Communications*, 11(9):3058–3067, 2012.

[41] Zhaoxi Fang, Tianlong Song, and Tongtong Li. Energy harvesting for two-way OFDM communications under hostile jamming. *IEEE Signal Processing Letters*, 22(4):413–416, April 2015.

[42] Michael P Friedlander, Hassan Mansour, Rayan Saab, and Oezguer Yilmaz. Recovering compressively sampled signals using partial support information. *IEEE Trans. on Information Theory*, 58(2):1122–1134, 2012.

[43] Shu Fu, Hong Wen, and Bin Wu. Power-fractionizing mechanism: Achieving joint user scheduling and power allocation via geometric programming. *IEEE Trans. on Vehicular Technology*, 2017.

[44] Hakim Ghazzai, Elias Yaacoub, Mohamed-Slim Alouini, and Adnan Abu-Dayya. Performance of green lte networks powered by the smart grid with time varying user density. In *Proc. of IEEE VTC-Fall*, pages 1–6, 2013.

[45] Mahdi Ben Ghorbel, Mohsen Guizani, Bassem Khalfi, and Bechir Hamdaoui. Cooperative joint power splitting and allocation approach for simultaneous energy delivery and data transfer. In *Wireless Communications and Mobile Computing Conference (IWCMC), 2015 International*, pages 184–187. IEEE, 2015.

[46] Mahdi Ben Ghorbel, Bechir Hamdaoui, Mohsen Guizani, and Bassem Khalfi. Distributed learning-based cross-layer technique for energy-efficient multicarrier dynamic spectrum access with adaptive power allocation. *IEEE Trans. on Wireless Communications*, 15(3):1665–1674, 2016.

[47] Mahdi Ben Ghorbel, Bassem Khalfi, Bechir Hamdaoui, and Mohsen Guizani. Resources allocation for large-scale dynamic spectrum access system using particle filtering. In *proc. of Globecom Workshops*, pages 219–224. IEEE, 2014.

[48] Mahdi Ben Ghorbel, Bassem Khalfi, Bechir Hamdaoui, and Mohsen Guizani. Power allocation analysis for dynamic power utility in cognitive radio systems.

In *Communications (ICC), IEEE International Conference on*, pages 3732–3737. IEEE, 2015.

[49] Asvin Gohil, Hardik Modi, and Shobhit K Patel. 5G technology of mobile communication: A survey. In *Intelligent Systems and Signal Processing (ISSP), 2013 International Conference on*, pages 288–292. IEEE, 2013.

[50] Inc. Google. Google spectrum database.

[51] Michael Grant, Stephen Boyd, and Yinyu Ye. Cvx: Matlab software for disciplined convex programming, 2008.

[52] M. Gregori and M. Payaro. Multiuser communications with energy harvesting transmitters. In *Proc. of IEEE Int'l Conference on Communications (ICC)*, pages 5360–5365, June 2014.

[53] Mohamed Grissa, Bechir Hamdaoui, and Attila A Yavuz. Location privacy in cognitive radio networks: A survey. *IEEE Communications Surveys & Tutorials*, 2017.

[54] Mohamed Grissa, Attila Yavuz, and Bechir Hamdaoui. Lpos: Location privacy for optimal sensing in cognitive radio networks. In *proc. of IEEE GLOBECOM*, pages 1–6. IEEE, 2015.

[55] Mohamed Grissa, Attila Yavuz, and Bechir Hamdaoui. An efficient technique for protecting location privacy of cooperative spectrum sensing users. In *proc of IEEE INFOCOM WKSHPS*, pages 915–920, 2016.

[56] Mohamed Grissa, Attila A Yavuz, and Bechir Hamdaoui. Cuckoo filter-based location-privacy preservation in database-driven cognitive radio networks. In *World Symposium on Computer Networks and Information Security (WSCNIS)*, pages 1–7. IEEE, 2015.

[57] Mohamed Grissa, Attila A Yavuz, and Bechir Hamdaoui. Location privacy preservation in database-driven wireless cognitive networks through encrypted probabilistic data structures. *IEEE Transactions on Cognitive Communications and Networking*, 3(2):255–266, 2017.

[58] Mohamed Grissa, Attila A Yavuz, and Bechir Hamdaoui. Preserving the location privacy of secondary users in cooperative spectrum sensing. *IEEE Trans. on Information Forensics and Security*, 12(2):418–431, 2017.

[59] Mohamed Grissa, Attila A Yavuz, and Bechir Hamdaoui. When the hammer meets the nail: Multi-server pir for database-driven crn with location privacy assurance. *arXiv preprint arXiv:1705.01085*, 2017.

[60] Yanju Gu and Sonia Aïssa. Rf-based energy harvesting in decode-and-forward relaying systems: Ergodic and outage capacities. *IEEE Trans. on Wireless Communications*, 14(11):6425–6434, 2015.

[61] Mohsen Guizani, Bassem Khalfi, Mahdi Ben Ghorbel, and Bechir Hamdaoui. Large-scale cognitive cellular systems: resource management overview. *IEEE Communications Magazine*, 53(5):44–51, 2015.

[62] Youngjune Gwon and HT Kung. Scaling network-based spectrum analyzer with constant communication cost. In *Proceedings of IEEE INFOCOM*, pages 737–745, 2013.

[63] Bechir Hamdaoui. Adaptive spectrum assessment for opportunistic access in cognitive radio networks. *IEEE Trans. on Wireless Communications*, 8(2):922–930, 2009.

[64] Bechir Hamdaoui, Bassem Khalfi, and Mohsen Guizani. Compressed wideband spectrum sensing: Concept, challenges and enablers.

[65] Bechir Hamdaoui and Kang G Shin. OS-MAC: An efficient MAC protocol for spectrum-agile wireless networks. *IEEE Transactions on Mobile Computing*, 7(8):915–930, 2008.

[66] Rami Hamdi, Mahdi Ben Ghorbel, Bechir Hamdaoui, Mohsen Guizani, and Bassem Khalfi. Implementation and analysis of reward functions under different traffic models for distributed dsa systems. *IEEE Transactions on Wireless Communications*, 14(9):5147–5155, 2015.

[67] Z-C Hao and J-S Hong. Highly selective ultra wideband bandpass filters with quasi-elliptic function response. *IET microwaves, antennas & propagation*, 5(9):1103–1108, 2011.

[68] Tanbir Haque, Rabia Tugce Yazicigil, Kyle Jung-Lin Pan, John Wright, and Peter R Kinget. Theory and design of a quadrature analog-to-information converter for energy-efficient wideband spectrum sensing. *IEEE Trans. on Circuits and Systems I: Regular Papers*, 62(2):527–535, 2015.

[69] Timothy Harrold, Rafael Cepeda, and Mark Beach. Long-term measurements of spectrum occupancy characteristics. In *Proc. of IEEE Symposium on New Frontiers in Dynamic Spectrum Access Networks (DySPAN)*, pages 83–89, 2011.

[70] Haitham Hassanieh, Lixin Shi, Omid Abari, Ezzeldin Hamed, and Dina Katabi. Ghz-wide sensing and decoding using the sparse fourier transform. In *Proc. of IEEE INFOCOM*, pages 2256–2264, 2014.

[71] D.T. Hoang, D. Niyato, P. Wang, and D.I. Kim. Performance optimization for cooperative multiuser cognitive radio networks with RF energy harvesting capability. *IEEE Trans. on Wireless Communications*, 14(7):3614–3629, July 2015.

[72] Steven Siying Hong and Sachin Rajsekhar Katti. Dof: a local wireless information plane. In *ACM SIGCOMM Computer Communication Review*, volume 41, pages 230–241, 2011.

[73] Kaibin Huang and Xiangyun Zhou. Cutting the last wires for mobile communications by microwave power transfer. *IEEE Communications Magazine*, 53(6):86–93, 2015.

[74] Ozlem Durmaz Incel. A survey on multi-channel communication in wireless sensor networks. *Comp. Net.*, 55(13):3081–3099, 2011.

[75] Jing Jiang, Hongjian Sun, David Baglee, and H Vincent Poor. Achieving autonomous compressive spectrum sensing for cognitive radios. *IEEE Trans. on Vehicular Technology*, 65(3):1281–1291, 2016.

[76] Hyungsik Ju and Rui Zhang. Throughput maximization in wireless powered communication networks. *IEEE Trans. on Wireless Communications*, 13(1):418–428, 2014.

[77] M Amin Khajehnejad, Weiyu Xu, A Salman Avestimehr, and Babak Hassibi. Analyzing weighted minimization for sparse recovery with nonuniform sparse models. *IEEE Trans. on Signal Processing*, 59(5):1985–2001, 2011.

[78] Bassem Khalfi, Mahdi Ben Ghorbel, Bechir Hamdaoui, and Mohsen Guizani. Distributed fair spectrum assignment for large-scale wireless dsa networks. In *International Conference on Cognitive Radio Oriented Wireless Networks*, pages 631–642. Springer, 2015.

[79] Bassem Khalfi, Mahdi Ben Ghorbel, Bechir Hamdaoui, and Mohsen Guizani. Dynamic power pricing using distributed resource allocation for large-scale dsa systems. In *Wireless Communications and Networking Conference (WCNC)*, pages 1090–1094. IEEE, 2015.

[80] Bassem Khalfi, Bechir Hamdaoui, Mahdi Ben Ghorbel, Mohsen Guizani, and Xi Zhang. Joint data and power transfer optimization for energy harvesting wireless networks. In *Computer Communications Workshops (INFOCOM WKSHPS), 2016 IEEE Conference on*, pages 742–747. IEEE, 2016.

[81] Bassem Khalfi, Bechir Hamdaoui, Mahdi Ben Ghorbel, Mohsen Guizani, and Xi Zhang. Joint data and power transfer optimization for energy harvesting wireless networks. In *Proc. of IEEE INFOCOM WKSHPS,*, pages 742–747, 2016.

[82] Bassem Khalfi, Bechir Hamdaoui, and Mohsen Guizani. Extracting and exploiting inherent sparsity for efficient iot support in 5G: Challenges and potential solutions. *IEEE Wireless Communications Magazine*, Oct. 2017.

[83] Bassem Khalfi, Bechir Hamdaoui, Mohsen Guizani, and Nizar Zorba. Exploiting wideband spectrum occupancy heterogeneity for weighted compressive spectrum sensing. In *Computer Communications Workshops (INFOCOM WKSHPS), IEEE Conference on*, pages 1–6, 2017.

[84] Bassem Khalfi, Bechir Hamdaoui, Mohsen Guizani, and Nizar Zorba. Efficient spectrum availability information recovery for wideband DSA networks: A weighted compressive sampling approach. *IEEE Trans. on Wireless Communications*, 17(4), April 2018.

[85] Sami Kirolos, Jason Laska, Michael Wakin, Marco Duarte, Dror Baron, Tamer Ragheb, Yehia Massoud, and Richard Baraniuk. Analog-to-information conversion via random demodulation. In *Proc. of IEEE Dallas/CAS Workshop on Design, Applications, Integration and Software*, pages 71–74, 2006.

[86] Yehuda Koren, Robert Bell, and Chris Volinsky. Matrix factorization techniques for recommender systems. *Computer*, 42(8), 2009.

[87] I. Krikidis, S. Timotheou, S. Nikolaou, Gan Zheng, D.W.K. Ng, and R. Schober. Simultaneous wireless information and power transfer in modern communication systems. *IEEE Communications Magazine*, 52(11):104–110, Nov 2014.

[88] Eva Lagunas, Shree Krishna Sharma, Symeon Chatzinotas, and Björn Ottersten. Compressive sensing based energy detector. In *Proc. of IEEE European Signal Processing Conference*, pages 1678–1682, 2016.

[89] Eva Lagunas, Shree Krishna Sharma, Symeon Chatzinotas, and Björn Ottersten. Compressive sensing based target counting and localization exploiting joint sparsity. In *Proc. of IEEE Acoustics, Speech and Signal Processing*, pages 3231–3235, 2016.

[90] Thanh Tu Lam, Marco Di Renzo, and Justin P Coon. System-level analysis of swipt mimo cellular networks. *IEEE Comm. Letters*, 20(10):2011–2014, 2016.

[91] Joonseok Lee, Seungyeon Kim, Guy Lebanon, Yoram Singer, and Samy Bengio. LLORMA: Local low-rank matrix approximation. *The Journal of Machine Learning Research*, 17(1):442–465, 2016.

[92] Khaled Ben Letaief and Wei Zhang. Cooperative communications for cognitive radio networks. *Proc. of the IEEE*, 97(5):878–893, 2009.

[93] Liang Liu, Rui Zhang, and Kee-Chaing Chua. Wireless information transfer with opportunistic energy harvesting. In *Proc. of IEEE Int. Symp. on Information Theory (ISIT)*, pages 950–954, July 2012.

[94] Miles Lopes. Estimating unknown sparsity in compressed sensing. In *Proc. of Int. Conf. on Machine Learning*, pages 217–225, 2013.

[95] Xiao Lu, Ping Wang, D. Niyato, Dong In Kim, and Zhu Han. Wireless networks with RF energy harvesting: A contemporary survey. *IEEE Communications Surveys Tutorials*, 17(2):757–789, 2nd Q 2015.

[96] Yingqi Lu, Pai Zhu, Donglin Wang, and Michel Fattouche. Machine learning techniques with probability vector for cooperative spectrum sensing in cognitive radio networks. In *Proc. of Wireless Communications and Networking Conference (WCNC)*, pages 1–6. IEEE, 2016.

[97] A Mancuso, S Probasco, and B Patil. Protocol to access white-space (paws) databases: Use cases and requirements. Technical report, 2013.

[98] MA Mehaseb, Y Gadallah, A Elhamy, and H Elhennawy. Classification of LTE uplink scheduling techniques: An M2M perspective. *IEEE Communications Surveys & Tutorials*, 18(2):1310–1335, 2016.

[99] M Mehdawi, NG Riley, M Ammar, A Fanan, and M Zolfaghari. Spectrum occupancy measurements and lessons learned in the context of cognitive radio. In *Proc. of IEEE Telecommunications Forum Telfor (TELFOR)*, pages 196–199, 2015.

[100] Jia Jasmine Meng, Wotao Yin, Husheng Li, Ekram Hossain, and Zhu Han. Collaborative spectrum sensing from sparse observations in cognitive radio networks. *IEEE Journal on Selected Areas in Communications*, 29(2):327–337, 2011.

[101] M. Mishali and Y. C. Eldar. From theory to practice: Sub-Nyquist sampling of sparse wideband analog signals. *IEEE Journal of Selected Topics in Signal Processing*, 4(2):375–391, Apr. 2010.

[102] Rohan Murty, Ranveer Chandra, Thomas Moscibroda, and Paramvir Bahl. Senseless: A database-driven white spaces network. *IEEE Trans. on Mobile Computing*, 11(2):189–203, 2012.

[103] D. Needell and R. Vershynin. Signal recovery from incomplete and inaccurate measurements via regularized orthogonal matching pursuit. *IEEE Journal of Selected Topics in Signal Processing*, 4(2):310–316, Apr. 2010.

[104] Deanna Needell, Rayan Saab, and Tina Woolf. Weighted ℓ_1-minimization for sparse recovery under arbitrary prior information. *arXiv preprint arXiv:1606.01295*, 2016.

[105] Deanna Needell and Joel A Tropp. Cosamp: Iterative signal recovery from incomplete and inaccurate samples. *Applied and Computational Harmonic Analysis*, 26(3):301–321, 2009.

[106] Derrick Wing Kwan Ng, Ernest S Lo, and Robert Schober. Wireless information and power transfer: Energy efficiency optimization in ofdma systems. *IEEE Trans. on Wireless Communications*, 12(12):6352–6370, 2013.

[107] S. Khoshabi Nobar, K. Adli Mehr, and J. Musevi Niya. Rf-powered green cognitive radio networks: Architecture and performance analysis. *IEEE Communications Letters*, 20(2):296–299, Feb 2016.

[108] MohammadJavad NoroozOliaee, Bechir Hamdaoui, Xiuzhen Cheng, Taieb Znati, and Mohsen Guizani. Analyzing cognitive network access efficiency under limited spectrum handoff agility. *IEEE Transactions on Vehicular Technology*, 63(3):1402–1407, 2014.

[109] MohammadJavad NoroozOliaee, Bechir Hamdaoui, and Kagan Tumer. Efficient objective functions for coordinated learning in large-scale distributed osa systems. *IEEE Trans. on Mobile Computing*, 12(5):931–944, 2013.

[110] Afif Osseiran, Jose F Monserrat, and Patrick Marsch. *5G Mobile and Wireless Communications Technology*. Cambridge University Press, 2016.

[111] Maria Rita Palattella, Mischa Dohler, Alfredo Grieco, Gianluca Rizzo, Johan Torsner, Thomas Engel, and Latif Ladid. Internet of things in the 5g era: Enablers, architecture, and business models. *IEEE Journal on Selected Areas in Communications*, 34(3):510–527, 2016.

[112] Vilaskumar M Patil and Siddarama R Patil. A survey on spectrum sensing algorithms for cognitive radio. In *2016 International Conference on Advances in Human Machine Interaction (HMI)*, pages 1–5. IEEE, 2016.

[113] Fabian Pedregosa, Gaël Varoquaux, Alexandre Gramfort, Vincent Michel, Bertrand Thirion, Olivier Grisel, Mathieu Blondel, Peter Prettenhofer, Ron Weiss, Vincent Dubourg, et al. Scikit-learn: Machine learning in python. *Journal of Machine Learning Research*, 12(Oct):2825–2830, 2011.

[114] Valentin V Petrov. Limit theorems of probability theory: sequences of independent random variables. Technical report, Oxford, New York, 1995.

[115] Z. Qin, Y. Gao, M. D. Plumbley, and C. G. Parini. Wideband spectrum sensing on real-time signals at sub-Nyquist sampling rates in single and cooperative multiple nodes. *IEEE Trans. on Signal Processing*, 64(12):3106–3117, Jun. 2016.

[116] Z Qin, Yang Gao, and Mark Plumbley. Malicious user detection based on low-rank matrix completion in wideband spectrum sensing. *IEEE Trans. on Signal Processing*, 2017.

[117] Zhijin Qin, Yue Gao, and Clive G Parini. Data-assisted low complexity compressive spectrum sensing on real-time signals under sub-Nyquist rate. *IEEE Trans. on Wireless Communications*, 15(2):1174–1185, 2016.

[118] Zhijin Qin, Yue Gao, Mark D Plumbley, and Clive G Parini. Wideband spectrum sensing on real-time signals at sub-Nyquist sampling rates in single and cooperative multiple nodes. *IEEE Trans. on Signal Processing*, 64(12):3106–3117, 2015.

[119] Zhijin Qin, Yue Gao, Mark D Plumbley, and Clive G Parini. Wideband spectrum sensing on real-time signals at sub-nyquist sampling rates in single and cooperative multiple nodes. *IEEE Trans. on Signal Processing*, 64(12):3106–3117, 2016.

[120] RadioSoft. White space database.

[121] Theodore S Rappaport, Yunchou Xing, George R MacCartney, Andreas F Molisch, Evangelos Mellios, and Jianhua Zhang. Overview of millimeter wave communications for fifth-generation (5g) wireless networks with a focus on propagation models. *IEEE Trans. on Antennas and Propagation*, 65(12):6213–6230, 2017.

[122] Fred Richter, Albrecht J Fehske, and Gerhard P Fettweis. Energy efficiency aspects of base station deployment strategies for cellular networks. In *Proc. of IEEE VTC-Fall,*, pages 1–5, 2009.

[123] Javier Rubio and Antonio Pascual-Iserte. Harvesting management in multiuser mimo systems with simultaneous wireless information and power transfer. In *Proc. of IEEE VTC-Spring*, pages 1–5, May 2015.

[124] Fatima Salahdine, Naima Kaabouch, and Hassan El Ghazi. Bayesian compressive sensing with circulant matrix for spectrum sensing in cognitive radio networks. In *Proc. of IEEE Annual Ubiquitous Computing, Electronics & Mobile Communication Conference (UEMCON)*, pages 1–6, 2016.

[125] Fatima Salahdine, Naima Kaabouch, and Hassan El Ghazi. A survey on compressive sensing techniques for cognitive radio networks. *Physical Communication*, 20:61–73, 2016.

[126] Fatima Salahdine, Naima Kaabouch, and Hassan El Ghazi. A bayesian recovery technique with toeplitz matrix for compressive spectrum sensing in cognitive radio networks. *International Journal of Communication Systems*, 2017.

[127] S. K. Sharma, E. Lagunas, S. Chatzinotas, and B. Ottersten. Application of compressive sensing in cognitive radio communications: A survey. *IEEE Communications Surveys & Tutorials*, 18(03):1838–1860, 2016.

[128] Shree Krishna Sharma, Symeon Chatzinotas, and Björn Ottersten. Compressive sparsity order estimation for wideband cognitive radio receiver. *IEEE Trans. on Signal Processing*, 62(19):4984–4996, 2014.

[129] Lixin Shi, Paramvir Bahl, and Dina Katabi. Beyond sensing: Multi-ghz realtime spectrum analytics. In *Proc. of USENIX Symposium on Networked Systems Design and Implementation (NSDI)*, pages 159–172, 2015.

[130] Yi Shi, Liguang Xie, Y Thomas Hou, and Hanif D Sherali. On renewable sensor networks with wireless energy transfer. In *Proc. of IEEE INFOCOM*, pages 1350–1358, 2011.

[131] Alex J Smola and Bernhard Schölkopf. A tutorial on support vector regression. *Statistics and computing*, 14(3):199–222, 2004.

[132] Inc. Spectrum Bridge. White space database.

[133] Boyd Stephen and Vandenberghe Lieven. *Convex Optimization*. Cambridge University Press, 2004.

[134] Hongjian Sun, Arumugam Nallanathan, Shuguang Cui, and Cheng-Xiang Wang. Cooperative wideband spectrum sensing over fading channels. *IEEE Trans. on Vehicular Technology*, 65(3):1382–1394, 2016.

[135] Hongjian Sun, Arumugam Nallanathan, Cheng-Xiang Wang, and Yunfei Chen. Wideband spectrum sensing for cognitive radio networks: a survey. *IEEE Wireless Communications*, 20(2):74–81, 2013.

[136] Z. Sun and J. N. Laneman. Performance metrics, sampling schemes, and detection algorithms for wideband spectrum sensing. *IEEE Trans. on Signal Processing*, 62(19):5107–5118, Oct. 2014.

[137] Tanim M Taher, Roger B Bacchus, Kenneth J Zdunek, and Dennis A Roberson. Long-term spectral occupancy findings in chicago. In *New Frontiers in Dynamic Spectrum Access Networks (DySPAN), 2011 IEEE Symposium on*, pages 100–107. IEEE, 2011.

[138] Karaputugala Madushan Thilina, Kae Won Choi, Nazmus Saquib, and Ekram Hossain. Machine learning techniques for cooperative spectrum sensing in cognitive radio networks. *IEEE JSAC*, 31(11):2209–2221, 2013.

[139] Zhi Tian and Georgios B Giannakis. Compressed sensing for wideband cognitive radios. In *Acoustics, Speech and Signal Processing, 2007. ICASSP 2007. IEEE International Conference on*, volume 4, pages IV–1357. IEEE, 2007.

[140] Zhi Tian, Yohannes Tafesse, and Brian M Sadler. Cyclic feature detection with sub-Nyquist sampling for wideband spectrum sensing. *IEEE Journal of Selected topics in signal processing*, 6(1):58–69, 2012.

[141] Bin Tong, Zi Li, Guiling Wang, and Wensheng Zhang. How wireless power charging technology affects sensor network deployment and routing. In *Proc. of IEEE ICDCS*, pages 438–447, June 2010.

[142] Taha Touzri, Mahdi Ben Ghorbel, Bechir Hamdaoui, Mohsen Guizani, and Bassem Khalfi. Efficient usage of renewable energy in communication systems using dynamic spectrum allocation and collaborative hybrid powering. *IEEE Transactions on Wireless Communications*, 15(5):3327–3338, 2016.

[143] Joel A Tropp and Anna C Gilbert. Signal recovery from random measurements via orthogonal matching pursuit. *IEEE Trans. on information theory*, 53(12):4655–4666, 2007.

[144] Joel A Tropp, Jason N Laska, Marco F Duarte, Justin K Romberg, and Richard G Baraniuk. Beyond nyquist: Efficient sampling of sparse bandlimited signals. *IEEE Trans. on Information Theory*, 56(1):520–544, 2010.

[145] Lav R Varshney. Transporting information and energy simultaneously. In *Proc. of IEEE Int'l Symp. on Infor. Theory*, pages 1612–1616, 2008.

[146] Namrata Vaswani and Wei Lu. Modified-CS: Modifying compressive sensing for problems with partially known support. *IEEE Trans. on Signal Processing*, 58(9):4595–4607, 2010.

[147] Javad Vazifehdan, R Venkatesha Prasad, Martin Jacobsson, and Ignas Niemegeers. An analytical energy consumption model for packet transfer over wireless links. *IEEE Communications Letters*, 16(1):30–33, 2012.

[148] Pavithra Venkatraman, Bechir Hamdaoui, and Mohsen Guizani. Opportunistic bandwidth sharing through reinforcement learning. *IEEE Trans. on Vehicular Technology*, 59(6):3148–3153, 2010.

[149] Jin Wang, Shaojie Tang, Baocai Yin, and Xiang-Yang Li. Data gathering in wireless sensor networks through intelligent compressive sensing. In *Proceedings of IEEE INFOCOM*, pages 603–611, 2012.

[150] Yue Wang, Zhi Tian, and Chunyan Feng. Sparsity order estimation and its application in compressive spectrum sensing for cognitive radios. *IEEE Trans. on wireless communications*, 11(6):2116–2125, 2012.

[151] Liguang Xie, Yi Shi, Y Thomas Hou, Wenjing Lou, Hanif Sherali, and Scott F Midkiff. Bundling mobile base station and wireless energy transfer: Modeling and optimization. In *Proc. of IEEE INFOCOM*, pages 1636–1644, 2013.

[152] Liguang Xie, Yi Shi, Y Thomas Hou, Wenjing Lou, Hanif D Sherali, and Scott F Midkiff. On renewable sensor networks with wireless energy transfer: the multi-node case. In *Proc. of IEEE SECON*, pages 10–18, 2012.

[153] Liguang Xie, Yi Shi, Y Thomas Hou, and Hanif D Sherali. Making sensor networks immortal: An energy-renewal approach with wireless power transfer. *IEEE/ACM Trans. on Netw.*, 20(6):1748–1761, 2012.

[154] Weiyu Xu, M Amin Khajehnejad, A Salman Avestimehr, and Babak Hassibi. Breaking through the thresholds: an analysis for iterative reweighted ℓ_1- minimization via the grassmann angle framework. In *Proc. of IEEE Int. Conf. on Acoustics, Speech and Signal Processing*, pages 5498–5501, 2010.

[155] Zhou Xun, Zhang Rui, and Ho Chin Keong. Wireless information and power transfer: Architecture design and rate-energy tradeoff. *IEEE Trans. on Communications*, 61(11):4754–4767, November 2013.

[156] E. Yaacoub and Z. Dawy. A survey on uplink resource allocation in ofdma wireless networks. *IEEE Communications Surveys Tutorials*, 14(2):322–337, 2012.

[157] R. T. Yazicigil, T. Haque, M. Kumar, J. Yuan, J. Wright, and P. R. Kinget. How to make analog-to-information converters work in dynamic spectrum environments with changing sparsity conditions. *IEEE Trans. on Circuits and Systems I: Regular Papers*, PP(99):1–10, 2017.

[158] Rabia Tugce Yazicigil, Tanbir Haque, Michael R Whalen, Jeffrey Yuan, John Wright, and Peter R Kinget. Wideband rapid interferer detector exploiting compressed sampling with a quadrature analog-to-information converter. *IEEE Journal of Solid-State Circuits*, 50(12):3047–3064, 2015.

[159] Mümtaz Yılmaz, Damla Gürkan Kuntalp, and Akan Fidan. Determination of spectrum utilization profiles for 30 MHz–3 GHz frequency band. In *Proc. of IEEE International Conference on Communications (COMM)*, pages 499–502, 2016.

[160] Wotao Yin, Simon Morgan, Junfeng Yang, and Yin Zhang. Practical compressive sensing with toeplitz and circulant matrices. In *Proc. of SPIE*, volume 7744, page 77440K, 2010.

[161] M-H Yoon, Y Shin, H-K Ryu, and J-M Woo. Ultra-wideband loop antenna. *Electronics letters*, 46(18):1249–1251, 2010.

[162] Weiliang Zeng, Yahong Rosa Zheng, and Robert Schober. Online resource allocation for energy harvesting downlink multiuser systems: Precoding with modulation, coding rate, and subchannel selection. *IEEE Trans. on Wireless Communications*, 14(10):5780–5794, 2015.

[163] Chao Zhai, Ju Liu, and Lina Zheng. Relay-based spectrum sharing with secondary users powered by wireless energy harvesting. *IEEE Trans. on Communications*, 64(5):1875–1887, 2016.

[164] Huan Zhao, Quanming Yao, James T Kwok, and Dik Lun Lee. Collaborative filtering with social local models. pages 1–10, Nov. 2017.

[165] Qing Zhao and Brian M Sadler. A survey of dynamic spectrum access. *IEEE signal processing magazine*, 24(3):79–89, 2007.

[166] Mariya Zheleva, Ranveer Chandra, Aakanksha Chowdhery, Ashish Kapoor, and Paul Garnett. Txminer: Identifying transmitters in real-world spectrum measurements. In *Proc. of IEEE Int. Symposium on Dynamic Spectrum Access Networks (DySPAN)*, pages 94–105, 2015.

[167] Xun Zhou, Chin Keong Ho, and Rui Zhang. Wireless power meets energy harvesting: a joint energy allocation approach in ofdm-based system. *IEEE Trans. on Wireless Comm.*, 15(5):3481–3491, 2016.

[168] Nizar Zorba and Christos Verikoukis. Energy optimization for bidirectional multimedia communication in unsynchronized tdd systems. *IEEE Systems Journal*, 10(2):797–804, 2016.